

**University of Pretoria**  
**FACULTY OF HEALTH SCIENCES**  
**DEPARTMENT OF PHYSIOLOGY**

**The effect of systemic lipopolysaccharides on the  
cardiovascular system in Sprague-Dawley rats**

by

Glory Isabella Tambwe

Submitted in partial fulfilment of the requirements for the degree of:  
*Master of Science (Human Physiology)*

**2021**

**Master of Science Candidate and Principal Investigator:**

Name and surname: Glory Isabella Tambwe

Student No: 13063902

Department of Physiology

Faculty of Health Sciences

University of Pretoria

**Project Supervisor:**

Dr. Janette Bester

Department of Physiology

Faculty of Health Sciences

University of Pretoria

**Co-supervisor:**

Dr. Sajee Alummoottil

Department of Physiology

Faculty of Health Sciences

## **Abstract**

Literature has shown that there is a link between cardiovascular disease and cognitive deterioration. Cardiovascular and neurodegenerative diseases both share risk factors that include age, elevated cholesterol levels and blood pressure. Both conditions primarily affect middle aged and elderly populations and are characterised by a disruption in homeostasis. Research has found that systemic inflammation induces cardiovascular and neurological disease. In addition, cardiovascular disease is initiated the following: endothelial damage and inflammation, disrupting cellular (erythrocyte, fibrin network, platelet), cardiac myofibril and vascular morphology.

Systemic inflammation may result if the cardiovascular system is exposed to bacteria or bacterial metabolites. Polysaccharides are long monosaccharide chains linked to glycosidic bonds that occur in nature. These structures serve as energy reserves and structural components in all organisms. The lipopolysaccharide endotoxin is a polysaccharide that is excreted from gram-negative bacteria and reside in gastrointestinal tract of healthy human beings. However, upon sustained abnormal gastrointestinal tract entry research suggests that lipopolysaccharides may aid in or play a primary role in the aetiology of cardiovascular disease and the neurodegenerative process through a low-grade systemic inflammatory immune response. The elderly may be are readily exposed to lipopolysaccharides through tooth loss (due to the dilation of the oral vasculature when tooth loss occurs) and impaired tight junction resulting in cardiovascular system entry. Research suggests that tooth loss and cardiovascular disease development are closely related through the resultant systemic inflammation. In addition, men experience an increased prevalence in various cardiovascular diseases that increase the risk of pathogenesis of neurodegeneration in a unique manner.

This study forms part of a larger study that investigated effects of lipopolysaccharides on the brain, cardiovascular system and liver in which the Alzheimer's disease population are the population of interest. The aim of this study was to investigate the effect of early endotoxin exposure on the cardiovascular system while also investigating its effect on cognition of male Sprague Dawley rats over a ten-day period. In addition, Manuka honey was introduced as a possible treatment for the systemic inflammatory effects of lipopolysaccharides.

Cognitive and behavioural tests evaluated anxiety-like behaviour, mobility and short- and long-term, familiar object-, and spatial memory using the Open field-, Novel object recognition-, and Y-Maze test behavioural tests.

The histological and ultrastructural analyses were conducted on the aorta, heart and blood following lipopolysaccharide exposure using light-, scanning electron- and transmission

electron microscopy. The aorta and myocardial tissue were studied through light- and transmission electron microscopy found that myocardium exposure to lipopolysaccharides resulted in cardiac myofibril damage and mitochondrial cristae destruction. While Manuka honey treatment prevented a significant amount of myofibril damage. Nevertheless, the treatment failed to prevent mitochondrial cristae destruction. Aortic exposure resulted in cellular abnormalities, elastin fragmentation and collagen deposition. Manuka honey administration resulted in the reduction of cellular abnormalities and elastin fragmentation in the aorta however, the treatment induced collagen depletion.

In addition, whole blood analysis through scanning electron microscopy, showed that the endotoxin resulted in a lack of erythrocyte and platelet morphological changes. However, exposure resulted in the abnormal formation of fused and thick aggregated fibrin networks. The therapeutic remedy assisted in counteracting the harmful effects of the endotoxin by producing fibrin fibres that were both standard in structure in some areas and thick and fused in structure in other areas.

Early endotoxin exposure did not result in a significant behavioural or cognitive alteration. However, Manuka honey coupled with LPS was shown to impair spatial memory.

In conclusion, cardiovascular organs such as the aorta, cardiac muscle and fibrin network morphology are vulnerable to the effects of short-term lipopolysaccharide exposure. Therefore, exposure may result in an elevation of cardiac-, aortic cellular and elastin destruction that may possibly conclude in cardiovascular disease and an elevation in thrombotic events. In addition, Manuka honey serves as an insufficient remedy for the harmful effects of lipopolysaccharides on the cardiovascular system.

**(Word count: 632)**

**Keywords:** Aorta, behaviour, blood, cardiovascular disease, cognition, lipopolysaccharide, Manuka honey, neurodegeneration.

## **Declaration**

I, Isabella Gloria Tambwe declare that this thesis entitled,

**“The effect of systemic lipopolysaccharides on the cardiovascular system in Sprague dawley rats”**

Which I herewith submit to the University of Pretoria for the degree Master of Science in Physiology. I declare that this is an original work that belongs to the documented principal investigator and has never been submitted for any academic award to this or any other tertiary institution for another degree. In addition, the following document has been submitted into Turnitin to determine its originality.

\_\_\_\_\_  
Glory Isabella Tambwe

\_\_\_\_\_  
30<sup>th</sup> March 2021

**Signed name**

**Date**

## Acknowledgements

This dissertation was written in loving memory of Lorraine Matangi Tambwe

“Alone we can do so little; together we can do so much.” – **Helen Keller**

I thank God, first and foremost for giving me the knowledge, strength, support and time that I have needed to complete my dissertation as well as for the giving me with me assistance through the following people:

Secondly, I would like to thank my supervisor Dr. Janette Bester for her assistance during the experimental, analysis and writing process, for her guidance, patience and constant encouragement throughout the completion of my dissertation. Thank you for all that you have done for us, for playing an instrumental role in my growth and development as a researcher and a person.

To my co-supervisor, Dr. Sajee Alummoottil, thank you for your kindness, encouragement, assistance during the termination process, constant feedback that has expanded my mind, writing range and understanding of this topic.

Thank you, Karabo Rathebe, Nonkululeko Dhlamini and Victoria Verrall for your support and assistance during the experimental phase (animal handling and the behavioural study).

To the staff at the University of the Witwatersrand Central animal service thank you so much for the training, and assistance that you have given me through the animal handling, treatment administration, and the termination process. Thank you all for your unending patience and kindness.

I would like to say heartfelt thank you to Mrs Erna van Wilpe and Mrs Charity Maepa at the Laboratory for Microscopy and Microanalysis. Thank you both for assisting me in my sample preparation, viewing and examination.

I would like to thank Dr. Helena Taute in the section of Cell Biology, Histology and Embryology of the Department of Anatomy. Thank you so much for all your assistance with sample preparation, assisting me with the machinery and your patience during this study.

Thank you, Dr. Abe Kasonga from the department of Physiology, for your assistance in the preparation of the total cholesterol enzyme-linked immunosorbent assay (ELISA). Thank you so much for your patience during the process.

To Dr. Willie Daniels thank you for your expertise during the behavioural analyse. It has provided me with a wealth of knowledge.

Last, but not least, I would like to thank my family and friends for their incredible support, love and patience during this time. Thank you for your encouragement and words of wisdom, for the delicious meals, and for all the love that you have given me. I would be nothing without you. I would like to give a special thanks to father (Dr. Mungela Tambwe) and my mother (Mrs Giteya Tambwe), thank you for all your love, support and wisdom. To my older sister, thank you for giving us an amazing example on what it means to live a meaningful life. To, my best friend Anya König, thank you for being there for me and always being willing to read my chapters. To Mr Herman Kalula thank you so much for your kindness, support and for assisting me with the statistical analyse.

The financial assistance of the National Research Foundation (NRF) towards this research is hereby acknowledged. Opinions and conclusions expressed are those of the author and are not inevitably to be attributed to the NRF.

## Table of Contents

<b>Abstract</b> .....	iii
<b>Declaration</b> .....	v
<b>List of Figures</b> .....	12
<b>List of Tables</b> .....	15
<b>List of abbreviations, chemical formulae, SI units and symbols</b> .....	17
<b>Chapter 1: Introduction</b> .....	22
<b>Chapter 2: Literature Review</b> .....	26
<b>2.1 The Cardiovascular System</b> .....	27
2.1.1 The Heart .....	28
2.1.2 Blood vessels .....	32
2.1.3 Blood cells and plasma.....	33
<b>2.2 The link of neurodegeneration and cardiovascular complications</b> .....	40
<b>2.3 Human Gastrointestinal Microbiome</b> .....	43
2.3.1 Lipopolysaccharides.....	43
<b>2.4 Cardiovascular System Modifications</b> .....	46
2.4.1 Cardiovascular systems affected by lipopolysaccharides .....	46
<b>2.6 Aims and Objectives</b> .....	48
<b>Chapter 3: Methods and Materials</b> .....	50
<b>3.1 Introduction</b> .....	51
<b>3.2 Study Design</b> .....	52
<b>3.3 Sampling criteria: Control and Experimental Groups</b> .....	55
3.3.1 Timeline, control and experimental compound preparations and animal distribution .....	55
<b>3.4 Methods</b> .....	59
3.4.1 Behavioural analysis .....	59
3.4.2 Termination.....	65



3.4.3 Biochemical analyses.....	68
3.4.4 Light microscopy .....	69
3.4.5 Ultrastructural analysis of erythrocytes, fibrin networks and platelets using Scanning Electron Microscopy .....	73
3.4.6 Morphological analysis of tissues using Transmission electron microscopy.....	77
<b>Chapter 4: Animal behaviour analyses.....</b>	<b>79</b>
<b>4.1 Chapter Objectives .....</b>	<b>80</b>
<b>4.2 Introduction .....</b>	<b>80</b>
<b>4.3 Results.....</b>	<b>81</b>
4.3.1 The Open field test analysis.....	81
4.3.2 The Novel object recognition test analysis .....	87
4.3.3 The Y-Maze test analysis .....	92
<b>4.5 Conclusion .....</b>	<b>99</b>
<b>Chapter 5: Body weight and temperature .....</b>	<b>100</b>
<b>5.1 Chapter Objectives .....</b>	<b>101</b>
<b>5.2 Introduction .....</b>	<b>101</b>
<b>5.3 Results.....</b>	<b>102</b>
5.3.1 Weight analysis .....	102
5.3.2 Core body temperature analysis .....	103
<b>5.4 Discussion.....</b>	<b>105</b>
<b>5.5 Conclusion .....</b>	<b>105</b>
<b>Chapter 6: Investigating the histology of the cardiovascular system .....</b>	<b>107</b>
<b>6.1 Chapter Objectives .....</b>	<b>108</b>
<b>6.2 Introduction.....</b>	<b>108</b>
<b>6.3 Results.....</b>	<b>110</b>
6.3.1 Light microscopy: Lipopolysaccharides effect on cardiac and aortic tissue and exploring Manuka honey as a treatment.....	110
6.3.2 Transmission electron microscopy: Lipopolysaccharides effect on cardiac and aortic tissue and exploring Manuka honey as a treatment.....	117

6.4 Discussion .....	120
6.5 Conclusion .....	124
<b>Chapter 7: Total cholesterol levels .....</b>	<b>125</b>
7.1 Chapter Objective .....	126
7.2 Introduction .....	126
7.3 Results .....	127
7.4 Discussion .....	130
7.5 Conclusion .....	130
<b>Chapter 8: Ultrastructural blood analysis .....</b>	<b>132</b>
8.1 Chapter Objective .....	133
8.2 Introduction .....	133
8.3 Results .....	134
8.3.1 The effect of lipopolysaccharides on blood haemostasis and exploring Manuka honey as a treatment .....	134
8.4 Discussion .....	143
8.5 Conclusion .....	145
<b>Chapter 9: Conclusion .....</b>	<b>147</b>
9.1 Introduction .....	148
9.2 Key findings .....	148
9.3 Relevance of the findings .....	152
9.4 Limitations of the study and future recommendations .....	152
<b>Chapter 10: Appendixes .....</b>	<b>155</b>
10.1 Appendix A .....	156
10.1.1 Materials and chemicals .....	156
10.2 Appendix B .....	158
10.2.1 Link for test raw data .....	158
10.3 Appendix C .....	159
10.3.1 University of Pretoria: Animal ethics committee approval .....	159

10.3.1 University of Pretoria: Faculty of health sciences research ethics committee approval.....	160
10.3.2 University of the Witwatersrand: Animal research ethics committee approval ...	161
<b>Chapter 11: References</b> .....	<b>162</b>

## List of Figures

### Chapter 2

Figure 2.1: Cardiovascular system.....	27
Figure 2.2: Heart cell histology.....	30
Figure 2.3: The Cardiac Muscle's Ultrastructure.....	31
Figure 2.4: The cellular coagulation model.....	34
Figure 2.5: Erythrocyte structure.....	36
Figure 2.6: The schematic diagram of gram-negative lipopolysaccharides.....	45

### Chapter 3

Figure 3.1: Study outline.....	54
Figure 3.2: Sampling criteria and doses.....	56
Figure 3.3: Rat grimace scale four action sites.....	58
Figure 3.4: The Open field test.....	60
Figure 3.5: Novel object recognition test.....	63
Figure 3.6: Y-Maze novelty preference test.....	64
Figure 3.7: Preparation sequence.....	67
Figure 3.8: Erythrocyte classifications.....	75
Figure 3.9: Platelet classifications.....	76
Figure 3.10: Fibrin network classifications.....	77

### Chapter 4

Figure 4.1: Open field test control and experimental group mobile profiles.....	86
Figure 4.2: Open field test control and experimental group zone profiles.....	87
Figure 4.3: Novel object recognition test trial 1 and 2 Block A (Familiar object) entries and times.....	91
Figure 4.4: Novel object recognition test trial 1 and 2 block C (Novel object) entries and times.....	92
Figure 4.5: Y-Maze test Distance and mean speed.....	94
Figure 4.6: Y-Maze familiar and novel arms entries and times.....	96

## **Chapter 5**

Figure 5.1: Daily body weight gain.....	102
Figure 5.2: Total mean weight of Sprague Dawley rats.....	103
Figure 5.3: Total mean core temperature of Sprague Dawley rats.....	104

## **Chapter 6**

Figure 6.1: Haematoxylin and Eosin cardiac muscle 20x sections.....	110
Figure 6.2: Haematoxylin and Eosin cardiac muscle 40x sections.....	111
Figure 6.3: Haematoxylin and Eosin cardiac muscle sections for the control and treated control group.....	112
Figure 6.4: Haematoxylin and Eosin cardiac muscle sections for the experimental and treated experimental group.....	113
Figure 6.5: Periodic Acid-Schiff cardiac muscle sections.....	113
Figure 6.6: Haematoxylin and Eosin aorta 20x sections.....	114
Figure 6.7: Haematoxylin and Eosin aorta 40x sections.....	115
Figure 6.8: Tunica adventitia width.....	115
Figure 6.9: Verhoeff-Van Gieson aorta sections.....	116
Figure 6.10: Detailed ultrastructure of cardiomyocyte longitudinal sections.....	118
Figure 6.11: Detailed ultrastructure of cardiomyocyte transverse sections displaying mitochondria.....	119
Figure 6.12: Detailed ultrastructure of aortic transverse sections.....	120

## **Chapter 7**

Figure 7.1: Mean total cholesterol of the control and experimental rat groups.....	128
--	-----

## **Chapter 8**

Figure 8.1: The SEM micrographs displaying the predominant erythrocyte structure found in the control and experimental group.....	135
Figure 8.2: SEM micrographs displaying PBS control group erythrocyte morphology.....	135
Figure 8.3: SEM micrographs displaying treated control group erythrocyte morphology.....	136

<b>Figure 8.4: SEM micrographs displaying experimental group erythrocyte morphology.....</b>	<b>136</b>
<b>Figure 8.5: SEM micrographs displaying treated experimental group erythrocyte morphology.....</b>	<b>137</b>
<b>Figure 8.6: SEM thrombin exposed samples displaying the platelets of the control and experimental rat group.....</b>	<b>137</b>
<b>Figure 8.7: SEM thrombin exposed samples displaying the platelets of the control and treated control group.....</b>	<b>138</b>
<b>Figure 8.8: SEM thrombin exposed samples displaying the platelets of the experimental and treated experimental group.....</b>	<b>139</b>
<b>Figure 8.9: SEM thrombin exposed samples prepared fibrin networks of the control and experimental rat group.....</b>	<b>140</b>
<b>Figure 8.10: SEM micrographs prepared from fibrin networks of the control group.....</b>	<b>140</b>
<b>Figure 8.11: SEM samples prepared from fibrin networks of experimental groups.....</b>	<b>141</b>
<b><u>Chapter 9</u></b>	
<b>Figure 9.1: Study summary.....</b>	<b>151</b>

## List of Tables

### Chapter 3

Table 3.1: Experimental period overview.....	55
Table 3.2: Materials, sample collection and storage.....	65-66
Table 3.3: Haemoxyltin and Eosin summary.....	69-70
Table 3.4: Periodic Acid-Schiff reactive tissue and cell components.....	71
Table 3.5: Verhoeff-Van Gieson staining identification.....	72
Table 3.6: Overall scoring system.....	74
Table 3.7: Cell membrane damage scoring system.....	74
Table 3.8: Erythrocyte scoring system.....	75
Table 3.9: Platelet scoring system.....	76
Table 3.10: Fibrin network scoring.....	76

### Chapter 4

Table 4.1: Open field- Test groups statistics.....	82-83
Table 4.2: Open field test- general group comparison between all test parameters.....	83-84
Table 4.3: Open field Test- Group statistical comparisons within test parameters.....	84-86
Table 4.4: Novel object recognition test- Overall group statistical comparisons.....	88
Table 4.5: Novel object recognition- Group statistical comparisons.....	88-90
Table 4.6: Y-Maze- Overall comparison of the parameters.....	93
Table 4.7: Y-Maze- Familiar time: Habituation vs testing time comparisons.....	93
Table 4.8: Familiar arm: times - Group statistical comparisons.....	94
Table 4.9: Novel arm: times - Group statistical comparisons.....	95

### Chapter 5

Table 5.1: Core temperature- Test groups statistics.....	103
Table 5.2: Core temperature- Group temperature comparisons.....	104

### Chapter 7

Table 7.1: Total cholesterol levels- Test groups statistics.....	127
--	-----

**Table 7.2: Total cholesterol concentration- Group temperature comparisons..... 128**

**Chapter 8**

**Table 8.1: Summary of Whole blood SEM analysis..... 141-142**



## List of abbreviations, chemical formulae, SI units and symbols

<b>Abbreviations</b>	
<b>A</b>	
<b>ADP</b>	Adenosine diphosphate
<b>AF</b>	Atrial fibrillation
<b>ANF</b>	Atrial natriuretic factor
<b>ANOVA</b>	Analysis of Variant
<b>AT</b>	Antithrombin
<b>ATP</b>	Adenosine triphosphate
<b>A<math>\beta</math></b>	Amyloid- $\beta$
<b>A<math>\beta</math>42</b>	Amyloid- $\beta$ 42
<b>B</b>	
<b>BMI</b>	Body mass index
<b>bpm</b>	Beats per minute
<b>C</b>	
<b>Ca<sup>2+</sup></b>	Calcium ion
<b>CAD</b>	Coronary artery disease
<b>CAS</b>	Central Animal Service
<b>CCL5</b>	Chemokine (C-C motif) ligand 5
<b>CD40-CD40L</b>	CD40-CD40 ligand
<b>cm</b>	Centimetre
<b>CNS</b>	Central nervous system
<b>CO<sub>2</sub></b>	Carbon Dioxide
<b>CV</b>	Cardiovascular
<b>D</b>	
<b>D</b>	Dyads
<b>ddH<sub>2</sub>O</b>	Distilled water
<b>DNA</b>	Deoxyribonucleic acid
<b>E</b>	
<b><i>E. coli</i></b>	Escherichia coli
<b>EAT</b>	Epicardial adipose tissue
<b>ELISA</b>	Enzyme-linked immunosorbent assay
<b>Epi's</b>	Eppendorf tubes
<b>F</b>	

<b>Factor</b>	Factor
<b>FLAME</b>	Florida Autopsied Multi-Ethnic
<b>G</b>	
<b>g</b>	Grams
<b>Gal-Gal</b>	Digalactoside
<b>GI</b>	Gastrointestinal
<b>GIT</b>	Gastrointestinal tract
<b>GP</b>	Glycoprotein
<b>GP IIb/IIIa</b>	Glycoprotein IIb/IIIa
<b>H</b>	
<b>H and E</b>	Haemoxilin and Eosin
<b>H<sup>+</sup></b>	Hydrogen ion
<b>HMDS</b>	Hexamethyldisilane
<b>HRP</b>	Horseradish Peroxidase
<b>I</b>	
<b>ICAM-1</b>	Intercellular adhesion molecule 1
<b>iDCMI</b>	Idiopathic dilated cardiomyopathy
<b>IL-10</b>	Interleukin-10
<b>IL-18</b>	Interleukin-18
<b>IL-1<math>\beta</math></b>	Interleukin-1 $\beta$
<b>IL-2</b>	Interleukin-2
<b>IL-4</b>	Interleukin-4
<b>IL-5</b>	Interleukin-5
<b>IL-6</b>	Interleukin-6
<b>IL-8</b>	Interleukin-8
<b>IP</b>	Intraperitoneal
<b>iRhom2</b>	Rhomboid protease-2
<b>K</b>	
<b>kg</b>	Kilograms
<b>L</b>	
<b>LBP</b>	Lipid A-binding protein
<b>LDL</b>	Low density lipoprotein
<b>LM</b>	Light microscopy
<b>LPS</b>	Lipopolysaccharides

<b>M</b>	
<b>m</b>	Meters
<b>MACE</b>	Major adverse cardiovascular events
<b>MAPK</b>	Mitogen-activated protein kinase
<b>MCI</b>	Mild cognitive impairment
<b>MD2</b>	Myeloid differentiation protein
<b>mg/kg</b>	Milligrams per kilogram
<b>mg</b>	Milligram
<b>ml</b>	Millimetre
<b>MMP</b>	Matrix metalloproteinases
<b>ms</b>	Metre per second
<b>N</b>	
<b>Na+</b>	Sodium ion
<b>NBD</b>	Nucleotide-binding domain
<b>NF</b>	Nuclear factor
<b>NF-kB</b>	Necrosis factor kB
<b>NF-kB</b>	Nuclear factor kappa-light-chain-enhancer of activated B cells
<b>NK</b>	Natural killer
<b>nm</b>	Nanometres
<b>NO</b>	Nitric Oxide
<b>NOX</b>	NADPH oxidase
<b>NOX-4</b>	NADPH oxidase-4
<b>O</b>	
<b>O.D absorbance</b>	Optical density absorbance
<b>O.D</b>	Optical density
<b>O<sub>2</sub></b>	Oxygen
<b>P</b>	
<b>PAMP</b>	Pathogen associated molecular pattern
<b>PARP</b>	Poly (ADP-ribose) polymerase
<b>PAS</b>	Periodic acid-Schiff
<b>PBMC</b>	Peripheral blood mononuclear cells
<b>PBS</b>	Phosphate buffered saline
<b>PLC</b>	Phospholipase C
<b>PF4</b>	Platelet factor-4
<b>pg</b>	Picograms
<b>PGE 2</b>	Prostaglandin E 2
<b>pH</b>	Power of hydrogen

<b>R</b>	
<b>RBC</b>	Red blood cells
<b>RGS</b>	Rat grimace scale
<b>ROS</b>	Reactive oxidative species
<b>S</b>	
<b>s</b>	Seconds
<b>SC</b>	Subcutaneous
<b>SDF-1</b>	Stromal cell-derived factor-1
<b>SEM</b>	Scanning electron microscopy
<b>SR</b>	Sarcoplasmic reticulum
<b>T</b>	
<b>TBD</b>	Thioredoxin binding domain
<b>TEG</b>	Thromboelastography
<b>TEM</b>	Transmission electron microscopy
<b>TF</b>	Tissue Factor
<b>TFPI</b>	Tissue factor pathway inhibitor
<b>TGF-<math>\alpha</math></b>	Tumour growth factor-alpha
<b>TLR4</b>	Toll-like receptor 4
<b>TLRs</b>	Toll-like receptors
<b>™</b>	Trademark
<b>TMD</b>	Transmembrane domains
<b>TNF</b>	Tumour necrosis factor
<b>TNF<math>\alpha</math></b>	Tumour necrosis factor alpha
<b>tPA</b>	Tissue plasminogen activator
<b>TRAF-6</b>	TNF receptor- associated factor 6
<b>TxA</b>	Thromboxane A 2
<b>U</b>	
<b>USA</b>	United States of America
<b>V</b>	
<b>Vet</b>	Veterinarian
<b>VVG</b>	
<b>VVG</b>	Verhoeff-Van Gieson
<b>vWF</b>	von Willebrand's Factor
<b>W</b>	
<b>WB</b>	Whole blood
<b>WBCs</b>	White blood cells

<b>Symbols</b>	
<b>%</b>	Percent
<b>°C</b>	Degrees Celsius
<b>±</b>	Plus, or minus
<b>5-HT6</b>	Serotonin 5-HT6
<b>A</b>	Alpha
<b>B</b>	Beta
<b>MI</b>	Microlitres

# **Chapter 1: Introduction**

Cardiovascular (CV) diseases are the number one cause of death resulting in seventeen point nine million deaths worldwide, three quarters of which occur in low-middle income countries, like South Africa<sup>3</sup>. In addition, these CV diseases result in increased mortality, reduces quality of life and the global prevalence of these diseases continues to increase<sup>4</sup>. Although, the disease aetiology is multifactorial, research has found that the following are CV disease risk factors: blood pressure, cholesterol, obesity, glucose control, and chronic inflammation<sup>5-6</sup>. These CV risk factors are also associated with an elevation of cognitive impairment and dementia. Although the underlying explanation of this association is unclear, inflammation plays a central role in CV and neurodegenerative disease aetiology<sup>7-8</sup>.

Ordinarily, increases in inflammation in specific areas is a survival mechanism that occurs following physical injury and infection<sup>9</sup>. Inflammation is characterised by immune and non-immune cell activation that protects the host through the elimination of pathogens, followed by the promotion of tissue repair and recovery<sup>10</sup>. However, chronic systemic inflammation due to continuous bacterial or toxin exposure results in the initiation of many overlapping pathogenic pathways. Evidence shows that the chronic systemic inflammation effects the life span and the health of an individual<sup>11</sup>.

The risk of developing a CV disease increases in as individuals age. Aging is characterised by the gradual physiological function decline resulting from an increased number of senescent cells in the body<sup>12</sup>. The increase number endothelial, cardiac and muscular senescent cells have been associated with CV dysfunction such as atherosclerosis, heart failure, hypertension, and stroke<sup>12</sup>. Atherosclerosis, coronary heart disease, heart failure, ischemic heart disease are CV diseases in which inflammation induces pathogenesis<sup>13</sup>. Atherosclerosis is a chronic CV disease characterised by lipid deposits, smooth muscle cell and fibrous matrix proliferation, concluding in atherosclerotic plaque formation<sup>14</sup>. Inflammation plays an important role in the initiation and development of atherosclerotic plaque through chronic acute and innate immune system activation producing flow-mediated inflammatory endothelial cell changes<sup>15</sup>. The condition results in sustained endothelial damage, atherosclerotic plaque and atrial wall inflammation<sup>14</sup>. Atrial wall inflammation results in the narrowing of the arterial lumina, thus reducing the blood flow of that region. While plaque rupture results in thrombosis<sup>14</sup>. In cardiac muscle, inflammation induces cardiac fibrosis<sup>16</sup>. Cardiac fibrosis is defined as a process in which there is an imbalance in cardiac extracellular matrix (ECM) production and degradation, inducing cardiac dysfunction resulting in pathology<sup>16</sup>. Cardiovascular dysfunction and atherosclerosis resulting from low-grade chronic systemic inflammation may contribute to the development of dementia e.g Alzheimer's disease (AD)<sup>17</sup>.

Research has found that gram-negative bacteria secrete the endotoxin lipopolysaccharide (LPS) that results in a chronic inflammatory state if exposed to the CV system possibly resulting an elevation of CV disease pathogenesis<sup>18-19</sup>. In addition, research has shown that recurrent exposure to subclinical LPS increases mortality and induces cardiac fibrosis and atherosclerotic plaque formation<sup>20</sup>.

Previous studies have also suggested that AD may be caused by infectious agents and emerging evidence has shown that the gastrointestinal microbiome affects neurodegenerative disease development and progression<sup>11</sup>. Systemic inflammation resulting from mild bacterial toxin exposure may induce CV disease and may affect the development of neurodegeneration (dementia i.e. AD)<sup>19</sup>. Systemic inflammation found in AD patients may result from LPS exposure, and may cause CV complications<sup>21</sup>.

This study has investigated the effect of early LPS-induced systemic inflammation exposure affects the CV system, while investigating the effect of the endotoxin on the cognition of male rats. Manuka honey was investigated as a treatment for the systemic inflammatory effects of LPS on the CV system. Manuka honey was used as a possible treatment for systemic inflammatory effects of LPS because previous studies have found that Manuka honey has anti-inflammatory and oxidant properties and is an effective wound healing agent<sup>22-23</sup>. The study investigates whether or not anti-inflammatory and wound healing properties of Manuka honey may counteract the any tissue damage that results from LPS exposure. Body- temperature and weight were used as health biomarkers. Lipopolysaccharide exposure occurred over a ten-day period following LPS exposure, histological and ultrastructural analyses were conducted on the aorta, blood and heart using light-, scanning electron-, and transmission electron microscopy. Light- and transmission electron microscopy found that LPS exposure resulted in cardiac myofibril damage and mitochondrial cristae destruction. In addition, Manuka honey prevented a significant amount of myofibril damage. However, the honey did not prevent mitochondrial cristae destruction. Lipopolysaccharide aortic exposure resulted in cellular abnormalities, elastin fragmentation and collagen depletion. The group exposed to Manuka honey and LPS showed a reduction of cellular abnormalities and elastin fragmentation however, collagen depletion was documented.

Whole blood analysis using scanning electron microscopy concluded that early endotoxin exposure did not produce erythrocyte or platelet morphological changes. However, LPS exposure resulted in the abnormal formation of fused and thick aggregated fibrin networks. Manuka honey counteracted a significant amount of the harmful effects on fibrin network formation. The Manuka honey and LPS exposed group displayed fibrin networks that were standard in structure in some areas and thick and fused in structure in other areas.



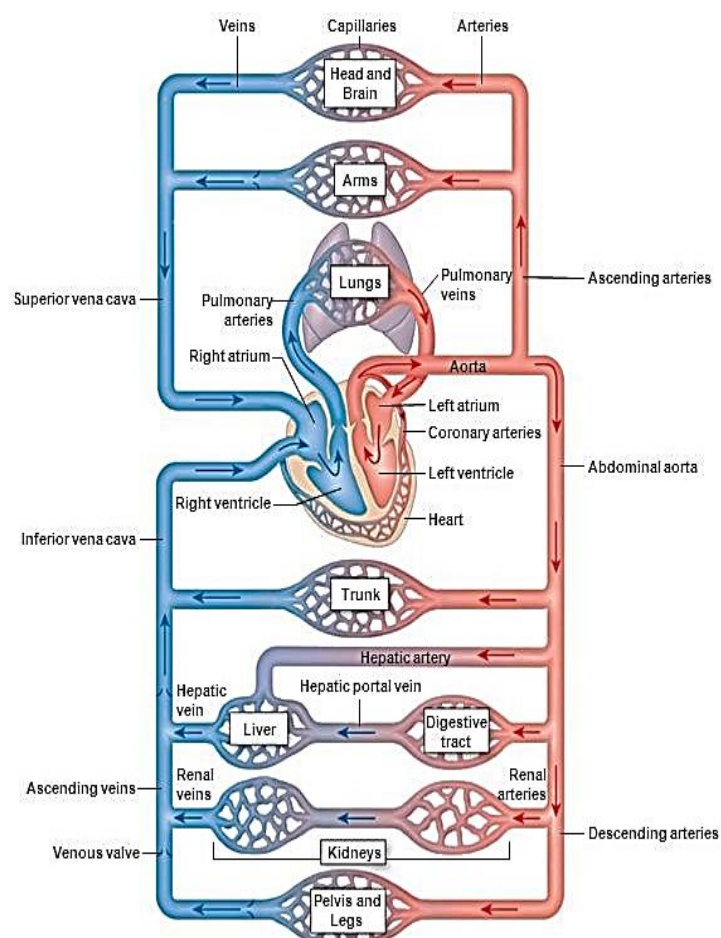
The Open field-, Novel object recognition-, and Y-Maze behavioural and cognitive tests concluded that early LPS exposure does not result in a significant behavioural or cognitive alteration. However, the Manuka honey and LPS showed impaired spatial memory when compared to the other groups.

In conclusion, early endotoxin exposure results in a change in the aorta, cardiac muscle, and fibrin network morphology. Early exposure results in an increase in cardiac, aortic cellular and elastin destruction, which may conclude in CV disease and an elevation in thrombotic events over time. In addition, Manuka honey is an insufficient treatment for the systemic inflammatory effects of LPS on the CV system.

# **Chapter 2: Literature** **Review**

## 2.1 The Cardiovascular System

The CV system consists of the heart, blood vessels, cellular elements and plasma as seen in figure 2.1. Pressure generated by the heart propels blood through a closed system of vessels, acting as a one-way circuit which ensures the continued systemic distribution of gases, nutrients, signal molecules and waste<sup>24</sup>. Pulmonary and systemic circulation follow one another in order to transport nutrients, oxygen and chemical signals to the body<sup>25</sup>. The internal organs of the body are arranged parallel to one another. As a result, nearly all systemic organs receive homogenous arterial blood<sup>26</sup>. The blood entering the organ supplies it with the required oxygen and nutrition, resulting in a direct proportionality between the supply of metabolic elements and blood supply<sup>26</sup>. The blood supply of organs are regulated by local metabolites, hormones and neurologically, creating a synergy between the organs of the body and allowing the CV system to fulfil the functional needs required by each organ<sup>24</sup>. Thus, when pathology occurs in the CV system, other organs systems are affected. Pathology of the CV system can arise through varying causes such as toxin exposure, blood pressure changes and gaseous exchange reductions<sup>24</sup>.



**Figure 2.1: Cardiovascular system.** The CV system consists of the heart, the cellular elements, the blood vessels and blood. This system functions as a transporting system for various substances such as nutrients, plays a key role in gaseous exchange, and removes waste and heat.<sup>24</sup>

### 2.1.1 The Heart

During exposure to infections, the pathogenesis caused by mild pro-inflammatory cytokine increase may result the impaired functioning of organs such as the heart. The heart is a complex interconnected muscular organ that consists of three muscle layers, the myocardium, endocardium, and epicardium<sup>18</sup>. Repetitive rhythmic contraction occurs through cellular communication between the autorhythmic and contractile myocardial cells<sup>27-28</sup>. However, environmental plasma disruptions result in myocardial disruptions concluding in CV disease. In addition, myocardial infarctions remain the leading cause of death in the CV category<sup>29</sup>. Pathological studies have identified that exposure to the chronic inflammatory response as one of the most common molecular and cellular contributing factors of heart injury<sup>29</sup>. Cytokine concentration influences the degree of cardiac injury<sup>30</sup>. Research has found that chronic inflammation can induce cardiac muscle inflammation that results from myofibroblasts inducing the following: chemokine expression resulting in the migration of immune cells to the heart, inducing endothelium adhesion molecule releasing, stimulating cardiac present monocytes to release gelatinases inducing the transmigration of immune cells through the basolateral membrane and producing nucleotide-binding oligomerization domain-like receptor with a pyrin domain 3 (NLRP3) inflammasome activity that resulting in interleukin-1  $\beta$  (IL-1 $\beta$ ) release<sup>31</sup>. The following process results from chronic inflammation and further induces a positive feedback loop of inflammation within the heart resulting in cardiac injury<sup>31</sup>.

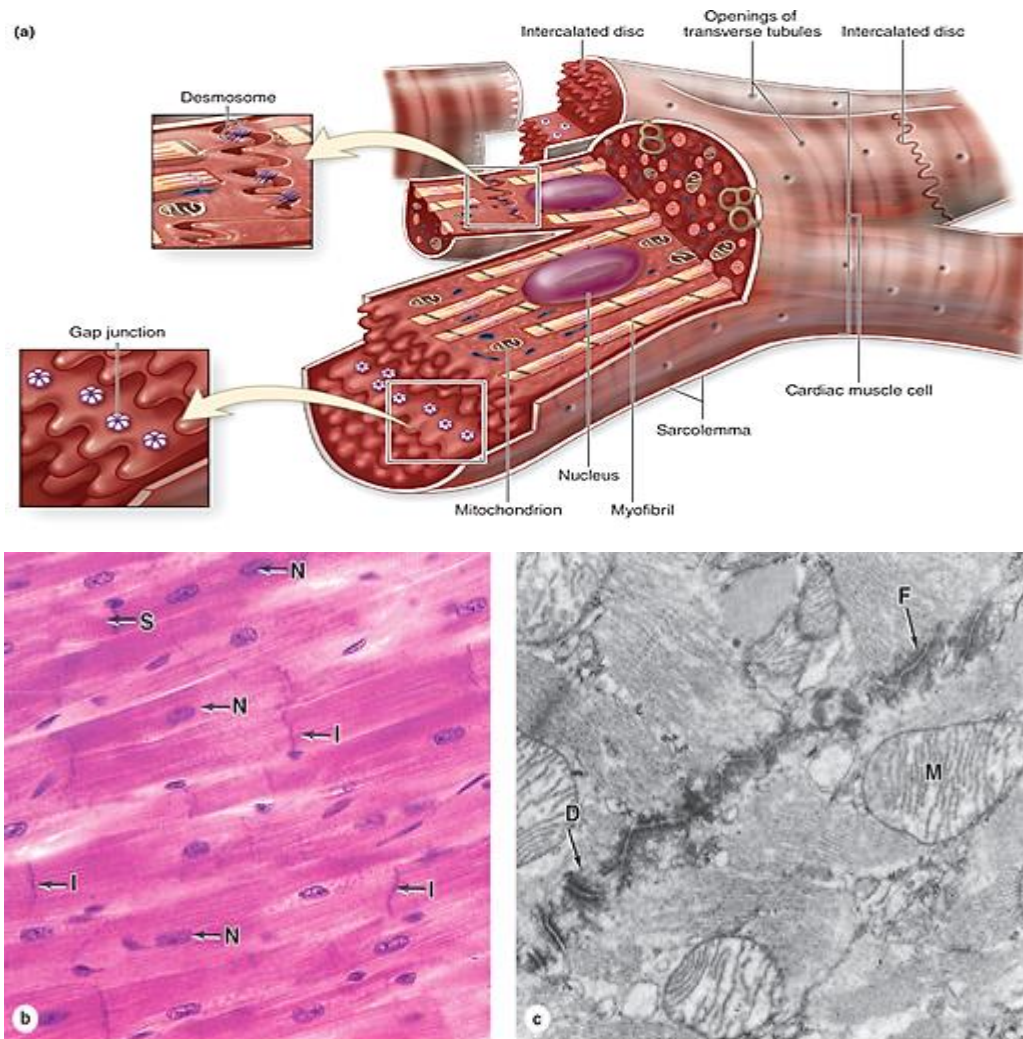
Middle aged and elderly individuals are particularly at risk since aging results in Inflamm-aging which presents as a state of chronic low-grade systemic inflammation<sup>30</sup>. As previously stated, LPS exposure induces a chronic systemic inflammatory state in patients, and thus those that are exposed may have a higher risk of CV disease development. Previous research has identified that LPS can induce myocardial infarctions which may result from further CV inflammation aggravation<sup>18</sup>. In addition, researchers have found that LPS level reductions in heart disease patients improved their outcomes, which has driven further research into the field<sup>32</sup>.

A study conducted by Lu et al. (2017) discovered that rhomboid protease-2 (iRhom2) is a positive LPS-induced inflammation regulator that is linked to cardiac injury<sup>18</sup>. In mammals, Rhomboid protease (e.g. iRhom-1 and iRhom-2) cleaves tumour growth factor-alpha (TGF- $\alpha$ )<sup>33</sup>. Rhomboid protease-1 and Rhomboid protease-2 are inactive rhomboid intramembrane serine protease homologs, with catalytic residues, and are vital to TNF $\alpha$  converting enzyme (TACE) maturation and trafficking<sup>34-35</sup>. Rhomboid protease-2 regulates TACE thus controlling TNF- $\alpha$  secretion. Tumour necrosis factor-alpha induces inflammation thus alerting the body to an infection as well as aiding infection clearance, however it can induce inflammatory arthritis<sup>36</sup>.

Researchers have found that TACE and iRhom-2 can undergo quick cytokine, growth factor and pro-inflammatory mediator activation concluding in TNF- $\alpha$  activation, resulting in an inflammatory response leading to cardiac tissue injury. Cardiac histopathological changes are induced after LPS administration causing LPS-induced cardiac inflammation. These changes are accompanied with Toll-like receptor 4 (TLR-4)/ nuclear factor-kappa B (NF- $\kappa$ B), dependent cardiomyocyte and serum TNF- $\alpha$ , IL-1 $\beta$ , interleukin-6 (IL-6) and interleukin-18 (IL-18) elevation<sup>18</sup>.

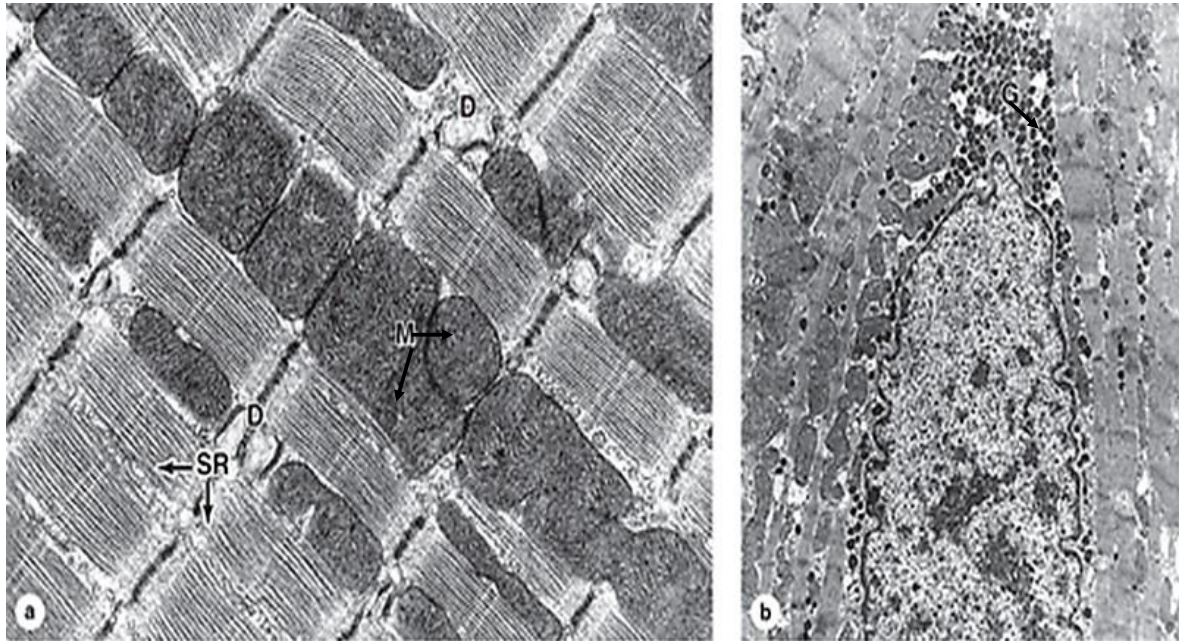
### Cardiomyocytes

In addition, LPS have a direct effect on the cardiomyocytes which work together to propel blood throughout the body due to their complex structure seen in figure 2.2. The endomysium surrounds the cardiomyocytes, containing a rich capillary network<sup>37-38</sup>. The perimysium separates layers and cardiomyocyte bundles that form larger fibrous connective tissue layer masses comprising of the “cardiac skeleton”. These cells are branched in structure and tightly interconnected by intercalated disks of neighbouring cells<sup>38</sup>. Transverse lines crossing the fibres at irregular intervals joins the cardiomyocytes in a manner that is only seen in cardiac muscle<sup>38</sup>. The intercalated discs represent the interfaces between adjacent cells and other junctional complexes as seen in figure 2.3 (a and b).



**Figure 2.2: Heart cell histology-** The cardiomyocytes work as a contractile unit which propel blood forward during contractions. (a) Illustrates the cardiac muscle and its characteristic features. Cardiac fibers consist of separate cells that are connected by intercalated discs. Transverse regions are desmosome abundant and other adherent junctions for firm adhesion. While longitudinal regions of the intercalated discs are filled with gap junctions. The image also shows that the cardiomyocytes have central nuclei. The cardiomyocytes branched structure allows the cells to interweave in a complicated arrangement with the fascicles, producing an efficient contraction mechanism for atrial ventricular emptying. (b) Light microscopy of a longitudinal section of cardiomyocytes present with nuclei (N) in the center of the muscle fibers and intercalated discs (I) widely spaced across the fibers. Striations (S) and fibroblast nuclei are also present (x 200); Hematoxylin and Eosin (H and E) staining). (c) Transmission electron microscopy (TEM) (x31 000) shows intercalated discs with a step-like structure and the interdigitated processes of adjacent cells. The transverse disk regions have many desmosomes (D) and fascia adherents (F) which firmly join the cardiomyocytes. The abundant gap junctions join the cells physiologically. The cell's sarcoplasm has numerous mitochondria (M) and the myofibrillar structures are less organized than in skeletal muscle.<sup>38</sup>

The function and structure of cardiomyocyte contractile apparatus are similar to those in skeletal muscles as seen in figure 2.3. Forty percent of the cell is occupied by the mitochondria, which is higher than in slow oxidative skeletal muscle fibres, this fulfils the high energy requirements<sup>38</sup>. Fatty acids stored as triglycerides are the heart's primary source of energy<sup>25,38</sup>. Glycogen granules and perinuclear lipofuscin pigment granules may also be present<sup>25,38</sup>.



**Figure 2.3: The Cardiac Muscle's Ultrastructure-** (a) Illustrates Transmission electron microscopy (TEM) (x 30 000) which shows that the cardiac muscle contains an abundant source of mitochondria (M) and few sarcoplasmic reticula (SR) between the myofibrils. The T-tubules are less organised and are generally associated with one extended terminal SR cistern, forming dyads (D) rather than the triads seen in skeletal muscle. (b) Displays cardiomyocytes (x 10 000) from the atrium display the presence of membrane-bound granules (G), primarily arrange at the nuclear pole. The granules are predominantly dominant in cardiomyocytes of the right atrium (approximately, 600 per cell). Smaller amounts are found in the left atrium and ventricles. These granules contain an atrial natriuretic factor (ANF) precursor. Atrial natriuretic factor targets kidney cells resulting in the loss of sodium and water, opposing aldosterone and antidiuretic hormone which result in sodium and water conservation in the kidneys.<sup>38</sup>

Researchers have found that LPS exposure can cause myocardial hypertrophy and autophagy, resulting in depolarisation disruptions<sup>39</sup>. Myocyte hypertrophy is an adaptive cardiac response characterised by cardiomyocyte enlargement and sarcomeric protein accumulation<sup>40-41</sup>. The process results in irreversible myocardial enlargement and expansion which is often followed by heart failure<sup>39</sup>. Previous studies have found that cardiac disruption results from cardiomyocyte inflammation, necrosis or apoptosis<sup>18,42</sup>. Lipopolysaccharides may bind to TLR-4 concluding in cytoplasmic accumulation, nuclear  $\beta$ -catenin translocation, myocardial hypertrophy gene transcription and expression<sup>43</sup>.

Lipopolysaccharides also induce cardiomyocyte autophagy<sup>20</sup>. Autophagy is a cellular degradation system which results in the damaged or redundant organelle, protein and/or cell component removal<sup>44</sup>. The process consists of three categories: Chaperone-mediated autophagy, macro-autophagy and microautophagy<sup>45</sup>. The process begins with membrane or phagophore cytoplasmic isolation forming the autophagosome followed by autophagosome-lysosomal fusion resulting in the autolysosome<sup>46</sup>. The contents are then dissolved. Previous studies have shown that autophagy is associated with numerous physiological and

pathological processes (e.g., aging, cell development, cell survival, cell death, immunity, and metabolism). Thus, playing a critical role in human pathogenic processes such as cancer, CV disease, metabolic disorders and muscle atrophy as a consequence of abnormal amounts of autophagy<sup>47-48</sup>. Excessive autophagy can result in pathological disease and autophagic cell death. Research has also shown that LPS-induced autophagy participates in numerous biological processes (e.g., liver autophagy, osteoclastogenesis, vascular endothelial cell autophagy), causing widespread pathogenesis<sup>39,49-50</sup>. In cardiomyocytes, LPS-Induced pathogenic autophagy and hypertrophy results in decreased cardiomyocyte viability<sup>39</sup>.

### 2.1.2 Blood vessels

The cardiomyocytes work together to pump oxygenated blood into the aorta. Bacteria may enter the CV system through the gastrointestinal tract (GIT) and travel through the circulatory system potentially influencing inflammatory and cytokine signalling<sup>51-52</sup>. Hypercoagulability may lead to CV complications such as a myocardial infarctions in patients<sup>53</sup>. There is growing evidence that high doses of LPS results in hypotension resulting from an LPS induced mean arterial blood pressure decrease<sup>53</sup>. However, research has shown that low dose LPS exposure induces cardiac tissue damage including myocardial dysfunction<sup>54-55</sup>. Low-grade chronic inflammation contributes to the development of atherosclerosis. Furthermore, inflammation induced by LPS exposure may contribute to CV stress experienced by the elderly or those suffering from pre-existing CV disease, which may contribute to dementia development<sup>567-8</sup>. Cerebral perfusion pressure results from sufficient cardiac output resulting in arterial pressure generated by the arterial walls followed by the microvascular resistance found in the brain, and venous drainage<sup>56</sup>. A study conducted by Roher et al. (2012) observed that AD patients experienced 20% lower cerebral blood flow than the control group, suggesting a connection between AD dementia and brain hypoperfusion. In addition, the study found a lower pulse pressure in AD patients, further illustrating lowered cerebral blood flow may result in decreased cognitive ability<sup>56</sup>. Cardiac damage may result in a decrease in cardiac output thus potentially resulting in brain hypoperfusion<sup>56</sup>. Cardiovascular disease prevalence and incidence differ in men and women, possibly resulting in varying risk levels and presentation. Cardiovascular pathology occurs as consequence of cellular dysfunction. Haemostatic deregulation may occur in the following areas: arterial, cardiac, venous and in the cellular components (platelets, erythrocytes, WBCs) of the CV due to endotoxins, pro-inflammatory cytokines, foreign particles, and ECM proteins exposure<sup>18,57-58</sup>.



### 2.1.3 Blood cells and plasma

Lipopolysaccharide induced cellular changes affect other organ systems and pathology is not restricted to the cardiac muscle and the CV vasculature. Cellular component changes have a detrimental effect on haemostasis and organism homeostasis. The blood consists of plasma, erythrocytes, white blood cells (WBCs) and the platelets, which play a crucial role in inflammation and the haemostatic cascade.

#### Haemostasis

Haemostasis is the process that results in blood clot formation upon blood vessel injury preventing further blood loss<sup>59</sup>. It consists of primary haemostasis and secondary haemostasis<sup>59</sup>. The following will describe normal haemostasis:

- Primary haemostasis

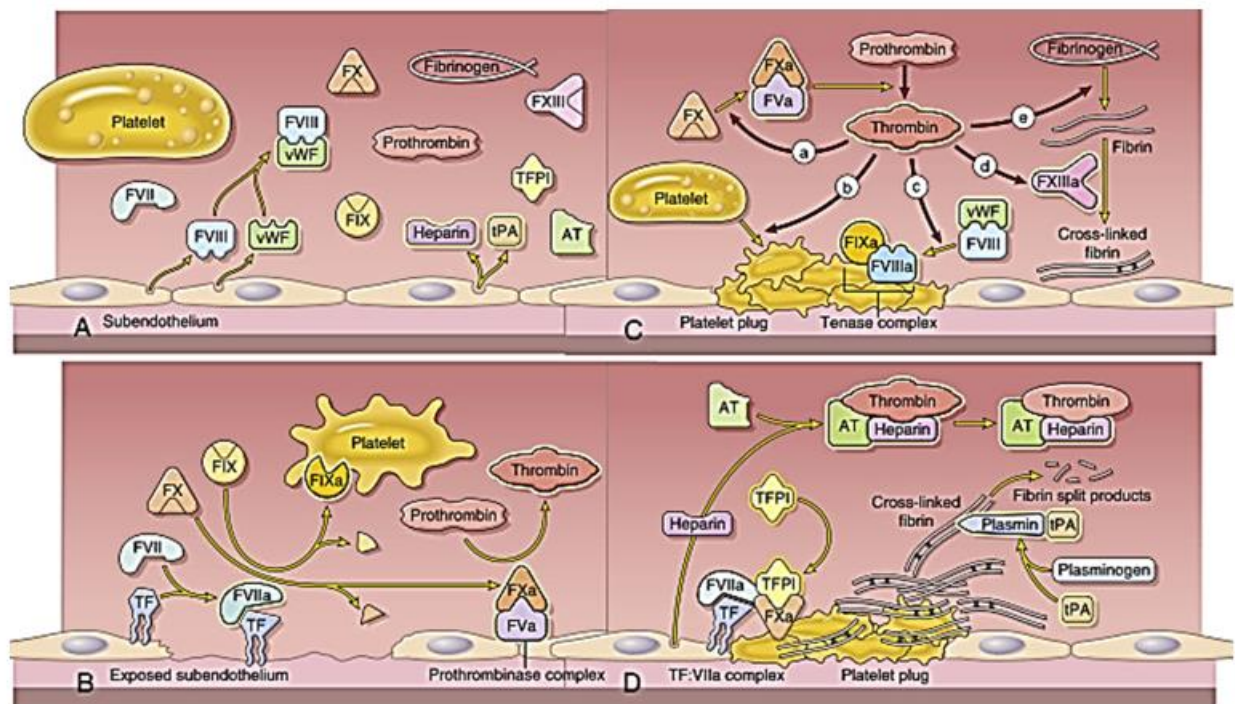
Primary haemostasis is defined as the process that occurs after the initial vascular endothelial injury, resulting in platelet deposition at the injury site<sup>59</sup>. Upon vascular injury, local vasoconstriction occurs as the endothelial matrix is exposed resulting in platelet adhesion to collagen or von Willebrand factor (vWF) on multiple receptors on the endothelial surface<sup>59</sup>.

During the process platelet activation occurs causing platelet aggregation and in subsequent the binding of multiple ligands such as collagen, fibrinogen, fibronectin, vitronectin and vWF. The activated platelet degranulate releasing agonists (adenosine diphosphate (ADP), serotonin, thromboxane A<sub>2</sub> (TxA) and vasopressin) that activate G protein coupled receptors to trigger additional aggregation causing the formation of a platelet plug at the injury site<sup>59</sup>. The activated integrins on surface of the platelets and the agonists both bind to and activate phospholipase C (PLC). Phospholipase C activation results in calcium release catalysing the degranulation and platelet shape change increasing platelet adhesiveness<sup>59</sup>.

Following platelet activation, glycoprotein IIb/IIIa (GPIIb/IIIa) undergoes a conformational change and the glycoprotein has an increased affinity for fibrinogen, promoting platelet aggregation resulting in platelet plug stabilisation<sup>59</sup>. In addition, the cytosolic portion of the GPIIb/IIIa binds to the platelet cytoskeleton mediating platelet spreading and clot retraction<sup>59</sup>.

- Secondary haemostasis:
  - The clotting cascade and clot propagation

Following primary haemostasis secondary haemostasis starts with proteases facilitating zymogen cleaving producing active enzymes that transform into thrombin activating and clot forming complexes<sup>59</sup>. After the formation of the platelet plug, the coagulation cascade proceeds through the following mechanisms, in which tissue factor (TF) causes clotting factor activation, resulting in the amplification of clotting factors and the facilitation of clot formation by thrombin as seen in figure 2.4<sup>59</sup>.



**Figure 2.4: The cellular coagulation model:** The coagulation process forms part of the haemostatic process however before an abrasion the endothelium is intact (as depicted in figure 2.4 (A)) and inactive procoagulants (factors VII, VIII, IX, X, XIII, prothrombin, and fibrinogen) and platelet circulate. The following anticoagulants: heparin, tissue factor pathway inhibitor (TFPI), tissue plasminogen activator (tPA) prevent spontaneous clot formation. (B) When vascular injury occurs the initial stage of haemostasis begins. The subendothelial TF is exposed and the circulating factor VII forms the TF:Factor VII complex. The TF: Factor VII activates factor IX and factor X. The activated factor IX binds to the platelets. The activated factor X activates factor V resulting in the formation of the prothrombinase complex converting prothrombin into thrombin. (C) Thrombin (a) activates factor X and factor V resulting in the formation of the prothrombinase complexes generating a secondary thrombin burst (b) activating platelets and separating factor VIII from vWF activating factor VIII (d) converting fibrinogen to fibrin, (e) activating XI which (f) activates factor XIII a cross-linked fibrin stabilizer. Following those steps, a stable clot is formed. (D) Following clot formation, antithrombin (AT) binds to heparin inhibiting thrombin activity. Tissue factor pathway inhibitor binds to an activated factor X resulting in the inhibition of the TF: Factor VII complex. Following that, plasminogen activation through tPA activation results in plasmin formation which binds to fibrin clot resulting in fibrin cleaving. Fibrin is cleaved into soluble products such as the D-dimer and other fibrin degradation products, which inhibit thrombin activity while the unbound plasmin is inhibited by  $\alpha$  2-antiplasmin.<sup>59</sup>

## Plasma

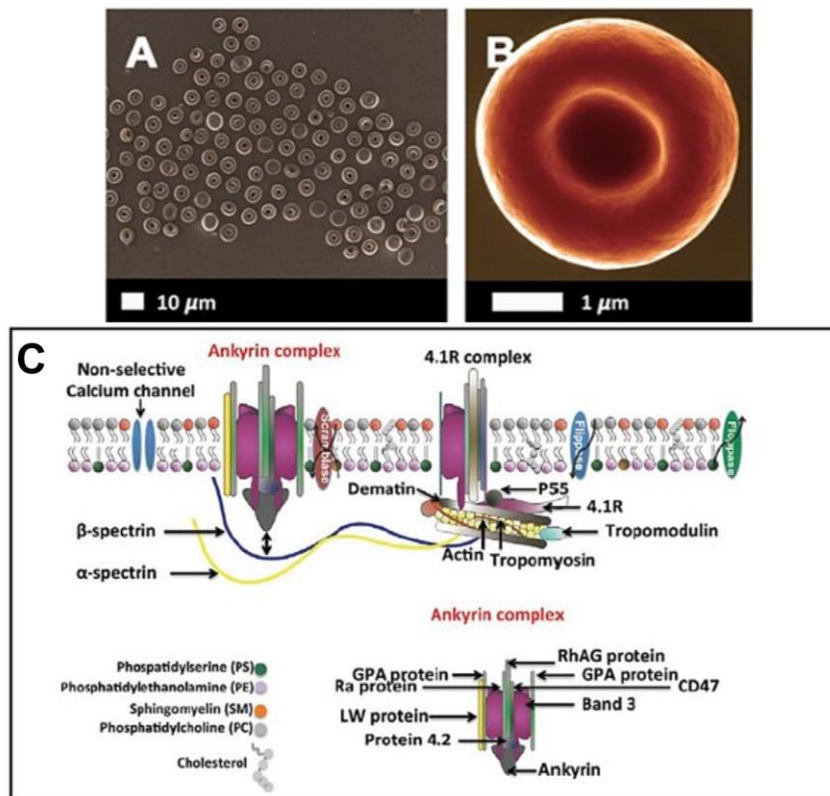
Blood plasma is the medium in which haemostasis occurs and where most haemostatic cellular agents reside. It consists of 92% water and suspends cellular elements, nutrients, organic matter, gases and proteins. The blood plasma proteins are: Albumins, Globulins, Transferrin

and Fibrinogen<sup>60</sup>. Fibrinogen plays an important role in the coagulation system, because once cleaved into fibrin monomers, it is an essential component of red and white thrombi and contributes to blood viscosity<sup>61</sup>. This process is initiated by the conversion of fibrinogen into fibrin monomers as a result of a thrombin reaction, resulting in the release of fibrinopeptide A and B from the A $\alpha$  and B $\beta$  amino terminal chains creating new amino termini. Thus, forming knobs that allow other fibrin monomers to fit into the holes eventuating in a fibrin gel. Following that, Factor XIII catalyses the formation of interchain covalent cross-links between the fibrin monomers thus strengthening the clot<sup>62</sup>.

During the early stages of polymerisation, the fibrin monomer molecules are bound together by a weak noncovalent hydrogen bond<sup>26</sup>. The freshly formed fibres are not cross-linked to one another, concluding in weak clots which easily break apart. Fibrin-stabilising factor strengthens the fibrin reticulum a few minutes after initial clot formation takes place<sup>63</sup>. One of the ways in which the process may change is when there is a thrombin production reduction. The absence of adequate thrombin levels would result in fibrin-stabilising factor remaining deactivated causing frail clot formation, because of fibrin cross-link absence<sup>63</sup>. Blood clot strength insufficiency prevents competent haemostasis, thus ending in blood loss. A blood clot entraps blood cells, platelets and plasma. When there are adequate thrombin levels, fibrin fibres aid in maintaining haemostasis, preventing blood loss, thus allowing for the uninterrupted gaseous exchange<sup>26,63</sup>.

### Erythrocytes

Erythrocytes transport oxygen (O<sub>2</sub>) and carbon dioxide (CO<sub>2</sub>) and they contribute to rheology. Their flexible biconcave disk structure allows them to complete this function, is seen in figure 2.5 (A and B). Erythrocytes' flexibility allows them to enter small capillaries. While navigating through the CV system, erythrocytes' biconcave shape increases their surface-to-volume ratio, allowing for an increase in the O<sub>2</sub> transport efficiency. Researchers have found that significant changes to this structure limits O<sub>2</sub> transport<sup>64</sup>.



**Figure 2.5: Erythrocyte structure-** Erythrocytes carry O<sub>2</sub> to and CO<sub>2</sub> from the organs of the body. Figure A illustrates a low magnification healthy whole blood (WB) smear which was prepared for Scanning electron microscopy (SEM). Figure B represents a single healthy erythrocyte. Figure C Shows the Schematic model of the erythrocyte membrane, most of the proteins are shown but their position relative to each other is unknown. Figure A and B: <sup>65</sup>, Figure C: <sup>66</sup>

A mature and healthy erythrocyte contains a complex plasma membrane consisting of a specialised lipid bilayer that interacts (through protein interactions) with the integral membrane proteins as illustrated in figure 2.5 (C). The double-layered erythrocyte surface consists of cholesterol, glycolipids and phospholipids. Cholesterol is equally spread through the two leaflets while the four main phospholipids are arranged asymmetrically. They consist of the amino phospholipids: phosphatidylserine and phosphoinositides, and are located in the inner membrane leaflet, enabling them to play a major role in the structural integrity of the cell membrane. Choline containing phospholipids are: phosphatidylcholine and sphingomyelin, located in the outer leaflet<sup>66</sup>. The cytosol is enriched with haemoglobin and several molecules e.g. calcium (Ca<sup>2+</sup>)<sup>64,66</sup>.

Enzymatic reactions such as membrane transport and signal transduction pathways are facilitated by the phospholipid bilayer, maintaining lipid homeostasis. The phospholipid bilayer contains hydrophilic heads and non-polar hydrophobic hydrocarbon tails. Moreover, there are various lipid and protein species that aggregate in the membrane domains; these molecules are called rafts. Rafts form specialised areas that act together and aid in many physiological

processes such as signal transduction. The membrane cholesterol molecules are unesterified structures that lie between both lipid bilayer layers. Lipid rafts are enriched with cholesterol, sphingolipids and also comprise of flotillins and stomatin<sup>66</sup>.

Three integral protein types (flippase, floppase and scramblase) facilitate transmembrane passage and lipid structural arrangement in the erythrocyte membrane. Flippase (aminophospholipidtranslocase) facilitates amino-containing phospholipid pumping from the outer to the inner leaflet<sup>66</sup>. Floppase controls the choline-containing phospholipid reverse transfer of cholesterol (against its concentration gradient) phosphatidylserine, and the superlattice from the inner leaflet to the outer leaflet<sup>66</sup>. Scramblase is a phospholipid non-specific bidirectional transport initiator, aiding in the particle transport (against their concentration gradients) in an energy independent manner<sup>66-67,23</sup>. Magnesium adenosine triphosphate (ATP) dependent flippase transfers phosphatidylethanolamine and phosphatidylserine from the outer monolayer to the inner monolayer at the expense of ATP, maintaining the correct phospholipid layer distribution<sup>66</sup>.

During eryptosis, intracellular  $\text{Ca}^{2+}$  followed by flippase inhibition and phospholipid scrambling activity activation, initiates phospholipid asymmetry loss and phosphatidylserine exposure<sup>68</sup>. The energy-independent flippase proteins allow these common phospholipids to swiftly equilibrate between the monolayers. Flippase also plays a role in the biosynthesis of many glycoconjugates<sup>69</sup>. Scramblase facilitates the bidirectional lipid flip-flop that occurs in a non-selective fashion from the inner and outer leaflet. This occurs down the concentration gradient<sup>70</sup>. The scramblase becomes a lipid channel in the presence of  $\text{Ca}^{2+}$ , which allows lipid diffusion from one monolayer to another using a concentration gradient<sup>66</sup>.

The structural proteins (e.g Band 3) regulate erythrocyte structure and function. These proteins facilitate anion erythrocyte membrane transport. The erythrocyte membrane is an important cytoskeletal and protein binding site. Band 3 is a trans-membrane protein or multi-spanning ion transport channel. The tetramers tie the lipid bilayer to the skeleton through a cytoplasmic domain and ankyrin interaction, which is linked with spectrin<sup>66</sup>.

All of these components maintain the structural integrity as well as erythrocyte homeostasis resulting in the survival of the cell in the CV system<sup>66</sup>. In addition, the erythrocytes play an important role in haemostasis. Under normal physiological conditions erythrocytes affect platelets during haemostasis and thrombosis in the following ways: they effect platelet margination, clot permeability, and platelet reactivity<sup>71</sup>. Erythrocytes move through the blood vessel centre causing the margination of platelets facilitating effective adhesion when blood vessel injury occurs<sup>72</sup>. The peripheral layer formed by the axial accumulation of erythrocytes contains plasma containing clotting factors and neutrophils<sup>71</sup>. In addition, decreased

erythrocyte deformability reduces blood clot and thrombi permeability which may affect the entry of fibrinolytic agents thus effecting fibrinolysis<sup>71</sup>. Erythrocytes modulate platelet reactivity through chemical signalling or erythrocyte-platelet interactions thus affecting haemostasis through the promotion of aggregation and ATP activated degranulation<sup>71</sup>. Erythrocyte damage produces free haemoglobin that induces platelet aggregation in the absence of blood vessel injury, contributing to the risk of thrombotic complications. Thus, changes to erythrocyte structure resulting in early eryptosis may result in an elevation in platelet activation, thus promoting clot production in the absence of injury<sup>71</sup>.

In the absence of pathological conditions such as haemolysis and anaemia, erythrocytes maintain their shape and function under strenuous conditions<sup>73</sup>. However, pathological processes such as inflammation may result in morphological changes and dysfunction<sup>73</sup>. It has been found that physiological aging induces an erythrocyte membrane, metabolic pathway and haemoglobin change concluding in signal manifestations that trigger immune system recognition and removal<sup>74-76</sup>. In addition, Inflammatory lipases produced during the inflammatory process result in premature erythrocyte aging<sup>73</sup>. It has been documented, that LPS does not directly cause eryptosis (Eryptosis refers to a erythrocyte suicidal death, characterised by erythrocyte blebbing, phospholipid scrambling of the erythrocyte membrane and shrinkage) in cells and have no significant effects on erythrocyte and plasma parameters<sup>66,77</sup>. However, previous studies have shown that erythrocytes in AD patients displayed a highly irregular shape, especially under simultaneously elevated serum ferritin level conditions<sup>21,78</sup>. These toxins cause a small, but significant increase in haemolysis possibly indicating a reduction in the erythrocyte membrane integrity and may indirectly cause eryptosis<sup>79</sup>. Phosphatidylserine resides on the intracellular plasma membrane leaflet in healthy erythrocytes, however during early eryptosis, the cell membrane becomes symmetrical. During inflammation, a similar process is seen where the erythrocyte membrane leaflet phospholipids become increasingly symmetrical as the phosphatidylserine, in the membrane, become externalised. Thus, resulting in membranal erythrocyte vesicle formation, subsequent to microparticle shedding causing erythrocyte pathological shape alterations<sup>78,80</sup>. This may be due to LPS induced systemic inflammation.

Other studies have shown that LPS causes a small total and indirect bilirubin lactate dehydrogenase, and haptoglobin plasma level increase<sup>81</sup>. Bilirubin is a heme catabolite that is mainly derived from erythrocyte damage. Total bilirubin circulatory levels are mainly determined by disintegrated erythrocyte clearance<sup>81</sup>. This slight elevation is an indication of increased erythrocyte degradation. Lactate dehydrogenase is a cytosolic glycolytic enzyme that catalyses lactate to pyruvate reversible oxidation. Serum lactate dehydrogenase levels are elevated in hepatitis. The slight lactate dehydrogenase elevation suggests minor liver

stress. Haptoglobin is a human plasma protein that captures haemoglobin during haemolysis<sup>82</sup>. The haemoglobin-haptoglobin complex formation decreases oxidative properties of heme-haemoglobin and promotes the complexes macrophage scavenger receptor CD-163 recognition<sup>82</sup>. The slight haptoglobin elevation may be as a response to the haemolysis. In addition, it has also been shown that LPS causes a small, but significant increase in transferrin plasma levels. Thus, indicating that LPS causes a small increase in haemolysis and iron parameters plasma levels<sup>79</sup>. It is yet to be established that LPS causes the same effect *in vivo*. However, inflamm-aging found in the elderly coupled with the presence of LPS may increase the presence of premature aging.

## Cardiovascular system's link to immunity

### Platelets

When endothelial injury occurs platelets playing a crucial role in haemostasis by adhering to the vascular endothelium, aggregating to form a platelet plug and facilitating the formation of the fibrin crosslinks to stabilize the clot<sup>83</sup>. However, when exposed to inflammation and infection through direct platelet-bacteria interactions (bacterial surface proteins binding to platelet receptors) or indirectly resulting in platelet activation without endothelial matrix exposure occurs<sup>84</sup>.

The consequences of inflammation result in the following CV system pathological alterations: the condition predisposes an individual to endothelial dysfunction and increased arterial rigidity thus elevating the risk of atherosclerosis development<sup>85</sup>. Both WBCs and platelets take part in these cellular and humoral responses<sup>86</sup>. Following platelet-bacteria or platelet-bacteria metabolite interactions, platelets act as cellular scavengers, as they aid in bacteria deposition collection and phagocyte recruitment, which results in the elevation of inflammatory responses<sup>86</sup>.

A study conducted by Jaw et al. (2016) suggested an association between the systemic LPS circulation and an atherosclerotic burden<sup>87</sup>. Lipopolysaccharides result in systemic inflammation that may aggravate the existing atherosclerotic burden in middle aged and elderly individuals. Platelets play a significant and well-established role in atherosclerosis aetiology which presents as a systemic inflammatory immune response to oxidized low-density lipoprotein (LDL) and/or other unknown antigens which conclude in atheromatous plaque accumulation<sup>88</sup>. Inflammation is pathophysiological driving force in the development and progression of atherosclerosis<sup>88</sup>. Although platelet vascular endothelial adhesion occurs, this does not occur under normal physiological circumstances. A pro-inflammatory phenotype or

endothelial layer disruption results in platelet vascular wall adhesion<sup>88</sup>. Consequently, platelet activation leads to cytokine release induction which resulting in leukocyte mediation and recruitment to vascular endothelium, which can be observed in atherogenesis and late stage atherosclerosis<sup>88</sup>.

Inflammation results in atherosclerosis initiation and disease progression, plaque rupture and thrombosis<sup>89</sup>. Inflamed endothelial cells via the vWF, and/or the intercellular adhesion molecule 1 (ICAM-1) and vitronectin receptors interact with activated platelets under high shear stress conditions resulting in platelet vascular wall adhesion<sup>88</sup>. Adhesion results in platelet pro-inflammatory chemokine release, followed by leukocyte attraction to the vascular wall<sup>90</sup>. Platelet released inflammatory mediators result in vascular inflammation promotion at the lesion site. Chemokine (C-C motif) ligand 5 (CCL5) (also known as RANTES) and the CD40-CD40 ligand (CD40-CD40L) dyad promote platelet and inflammatory cell recruitment, generating atherosclerosis disease progression<sup>90-92</sup>. Moreover, platelet released stromal cell-derived factor-1 (SDF-1) or platelet factor-4 (PF4) support macrophage oxidised LDL uptake, promoting foam cell formation, contributing to the lipid core development of atherosclerotic plaques<sup>93</sup>. Platelets also play a pivotal role in plaque rupture and local thrombus formation. Atherosclerotic lesion rupture exposes ECM proteins, triggering platelet recruitment to the vascular wall resulting in thrombosis. In addition, activated platelets further secrete matrix metalloproteinases (MMP), (MMP-2 or MMP-9) advancing ECM degradation and local factor activation furthering plaque rupture and thrombus development<sup>94</sup>. The ruptured atherosclerotic plaque microenvironment is highly thrombotic and the activated platelets facilitate the thrombosis cascade, resulting in local thrombi formation which obstructs the blood vessels concluding in a possible myocardial infarction or stroke<sup>88</sup>. As previously described inflammation results in the changed morphological and functioning of erythrocytes and platelets resulting in pathogenesis. Both the erythrocytes and platelets play a crucial role in haemostasis. Lipopolysaccharides may affect haemostasis by promoting haemolysis and platelet activation through the induction of inflammation<sup>73,86,88</sup>.

## **2.2 The link of neurodegeneration and cardiovascular complications**

Studies have found that men have a higher atrial fibrillation (AF), coronary artery disease (CAD) and heart failure prevalence and an increased AF, myocardial infarction and heart



failure incidence<sup>95-98</sup>. Those afflicted by AF, CAD, heart failure and myocardial infarction have an increased dementia incidence.

Atrial fibrillation is the most common continuous arrhythmia and is increasing in prevalence globally<sup>99</sup>. The disease is associated with elevated mortality risk although research proposes that longevity increases following diagnosis, which is accredited to medical therapies reducing stroke, heart failure and the management of other comorbidities<sup>100-101</sup>. Increased longevity and the detrimental effects of arrhythmia result in long-term heart dysfunction and arrhythmia<sup>102</sup>. Patients are at higher risk of stroke and stroke patients have an elevated dementia risk. In addition, those suffering from AF have an elevated subclinical or silent stroke occurrence concluding in an elevated prevalence of all dementia isoforms including AD<sup>102</sup>. Atrial fibrillation in the absence of a stroke has been related to gradual cognitive dysfunction. A number of AF patients report mental fogging, mental deceleration or dysfunction during transitions from sinus rhythms due to AF<sup>102</sup>. The proposed mechanism to explain sudden mental decline in an individual with AF is that the disease unveils cerebral microvascular dysfunction<sup>102</sup>. An autopsy study conducted by Bangen et al. (2015) discovered that cerebral atherosclerosis is common in AD patients<sup>103</sup>. The most common impacted area was the circle of Willis which alters blood flow or regulates hypotension in all brain areas. As overall vascular risk factors increase, so do the dementia risk and the relative negative impact of AF<sup>104</sup>. Repetitive microvascular injury due to atrioventricular synchronicity loss brings about reduced blood flow which aids in ischaemic injury manifestation, which may cause leukoariosis ((leuko- white, ariosis-rarefaction) which refers to ischaemic abnormalities observed within the white matter of the brain), which may accelerate AD development<sup>105</sup>.

Coronary artery disease is an AD risk factor that is caused by atherosclerosis through epicardial adipose tissue (EAT) that infiltrates both the myocardium and major coronary artery branches<sup>106</sup>. Epicardial adipose tissue plays a pivotal role in CAD development and is a form of low-grade inflammation resulting in substantial CV damage<sup>106-108</sup>. Research conducted by Vianello et al. found that EAT in CAD presents with the following: elevated M1 macrophages and TLR-4 upregulation, however the aetiology is not completely understood<sup>109</sup>. Nevertheless, research has found that TNF receptor-associated factor 6 (TRAF-6) plays a fundamental function in TLRs in mitogen-activated protein kinase (MAPK) and NF- $\kappa$ B pathway signalling and activation. Tumour necrosis factor receptor-associated factor 6 plays a central role in CV inflammation<sup>110-111</sup>. Therefore, strict TRAF-6 regulation is required for the appropriate immune response for homeostasis to be achieved, otherwise dysregulation occurs and various diseases may manifest<sup>106</sup>.

Atrial fibrillation and CAD are examples of the consequences of cardiac dysregulation. These diseases cause the heart to function sub optimally and may lead to heart failure if ill-managed. There is a link between cognitive impairment and heart failure through angiopathy, inflammation and perfusion defects, regardless of if a patient presents with AD<sup>112</sup>. Evidence indicates that dementing processes and heart failure share risk factors. In addition, clinical studies associate CV diseases and dementia through analogous genetic and biochemical profiles and common triggers<sup>113</sup>. Many recent studies suggest that AD and heart failure share a common pathogenesis which include in myocardial protein aggregates presenting as idiopathic dilated cardiomyopathy (iDCM)<sup>112</sup>. Idiopathic dilated cardiomyopathy is a chronic cardiomyocyte disease that presents with the dilatation and systolic left or complete ventricular impairment which cannot be placed in one condition or it involves coronary heart disease that causes myocardial dilation and malfunction<sup>114</sup>. Studies have found myocardial protein aggregates deposit in iDCM patients, that are biochemically similar to those found in AD patients<sup>115-116</sup>. Nongenetic iDCM forms result from several aetiologies that include myocardial inflammation due to infection, drug, toxins or allergens exposure and systemic autoimmune or endocrine diseases<sup>117</sup>. This condition often concludes in heart failure<sup>117</sup>.

Inflammation often results in disease; however, the initial inflammatory trigger is poorly understood and consequences of inflammation are endless. Inflammation, oxidative stress, and endothelial dysfunction elevate the AD risk<sup>102</sup>. Mounting evidence has shown that LPS is associated with an increased major adverse CV events (MACE) incidence in patients due to its systemic inflammatory effects<sup>118</sup>. A study conducted by Pastori et al. (2017) found that LPS may contribute to MACE incidence in AF patients due to platelet activation<sup>118</sup>. Thus, contributing to a negative prognosis. In addition, the study found that those in the highest LPS tertile (> 100 pg/mL) had the highest MACE risk. Evidence shows that LPS induces systemic inflammation and atherosclerosis as illustrated earlier a study conducted by Carnevale et al. (2018) which showed that LPS and TLR-4 were in atherosclerotic lesions that were characterised by activated macrophages linking the endotoxin to coronary artery disease<sup>20</sup>. When LPS binds to the TLR-4/ myeloid differentiation protein (MD2) complexes on many different tissue surfaces including endothelia cells (e.g the coronary artery and the aorta), innate immune system cells, smooth muscle (e.g lungs and GIT) and adipose tissue. The entry of the endotoxin into the systemic circulations results in inflammatory mediator release resulting in the development and progression of atherosclerosis which may produce coronary artery disease and heart failure<sup>20,108</sup>. Furthermore, there is adequate evidence to suspect that the toxin may contribute to AD progression in humans through systemic inflammation<sup>21</sup>. Moreover, LPS exposure may further elevate their AF and CAD risk through homeostatic dysregulation and myocardial damage.

## **2.3 Human Gastrointestinal Microbiome**

The GIT is a part of the gastrointestinal system. A large body of evidence indicates that the gastrointestinal microbial community plays a crucial role in shaping human physiology in the following systems: human digestive system maintenance and immune homeostasis<sup>119</sup>. The complex human gastrointestinal microbiome forms a meta-organism where symbiotic associations and host interactions play a crucial role in human health<sup>52</sup>. The microbiome influences human physiology both locally, in the GIT, and remotely, in organs such as the brain, CV system and liver<sup>119</sup>. Gastrointestinal tract microbiome-derived metabolite exposure affects both the CV and nervous system<sup>57,120-121</sup>. In addition, the GIT affects normal prenatal and childhood neurodevelopment<sup>19</sup>. The dysfunction has been linked to autism spectrum disorders, depression, multiple sclerosis, Parkinson's disease, schizophrenia, stroke and aging<sup>19</sup>. Gastrointestinal microbiome derived metabolites enter the CV circulation, metabolite exposure can affect the development of diseases such as: atherosclerosis and atrial thrombosis<sup>121</sup>. Exposure to metabolites is predictive of arterial thrombosis development, it induces platelet hyperactivity elevating the incidence of thrombotic events<sup>121</sup>. Lipopolysaccharides are gastrointestinal metabolites secreted by gram-negative bacteria that naturally occur in the gastrointestinal microbiome<sup>30,122-123</sup>. Endotoxin CV system exposure results in systemic inflammation, resulting in the enhancement of inflamm-aging<sup>30,122-123</sup>. In addition, LPS exposure may elevate the CV disease risk.

### **2.3.1 Lipopolysaccharides**

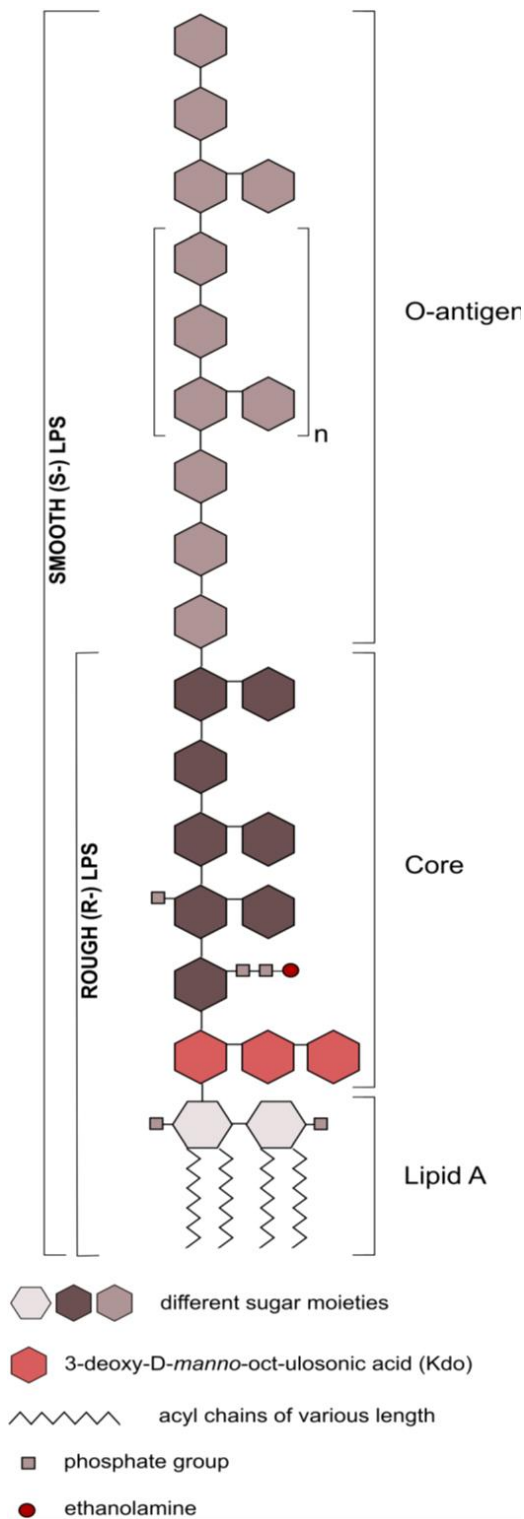
Lipopolysaccharides form the majority of the outer membrane's outer leaflet in gram-negative bacteria (i.e. *E. coli*), and fulfil two functions. Firstly, it protects the bacteria from harsh environments<sup>124-125</sup>. This occurs in the following manner: the toxin acts as a barrier against stress factors which makes LPS indispensable for bacterial variability in stressful environments<sup>126</sup>. The bacteria substitute Lipid A sugar moieties with phosphate groups to achieve outer membrane negativity which therefore interacts with available divalent cations in the encompassing milieu<sup>125</sup>. This mechanism reinforces the rigidity and tightness of the outer membrane hence resulting in bacterial resistance to external stress factors<sup>127</sup>. Secondly, LPS is a highly conserved bacterial structure within gram-negative bacterial species. Thus, making LPS a vital pathogen associated molecular pattern (PAMP) allowing bacterial recognition by the mammalian (e.g. human) innate immune system which can initiate bacterial infection clearance<sup>128</sup>. Swift LPS recognition and sensing of gram-negative bacteria greatly accounts for the innate immune system activation and response<sup>129</sup>. However, this must be a well-

balanced response. Uncontrolled bacterial growth within human bodies (GIT with leaky guts or tooth loss resulting in entry or within the CV as seen in sepsis) leads to large LPS quantities which can result in an overstressed systemic host immune response<sup>125</sup>.

Although, bacteria like *E. coli* are symbiotic bacteria that primarily reside in the gastrointestinal microbiome; aging results in the inability to maintain homeostasis in the body and elderly patients present with impaired gastrointestinal tight-junctions and tooth loss<sup>20</sup>. As humans age, tooth loss increases the possibility of bacterial entry into the CV because the dilation of oral vasculature resulting in bacterial or bacterial metabolite exposure to a variety of organs<sup>130</sup>. Both of these are ports of entry for bacteria to enter the circulatory system. A study conducted by Nikkari et al. (2001) found that blood from 'healthy' individuals can contain bacterial 16S ribosomal DNA showing evidence that some dormant bacteria does reside in blood<sup>131</sup>. The study raises the possibility for bacterial entry into the CV system and a 'normal' amount of CV bacteria<sup>131</sup>. Aberrant blood microbiota has been found in sequenced blood samples. However, in addition, microbiotas have been implicated in type 2 diabetes and CV disease<sup>132</sup>. Studies have implicated oral bacterial CV entry in the pathogenesis of periodontal disease-induced endocarditis and cerebral and/or myocardial infraction<sup>133</sup>. Once within the circulatory system the LPS molecules are detected by the innate immune system which induces an innate immune and an inflammatory response<sup>125,134</sup>. Lipopolysaccharide exposure also results in systemic inflammation that often concludes in weight loss and temperature changes. Weight loss and temperature changes are the first and/or only sickness behaviour exhibited by LPS exposed animals, however this is dose dependent<sup>135-136</sup>. Thus, body-weight and temperature can be used as a health marker when investigating the effects of LPS on the body.

### Structure and secretion

The endotoxin is synthesized in the cytoplasmic leaflet inner membrane and consists of three biologically, genotypically and chemically distinct domains which consist of the following<sup>125,137</sup>: (One) the O-specific polysaccharide or O-antigen, (two) the core oligosaccharide that is lipid A linked by 3-deoxy-d-manno-oct-ulosonic acid, (three) acylated and phosphorylated lipid A molecules are anchored in the bacterial outer membrane as seen in figure 2.6<sup>127</sup>. Lipopolysaccharides that consist of all three regions are called smooth (S)- form LPS, while O-antigen lacking LPS are called rough (R)-form LPS<sup>125</sup>.



**Figure 2.6: The schematic diagram of gram-negative lipopolysaccharides-** Lipopolysaccharides from gram-negative bacteria consist of three main subunits (From top to bottom): The O-antigen, the core region and lipid A.<sup>125</sup>

Following assembly in bacterial cytoplasmic leaflet, LPS tightly binds to the MsbA proteins which flip into the periplasmic leaflet by means of ATP-binding cassette transportation<sup>137</sup>. A study conducted by Wei and colleagues (2017) discovered that when MsbA is in an ADP or

nucleotide free state it displays an inward-facing configuration that opens transmembrane domains (TMD) that allow LPS entry<sup>137</sup>. Lipopolysaccharide's limit thioredoxin binding domain (TBD) opening and allow the adenosine ATP state in which there is nucleotide-binding domain (NBD) alignment for ATP to occur resulting in MsbA conformational changes. MsbA conformational changes inhibit LPS binding and allow periplasmic leaflet acyl chain entry<sup>137</sup>. Adenosine triphosphate hydrolysis then follows resulting in LPS release. After LPS is released transmembrane helices form a dense bundle and phosphate release results in MsbA regaining its inward-facing conformation<sup>137</sup>.

## **2.4 Cardiovascular System Modifications**

### **2.4.1 Cardiovascular systems affected by lipopolysaccharides**

#### **Blood: Hypercoagulability**

Researchers have discovered that neurodegenerative diseases patients experience hypercoagulable states, iron dysregulation and fibrin fibre structural changes<sup>21</sup>. It is well documented that LPS causes endotoxin-mediated hypercoagulation through cytokine activation. Such hypercoagulability, which is associated with pathological fibrin(ogen) concentration changes that directly affect the coagulation cascade. This disruption becomes the underlying cause of all thrombotic conditions including venous thromboembolism, ischemic stroke and ischemic cardiac disease as well as other pathologies<sup>58</sup>. As a result, an increase in the fibrin D-dimer product degradation is seen as a dependable CV risk biomarker<sup>58</sup>.

Research conducted by Pretorius et al. (2015) found that fibrin thickness was more heterogenous when LPS was added to the sample<sup>21</sup>. These dense matted deposits were previously seen in inflammatory conditions e.g., stroke and diabetes. The study found that blood exposed to LPS displays hypercoagulability, but also forms a denser clot as a result of coagulability parameter changes, however, the exact mechanism in which LPS plays a role in this outcome is unknown<sup>58</sup>. In addition, another study conducted by De Waal et al. found that LPS resulted in the fibrin(ogen) proteins of healthy individuals to polymerise into the amyloid form<sup>138</sup>. The structural change may result in pathological clotting<sup>138</sup>. Low amounts of LPS resulted in pathological clotting. The study also explored the fibrin network found in AD, Parkinson's disease and type 2 diabetes patients<sup>138</sup>. Amyloid formation was found in all of the illness groups and clotting formation could be reversed by adding LPS-binding agent<sup>138</sup>. Experimental studies have shown that gut-derived LPS are proatherogenic. Researchers have postulated a relationship between LPS and human atherosclerosis which was suggested by a forthcoming study that documented the association between LPS systemic circulation and the atherosclerotic burden<sup>87</sup>. Furthermore, LPS may contribute to thrombotic development in

humans, thus amplifying the platelet response to common agonists. Thus, promoting hypercoagulability which would further increase the likelihood of CV system complications.

### Cardiac muscle

Both, parasympathetic and sympathetic nervous systems control heart rate variability (HRV) which is important in regulating the oxygen supply of the human<sup>24,37,139</sup>. It is documented that the parasympathetic nervous system has an anti-inflammatory pathway that is implicated as an important factor in inflammation regulation<sup>140</sup>. Lipopolysaccharides may alter both cardiac muscle and the autonomic nervous system, potentially inducing pathogenesis.

It was displayed HRV analysis is a sensitive method used to study the autonomic nervous system activity in animals, allowing for the detection of sympathetic-parasympathetic balance fluctuations. The inflammatory response and the autonomic nervous system are closely linked due to an acute response to endotoxemia being observed. Inflammatory cytokine production alterations result in local or systemic inflammatory imbalances which are controlled by both the immune and central nervous systems<sup>141</sup>. This response includes innate immune system response as well as changes in autonomic nervous system activity<sup>142</sup>. An animal study conducted by Zila et al. (2015) found that LPS caused endotoxemia in rats concluding in a heart rate increase from 306 beats/min to 385 beats/min after LPS administration<sup>142</sup>. This indicates a decline in vagal activity. They speculated that other mechanisms resulted in a drop in vagal activity in rats with endotoxemia<sup>142</sup>. Recent studies have found that LPS cause myocardial inflammation leading to cardiotoxicity due to acute inflammation<sup>143</sup>. However, a wholistic study on how systemic LPS affects the CV system has never been conducted.

## 2.5 Exploring Manuka honey as a systemic inflammatory treatment

In addition to the absence of a wholistic study on the systemic inflammatory effects of LPS, there are no daily treatments for systemic inflammation for the endotoxin. This study proposes Manuka honey as a possible treatment for the systemic inflammatory effects of LPS because of its anti-inflammatory, anti-oxidant and wound healing properties<sup>23-22</sup>. Similar to other honeys, Manuka honey is comprised of fructose, glucose, maltose, oligosaccharides and sucrose, as well as enzymes which include catalase, diastase, glucose oxidase, invertase and peroxidase<sup>144</sup>. Sugar alone results in antibacterial properties in 61% of honeys<sup>145</sup>. Honey also holds anti-inflammatory, antioxidant and anti-hypertensive properties<sup>146</sup>. In addition, Manuka

honey possesses a low power of hydrogen (Ph) ranging from 3.5-4.5 resulting in increased angiogenesis and macrophage stimulation. Manuka honey results in hydrogen peroxide release that is antibacterial, and its unique advantageous antibacterial manuka factor (methylglyoxal) that aids in heal wounds<sup>23</sup>. Clinically, the Manuka factor has successfully treated gram-negative bacteria such as *E. coli* through bacterial clearance. *Escherichia coli* derived LPS was used in this study induces systemic inflammation<sup>21,23,147</sup>. The unique properties of Manuka honey contain both the beneficial characteristics of regular honey and the manuka factor, may be a suitable natural treatment for the systemic inflammatory effects of LPS, thus resulting in CV protection. This treatment may completely protect against systemic inflammatory effects of LPS or assist in injury reduction.

## **2.6 Aims and Objectives**

The aim of this study is to investigate the *in vivo* effect that systemically induced LPS has on the well-being, behaviour, memory and the CV system, of ten-week-old male Sprague-Dawley rats and the effect of Manuka honey as a treatment.

To achieve the aim the following objectives have been set:

1. Compare the behaviour and cognition of the experimental (LPS and LPS and Manuka honey treated) and control (Phosphate buffer saline (PBS) and PBS and Manuka honey) groups by conducting the following tests:
  - The Open field test evaluated overall activity (locomotion and mean speed), anxiety-like and exploratory behaviour.
  - The Y-Maze test evaluated short-term spatial novelty-object recognition (NOR) memory and,
  - The Novel object recognition test evaluated the ability of the test subject to recognise a familiar stimulus.
2. Measure and compare the body temperatures of the experimental, treated experimental, control and treated control group.
3. Measure and compare the weight gain rates of the experimental, treated experimental, control and treated control group.
4. Investigate the ultrastructure of aortic and cardiac muscle cells of the experimental, treated experimental, control and treated control group evaluating CV health using transmission electron microscopy.



5. Study the elastic fibre morphology of the aorta in the experimental, treated experimental, control and treated control groups by utilizing the Verhoeff-Van Gieson staining technique using light microscopy.
6. Study possible cardiomyocyte and aortic cell morphology aortic by comparing the nuclei, cytoplasm and connective tissue fibres of the experimental, treated experimental, control and treated control group by making use of the Haematoxylin and Eosin staining technique using light microscopy.
7. Study cardiac tissue fibre polysaccharide expression of the experimental, treated experimental, control and treated control group using Periodic Acid-Schiff staining technique using light microscopy.
8. Determine CV health by measuring total cholesterol concentrations of the experimental, treated experimental, control and treated control group using a sandwich ELISA assay.
9. Study the morphology of the erythrocyte, platelet and fibrin network structure of the experimental, treated experimental and control, treated control group using scanning electron microscopy.

# **Chapter 3: Methods and** **Materials**

### **3.1 Introduction**

This present study is a sub-section of a larger study that investigates the effect of LPS on the behaviour, cognition, weight, thermogenesis, total cholesterol levels and the morphology of the following tissues: brain (hippocampal matter), cardiovascular-, and hepatic systems. The study investigates if early low-dose LPS exposure produces similar symptoms found in those with early AD using a rat model. An AD population is the population of interest.

Animal models are used to investigate various conditions such as CV disease, neurodegenerative conditions, parasitic infections (e.g malaria) and spinal cord damage. These studies are vital in understanding the aetiology, pathophysiology and pharmacology of various diseases<sup>148</sup>. Rats and mice models have lead biomedical research for over a decade since they are particularly useful in CV and neurological research<sup>148</sup>.

This present study conducted behavioural studies to evaluate the effect of LPS on cognition and behaviour by comparing the control and experimental population. Specific neurological elements were considered when choosing our test subjects such as:

1. Hippocampal neurogenesis: rats experience greater hippocampal neurogenesis than mice<sup>149</sup>. New hippocampal neurons continue to form, even in adulthood, hence scientists have theorised that this process plays a key role in learning and memory<sup>150</sup>.
2. General stress behaviour: Mice often experience greater motor stress and anxiety, and require longer habituation periods and task training sessions than rats do<sup>151-152</sup>. Rats are typically unaffected by non-cognitive distractors (e.g external stress).

*Rattus norvegicus* rats commonly known as Sprague dawley rats were used in this study. Research indicates that rats grow rapidly during their childhood and attain sexual maturity at around six weeks of age but only gain social maturity five to six months later<sup>153</sup>. Laboratory rats have an average three year lifespan. When compared to the human aging process the physiological development of a ten-week-old male rat is the equivalent to a human young adult<sup>153</sup>. This study took the age of the rats into consideration and aimed to explore the effect of low physiological LPS levels of 0.05 mg/ml on these rats in order to explore the following:

1. The effect of early exposure on the male CV, neurological, and thermo-generation systems, as well as weight gain and total cholesterol levels.
2. Expand on the information of the neurological effects of early LPS exposure. In addition, explore Manuka honey as a possible treatment for the effects of LPS exposure.

The results obtained from this study can be used as a sex and age specific indication of the systemic effects of LPS exposure. However, the use of male rats provides a general overview

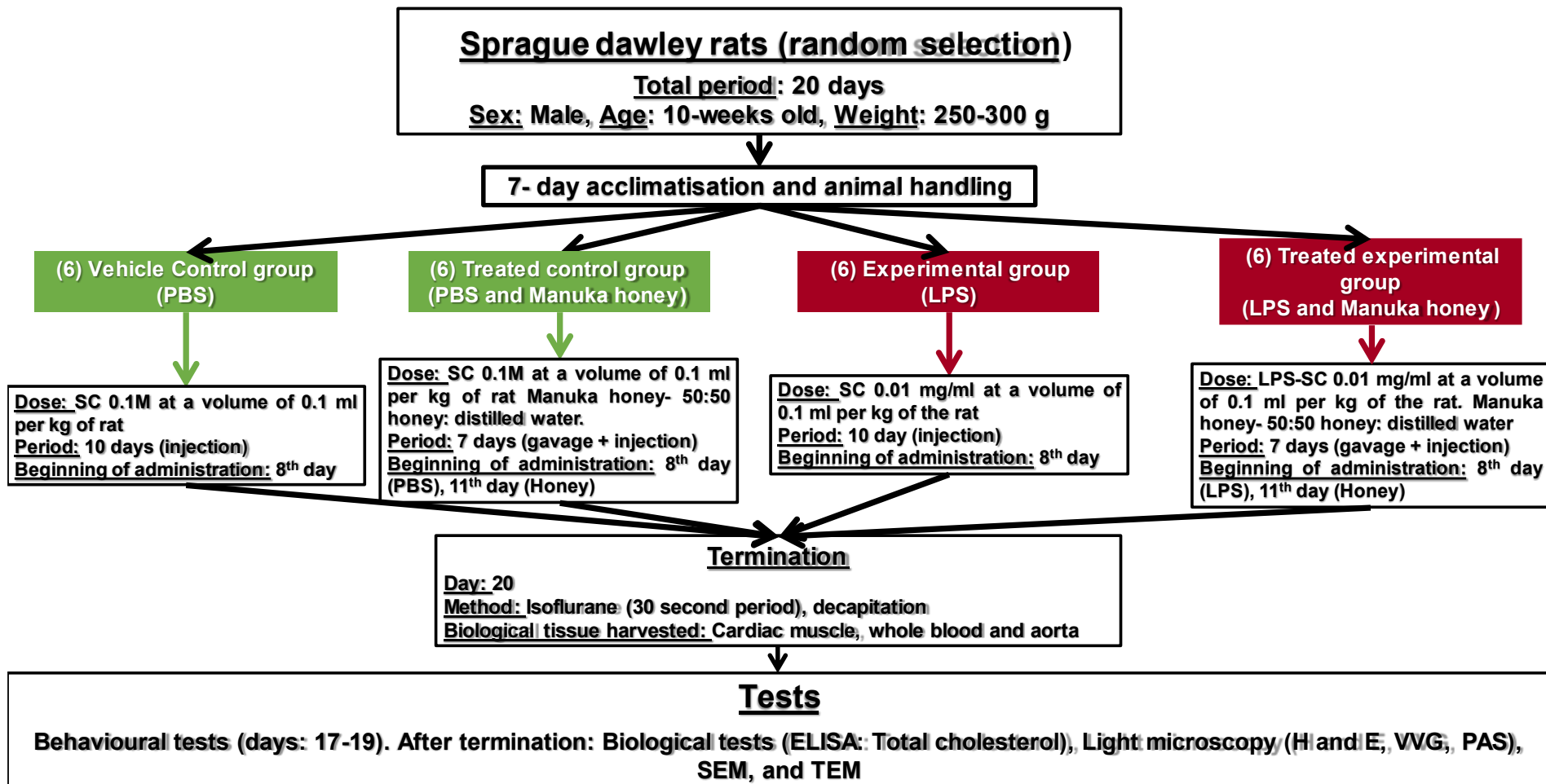
on the effects of LPS on the CV system and excludes the effects of female gonadal hormones as confounding factors. In addition, investigating the effects of LPS on the male CV system is the first step and future studies will compare the effects of LPS on the CV organs of male and female rats.

During normal aging, humans and rats experience cardiomyocyte swelling and a reduction in the number of cardiac cells present as a result of loss of function, amyloid and/or lipofuscin accumulation, and myocardium interstitial fibrosis transpire. These extend to the sinoatrial and atrioventricular nodes, and the atrioventricular bundle, thus altering cardiac conductivity<sup>154</sup>. The use of older rats would prohibit the clear differentiation between ordinary cardiac aging and LPS induced cardiac trauma. Using younger rats in the Sprague dawley rat model would produce greater success in comparative CV evaluations and would aid in producing definitive results<sup>155</sup>.

### **3.2 Study Design**

Twenty-four male rats (average weight: 250-300 g) were used in this study, following ethical approval from the University of Pretoria Animal Ethics (protocol number: 171-2020)- and the University of the Witwatersrand's Animal ethics committee (protocol number: 2019/07/44C). The rats were housed at the University of the Witwatersrand Central Animal Service (CAS) unit where the animals were randomly divided into two control groups (injected with PBS), and with PBS and Manuka honey (honey sourced only from the manuka plant) and two experimental groups (injected with *E. coli* serotype 055: B5) LPS as well as LPS and Manuka honey each group contained 6 rats. Standard irradiated "Epol" rat pellets and municipal water provided by *ad libitum* provided nourishment and hydration to each animal population. The test subjects were housed conventionally in cages with sizes laid down per the SANS 10386:2008 recommendations in the following conditions: room temperature 25-27 °C ( $\pm 2$  °C), relative 50% ( $\pm 20\%$ ) humidity and a twelve hour night/dark cycle. The rats were housed in pairs per cage and autoclaved pinewood shaving in addition to enrichment in the form of facial tissue paper was provided as bedding material as per the standard operating procedures at the University of the Witwatersrand CAS unit. The rats were acclimatised for seven days prior to dosage administration. Following that, the ten-day experimental period occurred in which the subcutaneous injection (SC) sites were alternated. Manuka honey was administered to the treated control and experimental groups through oral gavage on the 11<sup>th</sup> day for a seven-day period. Following that, behavioural tests such as the Open field test, The Novel object recognition test and the Y-Maze test were conducted on all the test subjects (from day seventeen to nineteen). Throughout the study, Dr Kimberly Jardine who was the principal

veterinarian (vet) supervised the health of the animals. The principal investigator conducted the behavioural tests after receiving training to do so. During the study, experiences of each animal group were monitored using the Rat Grimace scale (RGS) and welfare form. Following that, the rats were then be terminated after the total housing period of nineteen days. The test subjects were terminated on the 20<sup>th</sup> day during the process their blood and CV organs were harvested. The mode of euthanasia was by cardiac puncture after which perfusion with saline, decapitation, dissection, and organ harvesting which was conducted by the vet at University of the Witwatersrand CAS unit. The animals were terminated by cardiac puncture. The cardiac puncture was conducted to retrieve blood for the analyses of the blood components and the decapitation followed allowing all members of the research team to dissect their organs (brain, heart and liver) in a timely manner. This study only formed part of a larger study. The dissected CV organs and blood were studied using an enzyme-linked immunosorbent assays (ELISA) (Total cholesterol concentration test), Light microscopy (LM), Scanning electron microscopy (SEM) and Transmission electron microscopy (TEM). The project summary is illustrated in figure 3.1.



**Figure 3.1: Study outline-** The study was conducted in the following way, 24 male Sprague dawley rats were acquired and randomly assigned to control (PBS and PBS and Manuka honey group) and experimental (LPS, and a LPS and Manuka honey) groups. The control test subjects received subcutaneous (SC) PBS doses while and the experimental test subjects received SC LPS doses for ten days as well as honey oral gavage.

### 3.3 Sampling criteria: Control and Experimental Groups

#### 3.3.1 Timeline, control and experimental compound preparations and animal distribution

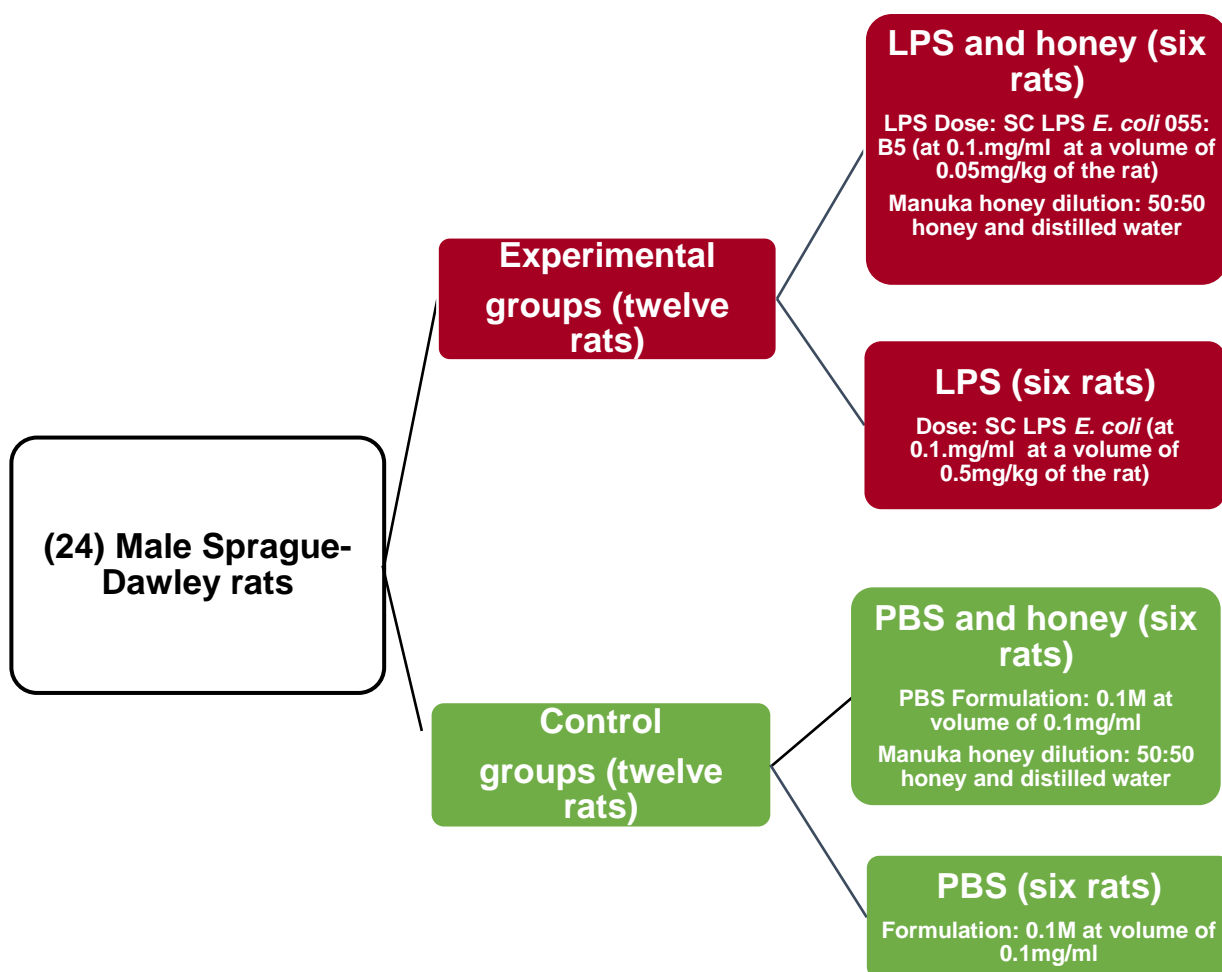
The animals experienced a seven-day acclimatisation period in which they grew accustomed to human contact. Proceeding acclimatisation, random animal division into the control and experimental testing groups occurred. Table 3.1 summaries the activities that took place during the study.

Table 3.1: Experimental period overview

<b>Animal study</b>							
<b>Group</b>	<b>Days in Experimental Period</b>						
	1-7	8-10	11-17	17	18	19	20
<b>Vehicle control</b>	<b>Acclimatisation</b>	PBS	PBS	<b>Open field</b>	<b>Novel object</b>	<b>Y-Maze</b>	<b>Termination</b>
<b>PBS + Honey (H)</b>		PBS	PBS + H				
<b>LPS</b>		LPS	LPS				
<b>LPS + Honey (H)</b>		LPS	LPS + H				

#### Compound Formulations

During the week of acclimatisation, vials containing LPS and PBS were autoclaved and the prepared substances were divided accordingly. The allocation and dilution of LPS, PBS, and Manuka honey are illustrated in the following figure 3.2. The LPS stock solution was dissolved in PBS and the Manuka honey was diluted in distilled water (Manuka honey 50:50 distilled water).



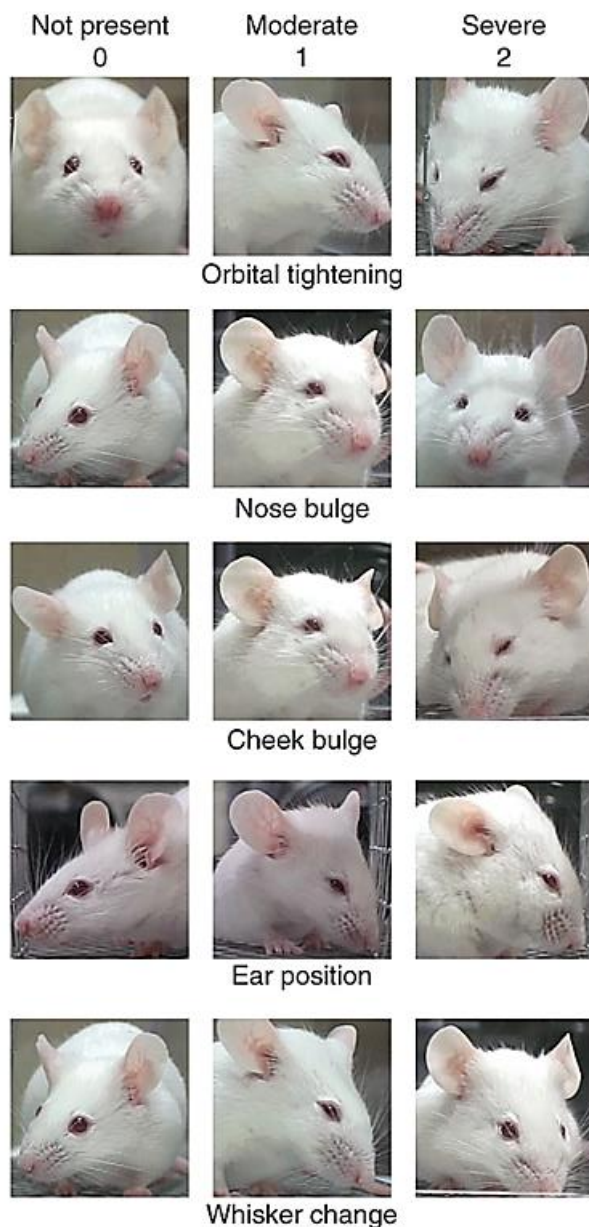
**Figure 3.2: Sampling criteria and doses-** The animals were randomly distributed into control and experimental groups (six rats each) where they were given either LPS, LPS and Manuka honey, PBS, PBS and Manuka honey.

After preparation, the LPS and PBS were stored in glass vials and stored at -20 °C until use. The Manuka honey solution was stored at four degrees Celsius (°C) until use. The weight, RGS score and welfare of each animal was documented daily. Upon administration day, one LPS and one PBS vial was thawed and administered. Before the LPS or PBS were administered the animals were weighed in the following way: the plastic container that was used to carry a test subject was cleaned and placed on the scale, following that the weight of the container was tared before the test subject was placed into the box. The weight of the animal was documented when all of its paws were on the bottom surface of the container and the scale remained on a single number. The weight of each test subject was documented to one decimal place. Following that, the animal was removed, and the container was cleaned with the F10 SC veterinary disinfectant. The weight of the test subject determined the dose of



LPS, LPS and Manuka honey, PBS and Manuka honey administered. The LPS and PBS were administered through SC injection while the Manuka honey were delivered through oral gavage (oral gavage is a procedure involving the passage of a gavage needle into the oesophagus resulting in the force feeding of an animal). The aim of this technique was to administer a specific, consistent Manuka honey dosage. All the compounds were administered at room temperature by a qualified animal nurse.

The pain experiences of the test subject were evaluated daily using the RGS (facial expression scale). The scale measures the degree of change in four 'action areas': orbital tightening, ear, cheek/nose flattening and whisker changes as seen in figure 3.3. Changes in the action sights have been identified as expressions the animal may display when experiencing various pain severities.



**Figure 3.3: Rat grimace scale four action sites-** The RGS observes four action sites which are orbital tightening, cheek and / or nose flattening, eyes changes and whisker changes, to determine if a rat is in no, moderate or severe pain. The pain is scored from zero to two by the severity of the facial expressions that the rat is exhibiting. Zero was considered no present pain and two signified that the animal was experiencing obvious pain.<sup>2</sup>

Severe pain was identified by the following: identifiable orbital tightening which is the narrowing of the orbital area and eye wrinkling; cheek and/or nose flattening was recognized as the flattening and elongation of the nose bridge as well as cheek flattening, inward ear curling and forward angling and widening of the space between the ears, whisker stiffening and angling on the face. In addition, the whiskers may clump together and may lose their

natural downward curve form<sup>156</sup>. No animal expressed above-described facial expression and thus were not in distress.

If the animals displayed persistent distressful signs they were evaluated by the vet. During the study, the welfare observations of each animal were closely documented. The following behavioural and physiological signs signified that an animal was experiencing severe distress and that termination was required: refusal to eat or drink, hunched posture, laboured breathing, self-mutilation, injection sights oozing pus, avoidant-, aggressive-, and fearful behaviours, constant diarrhoea and bloody stool, and whimpering vocalisations and 10% body weight loss. None of the animals required termination and did not experience any of the undesirable traits described.

### **3.4 Methods**

Animals were housed in cages throughout the experimental procedures as well as handled and restrained by the vet. Acclimatization and welfare monitoring of the animals were handled by the principal investigator: Glory Isabella Tambwe under the supervision of the vet. The groups used were subgroups of a larger research study. The study investigated whether the LPS induced symptoms that correspond with early AD symptoms. The study specifically focussed on rats that presented with behavioural changes that are found in an AD population and how the CV system in this population will be affected due to LPS exposure. We needed to do the behavioural tests to be able to confirm whether these rats experienced these behavioural changes. Nevertheless, this study specifically focuses on the CV system while completing the cognitive and behavioural objectives of the larger study by adding the behavioural study. The LPS endotoxin administered was expected to induce a systemic inflammatory response during the experimental period as found in literature. The animals were monitored for the following possible adverse effects: fatigue, loss of appetite and weight loss; as a precaution.

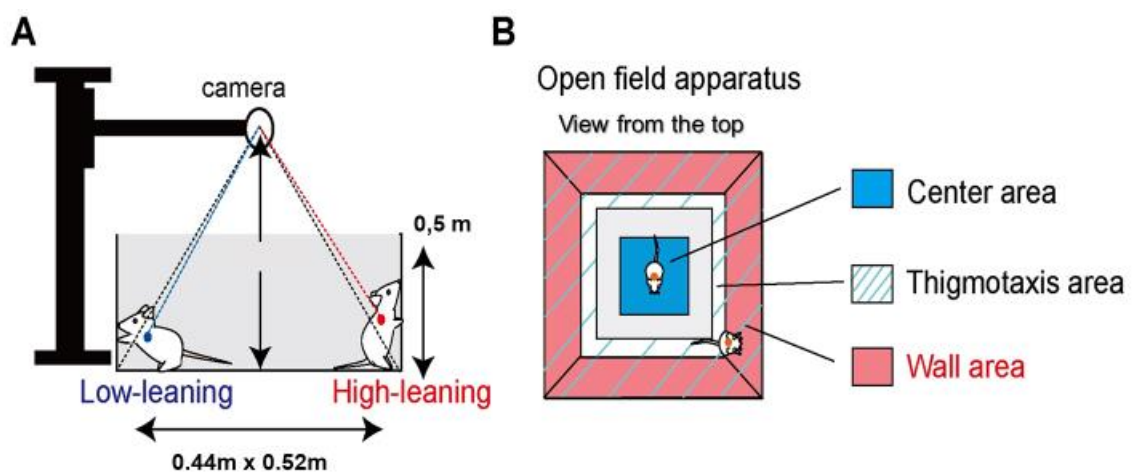
#### **3.4.1 Behavioural analysis**

Behavioural analyses were conducted to assess and compare the effect of LPS on cognition and behaviour, thus investigating if the effects of LPS on both factors share similarities to the early symptoms of AD. In addition, the effectiveness of Manuka honey as a treatment was also tested on the sample population. Behavioural tests were conducted after the experimental period using the Any-Maze video tracking software. The behaviour of each rat group was analysed using the Open field test, Y-Maze and the Novel object recognition test. The

movements of each animal were documented by three independent observers (Ms Nonkululeko Dhamini, Ms Victoria Verrall and Ms Karabo Rathebe) and the tracking software. In addition, the observations were recorded by a third-party observer that was unfamiliar to the experimental protocol thus limiting the bias. The tracking software allowed for the accurate definition quantification of rat zone entries using an overhead camera. Each test measured a different cognitive area providing a wholistic view of the effect of LPS on behaviour and cognition. In addition, effect of Manuka honey on resulting cognitive changes caused by LPS. The behavioural tests further widened the understanding of the effect that early LPS exposure has on neurodegenerative disease development by investigating memory and overall behaviour. The investigation of Manuka honey may provide a treatment for the behaviour and cognitive symptom induced by LPS exposure.

### Open field test

The animals received their last injections after performing the Open field test to prevent an elevation of anxiety as a result of the injection received. The Open field test is one of the most popular ethological tests that measures the overall activity of the animal as well as anxiety and exploratory behaviour<sup>1</sup>. In this study, the Open field test was used to both habituate the animals to the testing environment and illuminate anxiety as a confounding factor during the Novel object recognition and the Y-Maze behavioural tests. The test evaluated the time an animal spent in the central-, thigmotaxis (outer) and wall area. To achieve this the animals were allowed to freely explore an open arena surrounded by walls. In our scenario the animals were placed on a 0.44 m x 0.52 m plexiglass apparatus with 50 cm high walls. The plexiglass apparatus formed the field as seen in figure 3.4.



**Figure 3.4: The Open field test-** The animals were placed on a 0,44 m x 0,52 m plexiglass apparatus with 0,5m high walls. The plexiglass apparatus formed the field (A) Horizontal view of the testing area. (B) View from the top<sup>1</sup>.

The testing field was prepared by cleaning the grid with F10 SC veterinary disinfectant after each observation period preventing behavioural manipulation through olfactory cues left by the last test subject. The software divided testing field into squares. The number of squares that were crossed during the experimental period were counted and served as a measure of locomotor activity. The exploratory behaviour was assessed through the monitoring of the entry and exiting of the centre area and thigmotaxis area. When conducting the Open field test, studies have found that rodents prefer the thigmotaxis area, however, increased time in the central area were indications decreased anxiety<sup>157</sup>. Time in the central area indicated reduced stress levels while elevated thigmotaxis time indicated distress<sup>157</sup>. The behavioural responses of each animal were recorded using a video camera for a five-minute observation period in the field. Each animal was exposed to the Open field test twice. The first exposure was to habituate the animals to the field thus eliminating general anxiety caused by the exposure to an unfamiliar environment. The second was to measure the overall stress and anxiety experienced by the animal.

Stressed and anxious behaviour was identified by observing the following parameters: defecation, grooming, locomotion and exploration<sup>157</sup>. Research has shown that anxious and stressed animals displayed decreased locomotor activity and a reduction in exploratory behaviour<sup>158</sup>. In this study, reductions in locomotion and exploration were indications of stressed and anxious behaviour. Increased locomotion and exploration exhibited relaxed behaviour<sup>157</sup>. The following variables were tested: Total distance travelled, mean speed, time mobile, time immobile, immobile episodes, centre: entries, centre time.

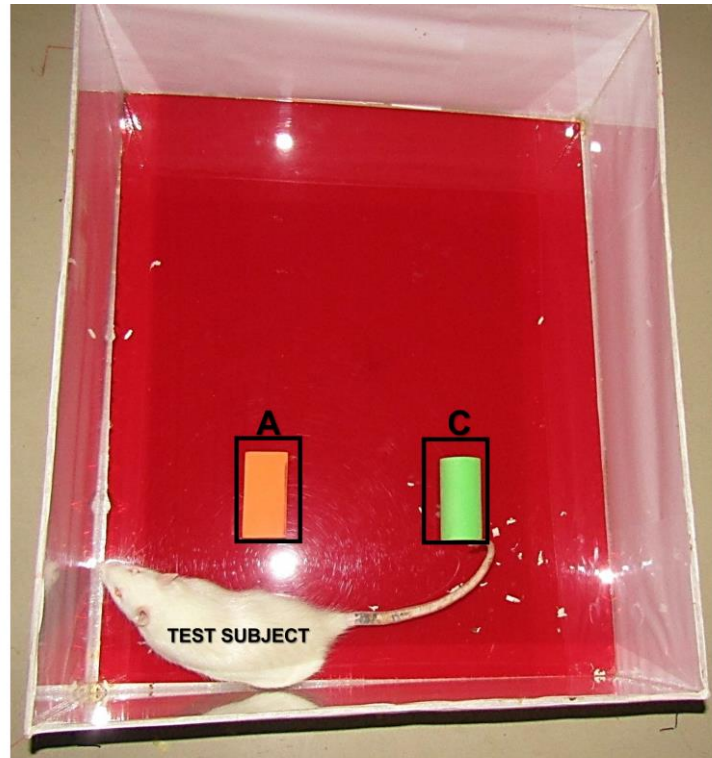
### The Novel object recognition test

The Novel object recognition test was conducted after the Open field test. The test evaluated the ability of an animal to recognise familiar stimuli, which was an indication of short-term and long-term memory<sup>159</sup>. The test was conducted to evaluate if the LPS exposed animals experienced a loss of memory and if so, if Manuka honey reduced or prevented the presentation of this symptom.

The Novel object recognition test is a non-spatial, non-aversive two-trial cognitive paradigm test that assessed recognition memory and relies on spontaneous exploratory behaviour<sup>159-162</sup>. The test was used for the following reasons: it does not involve multifaceted evaluation methods that involve complex tasks, long training periods and/or water or food deprivation<sup>160</sup>. Such methods are strenuous on animals. The advantages of the Novel object recognition test in this study were the rapid administration, swift data collection, it is cost effective, non-

rewarding and relies on the natural novelty preference of the rodent resulting in the production of high quality cognitive data<sup>160</sup>.

The test consisted of two trials and each trial consisted of two phases: familiarisation and the testing phase. During the familiarisation phase an animal was removed from its cage and placed in the testing block (0.44 m x 0.52 m) where two identical objects were placed. The animal was then released against the centre of the opposite wall with its back to the object. During the familiarisation phase, the test subject was given five minutes to explore identical familiar objects Block A and B. Following this, the animal and the blocks were removed. The testing area and blocks were cleaned with F10 SC veterinary disinfectant after each observation period to eliminate olfactory cues. The retention period followed and the animal was placed in a cage for an hour. Following that, the animal was removed from the cage and placed in the testing block. During the testing phase the testing block was arranged in the following way: the familiar object (Block A), used in familiarisation phase, was placed and remained in place while the identical block (Block B) was removed, and the area remained empty. Two and a half minutes into the testing phase, a second novel object (Block C) was placed where Block B had been placed during the familiarisation phase. Block C was a different colour and shape to Block A and B. The objects used in this experiment were small toys (eight to twelve centimetres in length) with a variety of colours and shapes that were fixed on the floor with removeable adhesive tape. The animal was allowed to explore for an additional two and a half minutes seen in figure 3.5.

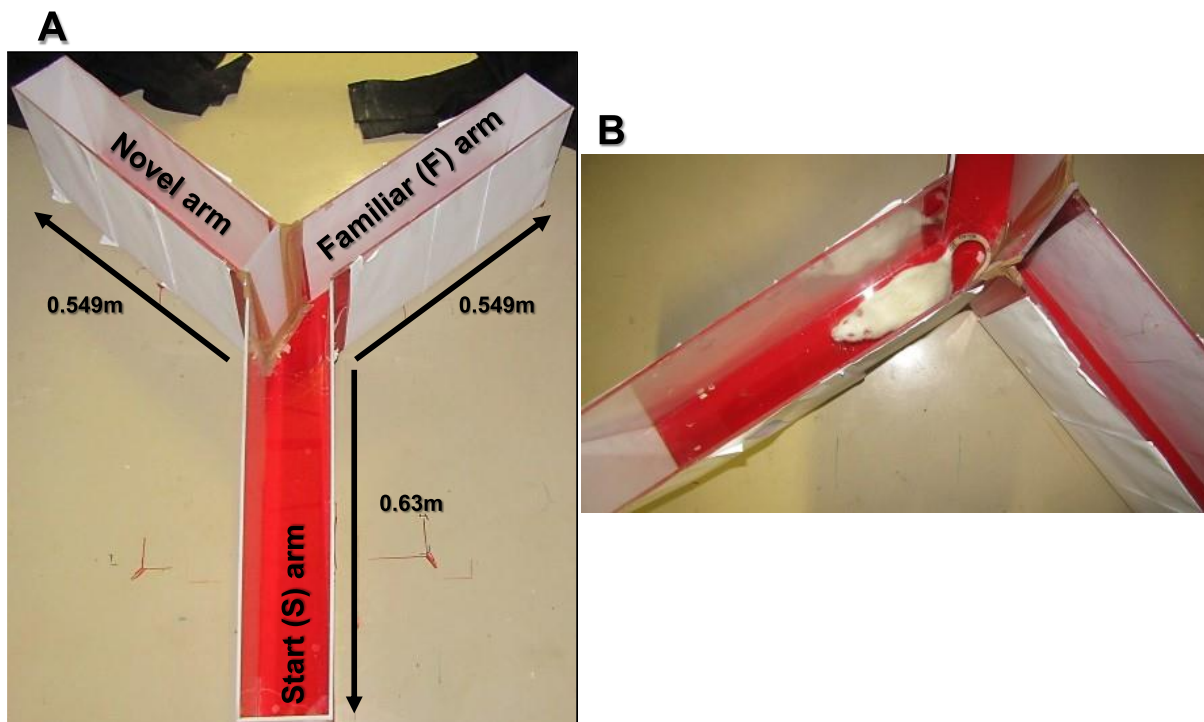


**Figure 3.5: Novel object recognition test-** During the habituation phase the animals were placed in the 0.44 m x 0.52 m testing box that first contained block A. The test subjects were allowed to explore for five minutes. During the testing phase the animals were placed in the testing block with block A for two minutes and a half then the block C, the novel object was placed in the testing block. **Actual image.**

The time that the animal was in a one-centimetre radius of the novel object (Block C) was recorded. The test subjects were expected to spend more time with the novel object (Block C) than the familiar object (Block A). Two trials were presided over in the same manner. During the first trial the short-term memory of the test subject was evaluated, however during the second trial the long-term memory of the animal was evaluated<sup>163</sup>. The following variables of each trial were documented: (familiar) block A entries, (familiar) block A time, (new) block C entries, and (new) block C time. Test subjects that remember the familiar objects will spend more time exploring the novel object<sup>163</sup>. During the first trial, the trial variables of the control, treated control, experimental, and treated experimental populations were compared. A declined short-term memory would be displayed as a significant difference (decrease) between the time the control group spends at the block C and the time a testing group resides at block C. During the second trial the same comparison is made between the groups however, the rats are expected to spend less time at Block A than they did in the first trial and more time at block C. However, primary determiner of if the test group is experiencing memory loss is if they display a significant difference (decrease) between the time the control group spends at the block C and the time a testing group resides at block C.

### The Y-maze novelty preference test

Following the Novel object recognition test, the Y-maze novelty preference test was conducted. The Y-maze test evaluated short-term spatial memory. The test consisted of the exploration of a Y shaped maze<sup>164</sup>. Each animal was placed in the Y-maze which consisted of three arms. The three arms were 120° degrees in relation to each other. The Familiar (F) and Novel arm (N) were 0.549 m in length and the walls were 0.5 m in height while the Start (S) arm was 0.63 m long and the walls were 0.5 m in height. The test was divided into two phases. During the first test phase (habituation trial), the N arm was obstructed and each animal was placed in the S arm as seen in figure 3.6. The animals were allowed to roam the maze for five minutes through to one F arm, while Any-Maze calculated the following: distance travelled, mean speed, number of entries and time spent in the familiar and start arms, number of entries and time. Following that, the animals were removed from the maze.



**Figure 3.6: Y-Maze novelty preference test-** The Y-maze in image A is the maze that was used for testing. During habituation each the test subject was placed at the S arm and allowed to explore for five minutes. During this phase the novel arm was barricaded. During the test phase the animals were allowed to explore the S, F and N arms. Image B illustrates a Sprague Dawley rat in the Y-maze. **Actual images.**

During the second trial (testing phase), each animal was allowed to rest before the testing phase in which exploration of all three arms was allowed. The N arm remained unobstructed and the following was documented: distance travelled, mean speed, number of entries and time spent in the familiar and start arms, number of entries and time, N arm entries and time spent. The more time spent in the N arm indicated that the test subject retained its short-term



memory. This phase took place for five minutes. The test results were then gathered and analysed. Following each test subject, the testing area was cleaned with F10 SC veterinary disinfectant to eliminate olfactory cues. The following data was collected: Total distance travelled, mean speed, F arms: entries, F arms: time, N arm: entries, N arm: time.




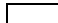

### 3.4.2 Termination

#### Termination procedure

Before termination began, animals were weighed and their body temperatures documented. The core body temperature of each animal was measured in °C by inserting a digital thermometer tip into the rectum, where it remained for a 30 second period before giving the temperature reading. Following that, the temperatures were recorded and later compared. The thermometer was cleaned and disinfected with F10 SC veterinary disinfectant. Following that, an animal received an Isoflurane dose for a 30 second period during that period a cardiac puncture was performed allowing for blood extraction into a sodium citrate (SEM) and a serum (Total cholesterol test) vacucare test tubes after which perfusion with saline was performed and decapitation using a gelatine was the mode of termination. Following that the organs were dissected. This method allowed for the least amount of tissue and coagulation changes. Appendix A provides detailed list of the materials and chemicals used during this project while Table 3.2 provides short summary of the materials needed for sample collection and storage. Figure 3.7 summarises the techniques used in the study.

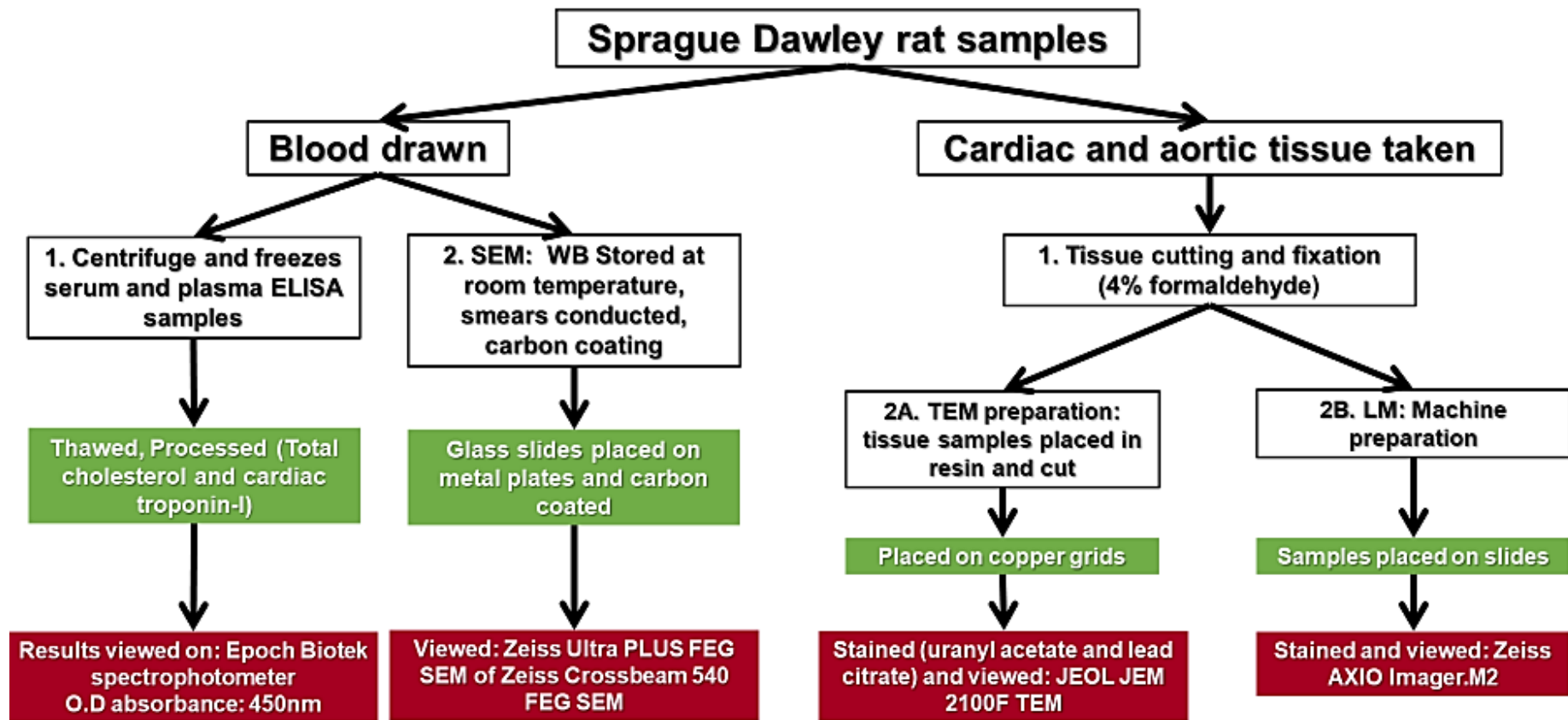
**Table 3.2: Materials, sample collection and storage**

<ul style="list-style-type: none"> <li>- Chemicals: Fixative- (All vials must contain) 4% formaldehyde (Merck: F8775-25ml)</li> <li>- Surgical Blades</li> <li>- Petri dish</li> <li>- Freezer box</li> <li>- Cooler bag</li> </ul>	<ul style="list-style-type: none"> <li>- Crushed ice</li> <li>- Eppendorf tubes (Epi's) (2 ml)</li> <li>- Permanent marker</li> <li>- Citrate blood tubes (2.7 ml)</li> <li>- Red serum blood tubes (5 ml)</li> </ul>	
<b>Sample collection</b>		
<b>Test</b>	<b>Sample</b>	<b>Consumable and number</b>
<b>Total cholesterol ELISA</b>	Blood: Serum	Serum red tube (40 tubes: 4 ml)

<b>Haemoxilin and Eosin (H and E)</b>	Tissue: Cardiac myocytes (Left ventricle) and aortic cells	 Longitudinally (4 mm x 4 mm)
<b>Verhoeff-Van Gieson (VVG)</b>	Tissue: Aortic cells	 Transverse rings
<b>Periodic Acid-Schiff (PAS)</b>	Tissue: Cardiac myocytes (Left ventricle)	 Longitudinally (4 mm x 4 mm)
<b>Scanning electron microscopy</b>	Blood: Whole	Citrate tube (40 tubes: 2 ml)
<b>Transmission electron microscopy</b>	Tissue: Cardiac myocytes (Left ventricle), and aortic	Cardiac tissue  Longitudinal (0,5 mm x 7 mm)
		Aortic tissue  Thin transverse circles

## Storage

<ul style="list-style-type: none"> <li>- SEM smears: Room temperature</li> <li>- ELISA blood samples <ul style="list-style-type: none"> <li>a) Centrifuge within 30 mins of collection</li> <li>b) Temperature: -80 °C in epi's</li> </ul> </li> </ul>	<ul style="list-style-type: none"> <li>- Light microscopy tissue (heart and aorta) <ul style="list-style-type: none"> <li>a) Stored in 4% formaldehyde</li> <li>b) Parafilm</li> </ul> </li> <li>- TEM tissue samples <ul style="list-style-type: none"> <li>a) Store in 4% formaldehyde</li> <li>b) Room temperature</li> </ul> </li> </ul>
--	--



**Figure 3.7: Preparation sequence-** Blood was acquired through cardiac puncture, left ventricular cardiac and aortic tissue during the termination. The samples were processed in the following order: 30 minutes after the blood was drawn the ELISA blood samples were centrifuged and frozen (-80 °C). The samples were later, thawed, processed and an O.D absorbance (optical density absorbance) was read at 450 nm. SEM and LM was prepared from whole blood samples. The TEM samples were processed from tissue samples.

### 3.4.3 Biochemical analyses

The biochemical analyses used in this study were ELISAs which was used to measure the total cholesterol of each testing population. The results were used to determine the impact on cholesterol homeostasis<sup>165</sup>.

#### Total cholesterol (Rat) ELISA Kit test

Method rationale: The total cholesterol test was utilised because cholesterol concentration in the CV system gives an indication of a cholesterol homeostasis disruption. Such a disruption indicates the effect of LPS on cholesterol regulation as well as the ability of Manuka honey to treat the disruption.

#### Method:

The QuickDetect™ total cholesterol (Rat) ELISA (Biovision kit: K4436-100) was used: The reagents, samples, and standards solutions were prepared according to manufactures instructions which were as follows: 40 µl of sample dilution buffer and 10 µl were added into the wells (the dilution factor of five). Seven samples from each group were used and later compared, the samples were tested twice. One well remained empty as a blank control. Following that, the blood serum samples were loaded onto the bottom without touching the well walls and the wells were gently shaken on a plate shaker. The samples were sealed and incubated for 30 minutes at 37 °C. After the incubation the seal were removed and the samples were aspirated and refilled with the wash solution. The washing procedure was repeated five times. Fifty microlitres of Horseradish Peroxidase (HRP)-Conjugate reagent was added to each well, except the blank control well and incubated for 30 minutes at 37 °C. Following that, the samples were aspirated and refilled with wash solution. The washing procedure was repeated five times. Following that, 50 µl of Chromogen Solution A and 50 µl Chromogen Solution B were added to each well. The samples were then mixed by gently shaking the well and incubated in the dark at 37 °C for fifteen minutes. Fifty microlitres of stop solution was added to each well to terminate the reaction. The colour in the well changed from blue to yellow. The absorbance readings were processed using Gen 5™ plate reader software, fifteen minutes after adding stop solution. The OD value for the blank control well was set as zero.

### 3.4.4 Light microscopy

#### Preparation:

The rat harvested hearts and aorta were longitudinally and transversely sectioned and fixed in the 4 % formaldehyde fixative. The samples were fixed for 24 hours at room temperature before the tissue samples were rinsed with 0.1 M PBS three times for 30 minutes. Following the rinsing, the samples were dehydrated with 50% ethanol for 30 minutes, 70% ethanol for an hour, 90% ethanol for an hour and lastly the samples were dehydrated twice in 100% ethanol for an hour. The samples were then placed in 100% ethanol overnight. The following day, the samples were treated with 50% xylene in ethanol for 30 minutes. Following that the samples were placed in xylene for two hours. The samples were also placed in wax I (30% white parafilm wax and 70% xylene) for an hour at a temperature of 60 °C then in wax II (70% wax and 30% xylene) for an hour at a temperature of 60 °C and lastly in wax III (100% wax) for two hours at a temperature of 60 °C. The samples were then placed on a grid to cool down at four degrees Celsius. Finally, the tissue was sectioned using the Leica RM 2255 microtome then placed on warm water at 45 °C in the Thermo scientific section flotation bath, then mounted on glass slides before being placed on the Raymond A lamb slide warmer to dry at 45 °C (Setting: five).

#### Deparaffination

The wax slides were emersed in xylene for ten minutes. Following that, the slides were placed in a new xylene container for five minutes to remove the wax. If the slides still contained wax, the slides remained in the xylene for an additional five minutes. The samples were then placed in series of ethanol concentrations: 100% ethanol for four minutes, following that, 90% ethanol for one minute, and lastly in 70% ethanol for one minute. Following that, the slides were placed distilled water for one minute. All of the steps were performed at room temperature.

#### Haemoxilyn and Eosin

Method rationale: The H + E staining was used to identify and investigate the effect of LPS on cardiomyocyte and aortic general cell morphology by comparing the nuclei, cytoplasm and connective tissue fibres of the control and experimental groups. Manuka honey was investigated as a possible treatment for the effects of LPS. Haematoxylin and Eosin staining reveals various tissue structures clearly allowing for cytological criteria, tissue sample quantity and classification examination<sup>166</sup>. Table 3.3 describes the properties of each stain.

#### Table 3.3: Haemoxilyn and Eosin summary

## Haemoxilyn and Eosin

Stain	Identified structure(s)	Colour (range)
Haematoxylin	Nuclei	Light blue to dark blue-purple
Eosin	Cytoplasm Connective tissue fibres (elastic fibres, mucins, muscle striations)	Pink to red

### Working chemical reagents:

1. Mayer's Haematoxylin: Fifty g of potassium aluminium was dissolved in in 1 L of 50% ethanol. Followed by, Haematoxylin being dissolved in the same solution. 0.2 grams of sodium iodate was added, then 1 g of citric acid and 50 g of chloral hydrate followed by distilled water resulting in the total volume of the solution equating to 1 litre. The solution remained undisturbed for three days before usage could occur.
2. Scott's buffer: Two grams of potassium bicarbonate and 20 g of magnesium sulphate were dissolved in 1 litre distilled water.
3. One percent Eosin solution: Two grams of Ethanol soluble Eosin was dissolved in 198 ml of 95% ethanol.

### Method:

Cardiac and aortic wax sections were deparaffinized as described above then placed in Mayer's Haematoxylin's fixative for fifteen minutes. The glass slides were placed in Scott's buffer for eight minutes. Following that, the samples were repeatedly submerged in distilled water for ten seconds then dipped in 1% eosin. The glass slides were rinsed in distilled water for one minute. The slides were briefly submerged in 70%, 90%, 100% ethanol, and then xylene. Following that, the samples were mounted with Entellan® new (Merck 12 Gaa) and a coverslip was placed over the samples. Photos were captured using the Zeiss AXIO Imager.M2 light microscope (Zeiss Group, 2 Roger Place Unit 1A, Gillitts Office Park 3640, Durban, South Africa). The tunica adventitia width of each group was measured using ImageJ and the values were compared.

### Periodic acid-Schiff

Method rationale: The PAS staining method identifies carbohydrates or glycoconjugates, table 3.4 lists PAS reactive tissue and cell components.

Table 3.4: Periodic Acid-Schiff reactive tissue and cell components

<b>Markers identified</b>
<b>Glycogen (specific to cardiomyocytes)</b>
<b>Starch</b>
<b>Mucin (sialomucin, neutral mucin)</b>
<b>Basement membranes</b>
<b><math>\alpha</math>-antitrypsin</b>
<b>Reticulin</b>
<b>Fungi (capsules)</b>
<b>Pancreatic zymogen granules</b>
<b>Thyroid colloid</b>
<b>Corpora amylacea</b>
<b>Russel bodies</b>

The stain reacts to the free aldehyde groups within the carbohydrates and the Schiff reagent reacts with the free carbohydrate aldehyde groups that result in a bright red or magenta end product concluding in polysaccharide identification<sup>167</sup>. Glycogen cardiomyocyte presentation is of primary interest in this study<sup>167</sup>. The Schiff reagent's glycoprotein reactivity within the basal lamina results in the PAS technique which is extremely valuable in basement membrane width assessment<sup>168</sup>. Increased basement membrane thickness occurs in a number of pathological conditions<sup>167</sup>. More specifically, the technique will identify cardiomyocyte hypoxia or normoxia depending on the colour displayed. During cardiomyocyte normoxia, a low glycogen accumulation rate is maintained and the cells are stained purple. During hypoxia, an elevated glycogen content would present in the cardiomyocytes thus the cells would stain bright or magenta while employing the PAS staining method<sup>169</sup>. The technique investigated if LPS induces cardiomyocyte hypoxia and if Manuka honey is an effective treatment.

#### Method:

The Periodic acid-Schiff kit was supplied with working chemical reagents in the kit. The cardiac muscle sections were deparaffinised as previously described and hydrated in distilled water. The slides were immersed in Periodic Acid Solution for five minutes at room temperature and then rinsed in distilled water then immersed Schiff's reagent for fifteen minutes at room temperature. The slides were rinsed with running tap water for five minutes then

counterstained in Haematoxylin Solution, Gill no 3 for 90 seconds. After this the slides were rinsed with running tap water. Then dehydrated with 70, 90, and 100% ethanol then xylene. The slides were cleared and mounted in resin. The samples were viewed using the Zeiss AXIO Imager.M2 light microscope.

### Verhoeff-Van Gieson

Method rationale: Verhoeff-Van Gieson (VVG) is a histochemical stain which enables the visualisation of elastic fibres, identification of normal and abnormal (pathological) aortic elastic fibres differentiation<sup>170</sup>. Elastic fibres are one of the connective tissue types and their main function is to provide elasticity and flexibility. As a result any abnormalities in blood vessel wall elasticity concludes in pathology<sup>171</sup>. Abnormal elastic fibre pattern detection aids in pathological condition diagnose<sup>171</sup>.

The VVG stain is particularly useful in evaluation elastic lamina pathologies found within elastic arteries like the aorta<sup>172</sup>. Using this stain atherosclerosis may present itself as elastin fibre fragmentation and atrophy within the lamina<sup>173</sup>. Pathogenesis may begin with lipid deposition, intimal fibrosis and increased local elastase concentrations within the arterial tissue. Degenerative valvular changes seen in patients with aortic stenosis presents as internal elastic lamina erosion and displacement. The stain allowed for the investigation of the effect of LPS on the elastic fibre organisation and if Manuka honey was an effective treatment for these changes. Verhoeff-Van Gieson allows the viewing of varying degrees of elastic fibre degradation within a blood vessel. This method defines the staining patterns presented in table 3.5

Table 3.5: Verhoeff-Van Gieson staining identification

<b>Tissue type</b>				
Red blood cells and cytoplasm	Muscle	Collagen	Nuclei	Elastic fibres
Yellow	Orange	Red	Blue/grey/black	Blue black to black

Working chemical reagents:

1. Ferric solution: Six ml of Ferric chloride solution was added to 74 ml of distilled water.
2. Elastic solution: Sixty ml's of the provided ethanol soluble Haematoxylin, 9 ml's of Ferric chloride, 24 ml's of Weigert iodine and 15 ml of distilled water were coalesced into a glass bottle.



### Method:

The aorta wax sections were deparaffinized (as previously described) and hydrated in distilled water. The slides were placed in a working elastic stain solution for five minutes then rinsed in running tap water. Following that, the slides were dipped in differentiating Ferric Chloride solution for 30 seconds and then rinsed in tap water. The slides were checked microscopically to determine correct colour appearance and if the targeted structures could be correctly identified. If the samples were over differentiated (Ferric Chloride produced an overpowering colour) the samples were returned to the working elastic stain solution. The slides were rinsed in 95% ethanol to remove the iodine<sup>174</sup>. Following that, the slides were rinsed with running tap water and then stained with in Van Gieson Solution for one minute. The slides were then rinsed in 95% ethanol and dehydrated with xylene. The slides were cleared and mounted in Entellan® new (Merck 12 Gaa) and viewed using Zeiss AXIO ImagerM2 light microscope.

### 3.4.5 Ultrastructural analysis of erythrocytes, fibrin networks and platelets using Scanning Electron Microscopy

Method rationale: Scanning electron microscopy was used to gather descriptive data on the erythrocytes, platelets and fibrin networks of the control and experimental group using whole blood (WB). The technique provided an ultrastructural view of the cell surface<sup>175</sup>.

### Method:

This technique did not require the preparation of working chemical reagents and the samples were prepared in the following way: 10 µl of the rat WB sample were placed on a 10 mm round coverslip. Following that, a 5 µl thrombin droplet was placed on a coverslip and 10 µl of the same blood sample was placed on the thrombin droplet. A bent pipette tip was used to carefully spread the sample droplet over the coverslip. The sample dried at room temperature for up to one minute. The WB sample and thrombin were allowed to dry one quarter of the coverslip's radius. When the blood and thrombin mixture formed a gel-like layer the coverslips were washed immediately. Duplicates of each sample were produced. The coverslips were transferred into 24 well plates and covered with PBS for fifteen minutes. The solution was then discarded and the sample was fixed with 4% formaldehyde for 30 minutes. The fixative was then removed and discarded following a PBS wash for three times three minutes each time. If the samples were still thick the sample plates were gently shaken five times allowing the PBS to wash over the blood sample. The samples were then transported to the fume cupboard where the third PBS wash was removed and discarded in the appropriate waste after which four to five 1% osmium tetroxide drops were placed directly on the coverslip. The same

number of distilled water (ddH<sub>2</sub>O) drops were placed on the coverslip, following that the samples were left covered and undisturbed for fifteen minutes. The osmium tetroxide/ddH<sub>2</sub>O solution was removed and the samples received three buffer washes (with PBS) for three minutes each. The first wash was discarded in the osmium tetroxide waste. An ethanol series dehydration took place in which the samples were washed in 30%, 50%, 70%, 90%, 100% ethanol for three minutes each. The 100% ethanol wash was repeated thrice. Then the ethanol was discarded in the fume cupboard and the samples were placed in hexamethyldisilazane (HMDS) for 30 minutes. The solution was then discarded and one HMDS drop was placed directly on the sample. The well was tilted to draw off excess solution. The edge of the coverslip was lifted to allow the bottom to dry using a blood collecting needle. The HMDS was left to evaporate. After the HMDS had evaporated, the glass plate was mounted on a steel plate and coated with carbon. Coated erythrocytes, fibrin network structures and platelets were visualised with a Zeiss Ultra PLUS FEG SEM (Zeiss Group, 2 Roger Place Unit 1A, Gillitts Office Park 3640, Durban, South Africa).

The images were classified into various categories that indicated erythrocyte, fibrin network and platelet structural normalcy. The cells were scored on an overall cell profile abnormality rating as displayed in table 3.6.

Table 3.6: Overall scoring system

<b>No or minimal change</b>	<b>Some visible cell or fibre changes</b>	<b>Most cells or fibres are altered</b>	<b>Large membrane changes and all cells or fibres are altered</b>
-	+	++	+++

An individual cell was scored according to its morphology as well as a membrane change. The manner in which the cell is scores is illustrated in table 3.7.

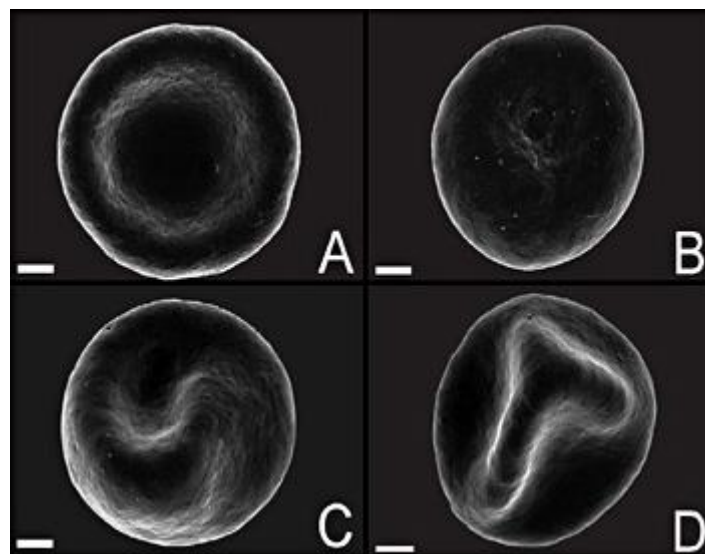
Table 3.7: Cell membrane damage scoring system

<b>No or little membrane changes</b>	<b>Mild membrane changes</b>	<b>Moderate membrane changes</b>	<b>Extreme membrane changes</b>
-	+	++	+++

An erythrocyte or group of erythrocytes were classified into four categories which were normal biconcave erythrocytes or spherocytes or echinocytes or knizocytes as seen in figure 3.8<sup>176</sup>. The degree of membrane damage was rated according to table 3.8.

Table 3.8: Erythrocyte scoring system

Normal	Spherocytes	Echinocytes	Knizocytes
-	+	++	+++

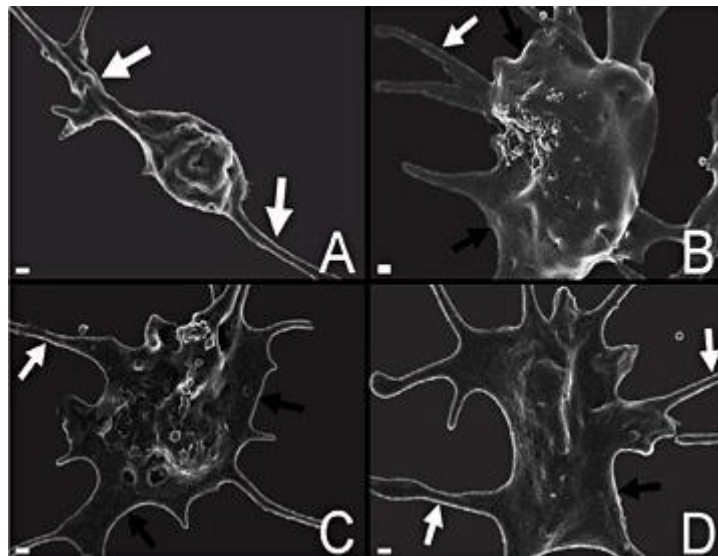


**Figure 3.8: Erythrocyte classifications-** These SEM images are examples of different erythrocyte categories that may be seen in our study. Normal erythrocyte biconcave (-) morphology is seen in Figure A. However, Figure B illustrates a spherocyte (+) which is a small, globular, completely haemoglobinated erythrocytes. Spherocytes are erythrocytes undergo a morphological change in which they become sphere-shaped. While Figure C illustrates an echinocyte (++) , which is an erythrocyte with a crenated or spiked surface that is synonymous with cellular membrane damage caused by various cytolytic compounds. Figure D illustrates a knizocyte (+++) is an erythrocyte that presents with two concavities, the erythrocyte type has been associated with hemolytic anemia.<sup>176</sup>

The platelet structure of the control and the experimental group were classified in three categories as displayed in figure 3.9 and the platelet abnormality scoring system is illustrated in table 3.9<sup>176</sup>. The platelets are classified into the following categories: normal, minor platelet spreading and complete platelet spreading.

Table 3.9: Platelet scoring system

Normal platelets	Minor platelet spreading	Complete platelet spreading
-	+	++

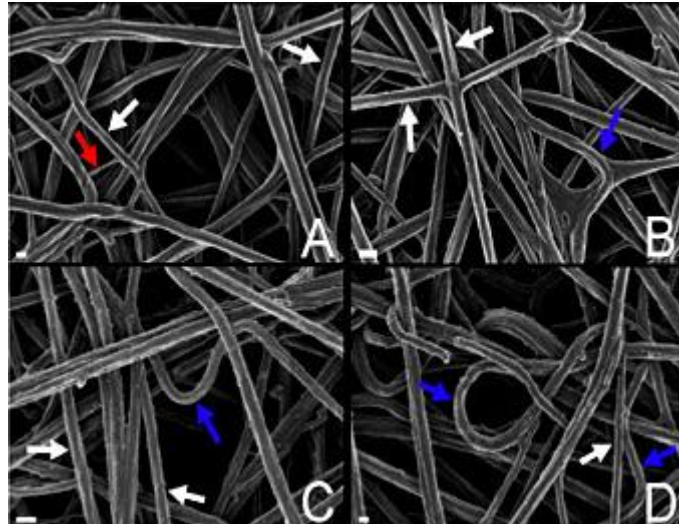


**Figure 3.9: Platelet classifications-** These SEM images are examples of different platelet categories used in this study. Figure A is an example of a normal platelet (+). While Figure B displays a platelet illustrates a minimal shape change and possess a few pseudopodia (white arrows) this is classified as minor platelet spreading (++) . Figure C and D display platelets that are completely spread (+++) and exhibit platelet spreading (black arrows).<sup>176</sup>

The fibrin network structure of the control and experimental group were classified as normal or abnormal based on the degree of tautness and fibre bending as seen in figure 3.10<sup>176</sup>. The fibrin networks were scored using the guidelines found in table 3.10.

**Table 3.10: Fibrin network scoring**

Normal	Mildly less taut and disordered	Moderately less taut and disordered	Completely disordered and less taut
-	+	++	+++



**Figure 3.10: Fibrin network classifications-** These SEM images are examples of the different possible fibrin network categories. A typical normal control fibrin network (+) can be seen in micrograph A. These networks have predominantly taut, straight fibers and a mixture of thin and thick fibrin fibers as indicated with the red and white arrows. Micrograph B-D are examples of an abnormal fibrin network, the fibrin fiber networks are less taut or bent as indicated with the blue arrows.<sup>176</sup>

The WB of the control and experimental groups were analysed and compared allowing for the investigation of the effect of LPS on erythrocyte, platelet and fibrin network structure. Manuka honey was the proposed treatment for the effects of LPS.

### 3.4.6 Morphological analysis of tissues using Transmission electron microscopy

Method rationale: Transmission electron microscopy was used to investigate the characteristics of cardiac and blood vessel tissue on a high magnification for both the LPS treated and control animal specimens. This technique is a significant tool in visualising the ultrastructure of pathology and normal cells and tissue<sup>177</sup>. Upon preparations, longitudinal and transverse cardiac muscle sections were processed to view various structures. The longitudinal sections allowed for the cardiac myofibril observation and investigation between the control and experimental groups while transverse sections were obtained to investigate mitochondrial ultrastructure. The aortic tissue was prepared in transverse sections resulting in the elastin and collagen fibre comparison between the above-mentioned groups. Collagen provides tensile strength and rigidity to the aorta. The high-resolution viewing of a cell or tissue allows for cellular pathology diagnosis with the central principle of electrons passing through the cell or tissue section resulting in the specimen image. Although LM techniques may have limitations on the information displayed through staining methods that show cell distribution and structure, it is limited in its membrane and organelle display. However, this is remedied

by the use of TEM. This results in the identification of tissue ultrastructure allowing for differences to be identified before physiological symptoms are present.

### Working chemical reagents:

1. Agar 100 resin: Forty-eight point nine grams of Glycidyl ether 100, 22.8 g of Dodecenylsuccinic anhydride, 28.3 g of Methyl nadic anhydride were incorporated together on a metallic stirrer. Following 30 minutes, Tris(dimethylaminomethyl)phenol was added and the contents was stirrer for another 30 minutes.
2. Two to one Ethanol: Agar 100 resin dilution: 100% ethanol was added to half of its quantity in Agar 100 resin.
3. One to two Ethanol: Agar 100 resin dilution: A single volume of 100% ethanol was added to double its volume in Agar 100 resin.

### Method

The heart and blood vessel tissue were first cut in five-by-five-millimetre blocks then fixed in 4% formaldehyde solution for 24 hours. The fixative solution was removed and the samples underwent three, fifteen minute 0.1 M PBS buffer washes. After the third buffer wash a 1% osmium tetroxide solution was added to complete the fixation step. The sample remained in the osmium tetroxide for an hour. Following that, the sample was washed three times with PBS, for 15 minutes each. The samples were dehydrated in a series of 30%, 50%, 70%, 90% ethanol then three times in 100% ethanol. Each dehydration step had a fifteenminute duration.

The infiltration process had two steps: a two to one Ethanol: Agar 100 resin mixture was added to the samples for an hour followed by a one to two Ethanol: Agar 100 resin mixture for two to four hours. The ethanol resin solution was removed. One hundred percent Agar 100 resin was added to the samples that were then assigned a sample number and embedded into rubber moulds. The embedded samples were placed in an oven for 36 hours at 60 °C for polymerization. Following the 36-hour period, the samples were removed from the oven and cut into semi-thin sections (0,35 µm) with the ultramicrotome. The sections were placed on glass slides and stained with Toluidine blue then samples were cut into ultra-thin (50-90 nm) sections and placed onto three mm diameter copper grids, stained with uranyl acetate and lead citrate for contrast. The stained samples were viewed using a JEOL JEM 2100F TEM (Zeiss Group, 2 Roger Place Unit 1A, Gillitts Office Park 3640, Durban, South Africa).

# **Chapter 4: Animal behaviour analyses**

## **4.1 Chapter Objectives**

Compare the behavioural profiles and memory of the experimental (LPS and LPS and Manuka honey treated) and control (PBS and PBS and Manuka honey) groups by conducting the following tests:

- The Open field test evaluated overall activity (locomotion and mean speed), anxiety-like and exploratory behaviour.
- The Y-Maze test evaluated short-term spatial novelty-object recognition (NOR) memory and,
- The Novel object recognition test evaluated the ability of the test subject to recognise a familiar stimulus.

## **4.2 Introduction**

Neurodegenerative diseases can affect the brain of an individual in different ways such as localised or general brain structure damage and/or the malfunction of various areas or receptors. The reduced homeostatic ability found in the elderly results in neurodegenerative diseases falling mainly within this age group. Alzheimer's disease is a neurodegenerative disease that primarily affects the elderly<sup>178</sup>. However, males experience young age onset, shorter disease duration and display atypical clinical presentations. Various CV diseases (e.g AF, coronary heart disease, and heart failure) have an elevated prevalence in men and increase the probability of neurodegenerative disease development<sup>95-98</sup>. Lipopolysaccharides are found in the brain matter of AD patients and may also result in CV disease pathogenesis<sup>95-97,179</sup>. In addition, clinicians have found that in early pathogenic stages, cognitively healthy elderly individuals present with high  $\beta$ -amyloid ( $A\beta$ ) levels<sup>178,180</sup>. These findings support the observations that  $A\beta$  positivity in these individuals is linked to episodic memory decline, greater medial temporal lobe area loss, increased  $A\beta$  accumulation, other cognitive aspects and elevated development rates to clinical classification of mild cognitive impairment or AD dementia<sup>61,178,181-182</sup>.

Elevated age is the greatest  $A\beta$  positivity risk factor in cognitively healthy adults<sup>178</sup>. A study conducted by Ossenkoppelle et al (2015) has shown that 10% of adults aged 60 to 70 years old, 25% of adults aged 71 to 80 years old and 40% of adults that are older than 80 years old, are  $A\beta$  positive<sup>183</sup>. This is significant since research has shown that LPS-type glycolipids have a high affinity for neuronal nuclear membranes. Nevertheless amyloid- $\beta$  42 ( $A\beta$ 42) peptides play an important role in facilitating LPS entry and translocation into the neuronal cells and



across the neuronal nuclear envelopes in human neuronal glial cells that are in primary co-culture<sup>184</sup>.

Alzheimer's disease clinically presents with neuron destruction in various parts of the brain that are important for memory such as the entorhinal cortex and hippocampus. As the pathology progresses, it later affects areas of the cerebral cortex that are responsible for language, reasoning and social behaviour<sup>185</sup>. There is a large quantity of evidence showing a close link between neuroinflammation and neuropsychiatric disorders such as depression and memory deficits<sup>186-187</sup>. Research has found that LPS brings about an inflammatory response that plays a crucial role in neuropsychiatric dysfunction of a rodent<sup>188</sup>. Lipopolysaccharides release many pro-inflammatory cytokines such as interleukin-1 $\beta$  (IL-1 $\beta$ ) and tumour necrosis factor alpha (TNF $\alpha$ )<sup>18,189</sup>. Interleukin-1 $\beta$  is vital to the oxidative and neuroinflammatory responses brought about by LPS and has been identified as a key mediator in behavioural dysfunction found in rodents<sup>188-189</sup>. The consequence of its administration in an animal model is anhedonia (the inability to experience pleasure in when participating in normally pleasurable activities), fatigue, impaired social interaction, memory deficits and weight loss<sup>190</sup>.

Lipopolysaccharides may also cause or worsen AD<sup>191</sup>. The current study tested the effects of LPS on memory and the psychological profiles of the animals by performing behavioural analyses using the Any-Maze video tracking software. These analyses were done in order to confirm that LPS induces an AD type of dementia as this is the type of population that is of interest.

The analyses that were conducted on the control and experimental groups are as follows: The Open field test, Y-Maze test, and the Novel object recognition test. The tests used are standardised behavioural and cognitive tests that have been formulated and currently used in research<sup>192-195</sup>.

The aim of this chapter was to explore the effect of LPS on the behavioural profile and memory as well as present Manuka honey as a possible treatment for the effects of LPS.

## **4.3 Results**

### **4.3.1 The Open field test analysis**

The overall mean scores of each animal group was compared using a One-way Analysis of Variance (ANOVA) test. The means of the test variables described in chapter three were compared and tested for statistical significance using a Two-Way ANOVA at a P-value  $\leq 0.05$ . The test revealed that there was no significant difference between the experimental and

control groups. The control and experimental groups did not present with any statistical differences within any category. All statistical tests were conducted using the GraphPad Prism 9.0.0 software. The statistical data is displayed in table 4.1, 4.2 and 4.3, figure 4.1 and 4.2. Refer to chapter ten Appendix B for the complete data set.

The group statistics (mean, median and p-values) are found in table 4.1, the means of the experimental and control groups were ranked from one being the lowest and four being the highest ranked group in that specific category. The control group presented with the lowest mean distance travelled, mean speed, overall mobile time, outer zone mobile time, third most centre zone entries and longest overall immobile time. While the treated control group presented with shortest time occupying the centre zone, the second lowest overall immobile time, outer zone mobile and immobile time, and centre zone entries, while displaying the second highest overall all mobile time, and the highest distance travelled, mean speed, and outer zone: mobile time. Meanwhile the experimental group displayed the following test results: the shortest time overall and outer zone: immobile time, second shortest centre zone time, the second fastest mean speed and second greatest mobile time spent in the outer zone. In addition, the treated experimental group presented with the lowest time centre zone entries, the second shortest distance travelled, slowest mean speed and overall mobile time, while displaying the third largest overall- and outer zone- immobile time and time occupying the centre zone.

**Table 4.1: Open field- Test groups statistics**

<b>Ranking</b>	<b>Group</b>	<b>Category</b>	<b>P-values</b>	<b>Mean ± SD</b>	<b>Median</b>
1	PBS	<b>Distance (m)</b>	0.799	16,046 ± 2,84	15,223
2	LPS + H			16,93 ± 2,11	17,005
3	LPS			17,11 ± 3,03	16,63
4	PBS + H			17,36 ± 4,15	17,368
1	PBS	<b>Mean speed (ms)</b>	0.806	0,089 ± 0,0158	0,085
2	LPS + H			0,094 ± 0,0117	0,095
3	LPS			0,095 ± 0,0169	0,093
4	PBS + H			0,096 ± 0,0231	0,097
1	PBS	<b>Overall mobile time (s)</b>	0.872	138,13 ± 12,685	141,25
2	LPS + H			138,89 ± 14,195	137,05
3	PBS + H			141,54 ± 15,221	144
4	LPS			142,12 ± 7,822	142,6

1	LPS	<b>Overall immobile time (s)</b>	0.872	37,88 ± 7,822	37,4
2	PBS + H			38,46 ± 15,221	36
3	LPS + H			41,11 ± 14,196	42,95
4	PBS			41,87 ± 12,685	38,75
1	PBS	<b>Outer zone: mobile time</b>	0.903	130,32 ± 11,739	131,85
2	LPS + H			132,65 ± 13,066	132,1
3	LPS			133,33 ± 8,072	135,9
4	PBS + H			134,43 ± 16,196	139,2
1	LPS	<b>Outer zone: immobile time</b>	0.854	37,88 ± 7,822	37,4
2	PBS + H			38,1 ± 14,831	36
3	LPS + H			41,11 ± 14,196	42,95
4	PBS			41,87 ± 12,685	38,75
1	LPS + H	<b>Centre entries</b>	0.621	0,8 ± 1,23	0
2	PBS + H			0,9 ± 0,74	1
3	PBS			1,2 ± 0,92	1
4	LPS			1,3 ± 0,95	2
1	PBS + H	<b>Centre time (s)</b>	0.860	0,47 ± 0,44	0,45
2	LPS			0,64 ± 0,60	0,7
3	LPS + H			0,71 ± 1,55	0
4	PBS			0,82 ± 0,68	0,75

**Abbreviations: H: Manuka honey, LPS: Lipopolysaccharide, m: meters, ms: meters per second, PBS: Phosphate-buffered saline, s: Seconds, SD: Standard deviation**

When all the testing criteria were compared between individual control and experimental groups using the One-way ANOVA test, no significant differences were found as documented in table 4.2.

Table 4.2: Open field test- general group comparison between all test parameters

Groups	P-value	Significant (yes or no)
PBS vs PBS+H	>0,9999	No
PBS vs LPS	>0,9999	No
PBS vs LPS+H	>0,9999	No
PBS+H vs LPS	>0,9999	No

PBS+H vs LPS+H	>0,9999	No
LPS vs LPS+H	>0,9999	No

A Two-way ANOVA was conducted and found that when the experimental and control groups were compared in each category, the data remained statistically insignificant as documented in table 4.3.

Table 4.3: Open field Test- Group statistical comparisons within test parameters

Groups	Category	P-value	Significant (yes/no)
PBS vs PBS+H	<b>Distance (m)</b>	0,9801	No
PBS vs LPS		0,9893	No
PBS vs LPS+H		0,9937	No
PBS+H vs LPS		0,9999	No
PBS+H vs LPS+H		0,9993	No
LPS vs LPS+H		>0,9999	No
PBS vs PBS+H	<b>Mean speed (ms)</b>	>0,9999	No
PBS vs LPS		>0,9999	No
PBS vs LPS+H		>0,9999	No
PBS+H vs LPS		>0,9999	No
PBS+H vs LPS+H		>0,9999	No
LPS vs LPS+H		>0,9999	No
PBS vs PBS+H	<b>Overall mobile time (s)</b>	0,7448	No
PBS vs LPS		0,6401	No
PBS vs LPS+H		0,9960	No
PBS+H vs LPS		0,9982	No
PBS+H vs LPS+H		0,8620	No
LPS vs LPS+H		0,7751	No
PBS vs PBS+H		0,7448	No

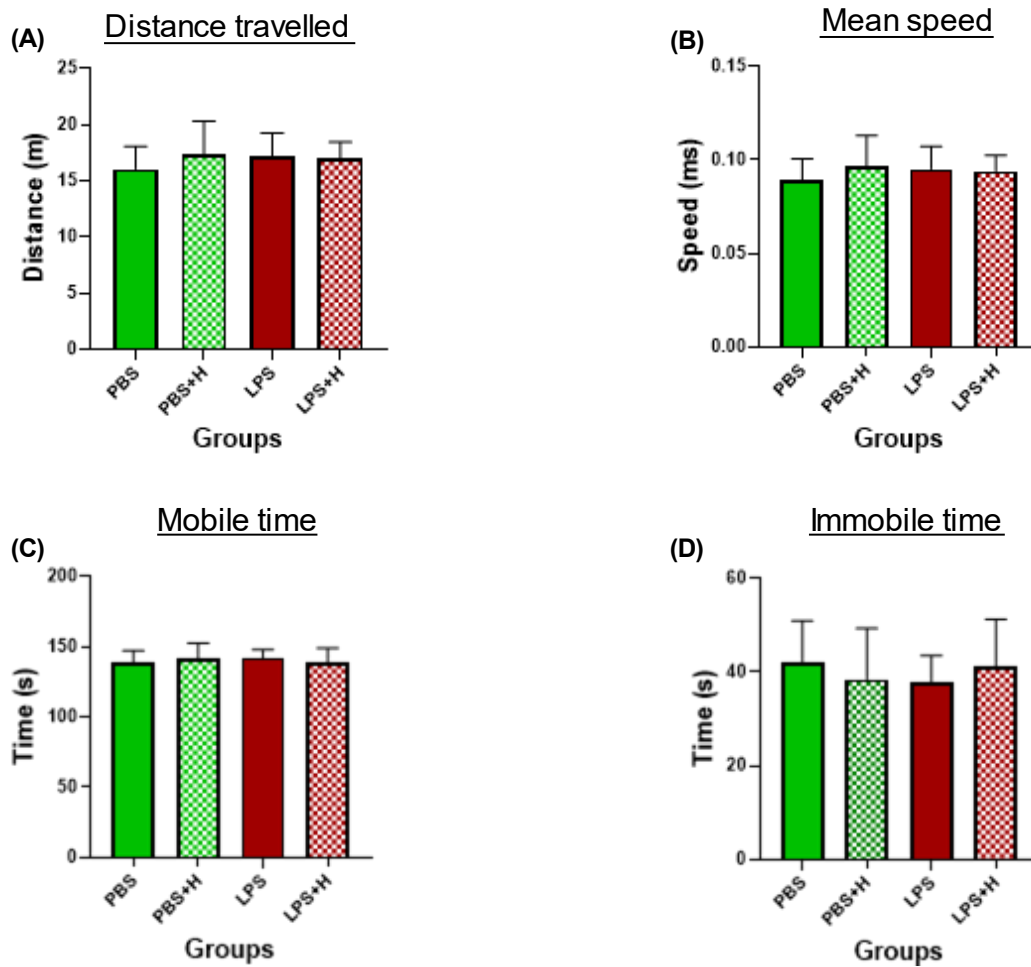
PBS vs LPS		0,6401	No
PBS vs LPS+H		0,9960	No
PBS+H vs LPS	<b>Overall immobile time (s)</b>	0,9982	No
PBS+H vs LPS+H		0,8620	No
LPS vs LPS+H		0,7751	No
PBS vs PBS+H		0,6176	No
PBS vs LPS		0,8101	No
PBS vs LPS+H	<b>Outer zone: mobile time (s)</b>	0,9013	No
PBS+H vs LPS		0,9881	No
PBS+H vs LPS+H		0,9527	No
LPS vs LPS+H		0,9971	No
PBS vs PBS+H		0,6808	No
PBS vs LPS		0,6401	No
PBS vs LPS+H	<b>Outer zone: immobile time</b>	0,9960	No
PBS+H vs LPS		>0,9999	No
PBS+H vs LPS+H		0,8101	No
LPS vs LPS+H		0,7751	No
PBS vs PBS+H		0,9997	No
PBS vs LPS		>0,9999	No
PBS vs LPS+H	<b>Centre entries</b>	0,9994	No
PBS+H vs LPS		0,9994	No
PBS+H vs LPS+H		>0,9999	No
LPS vs LPS+H		0,9988	No
PBS vs PBS+H		0,9996	No
PBS vs LPS		>0,9999	No
PBS vs LPS+H	<b>Centre time (s)</b>	>0,9999	No
PBS+H vs LPS		>0,9999	No
PBS+H vs LPS+H		0,9999	No
LPS vs LPS+H		>0,9999	No

---

Abbreviations: H: Manuka honey, LPS: Lipopolysaccharide, PBS: Phosphate-buffered saline, SD: Standard deviation

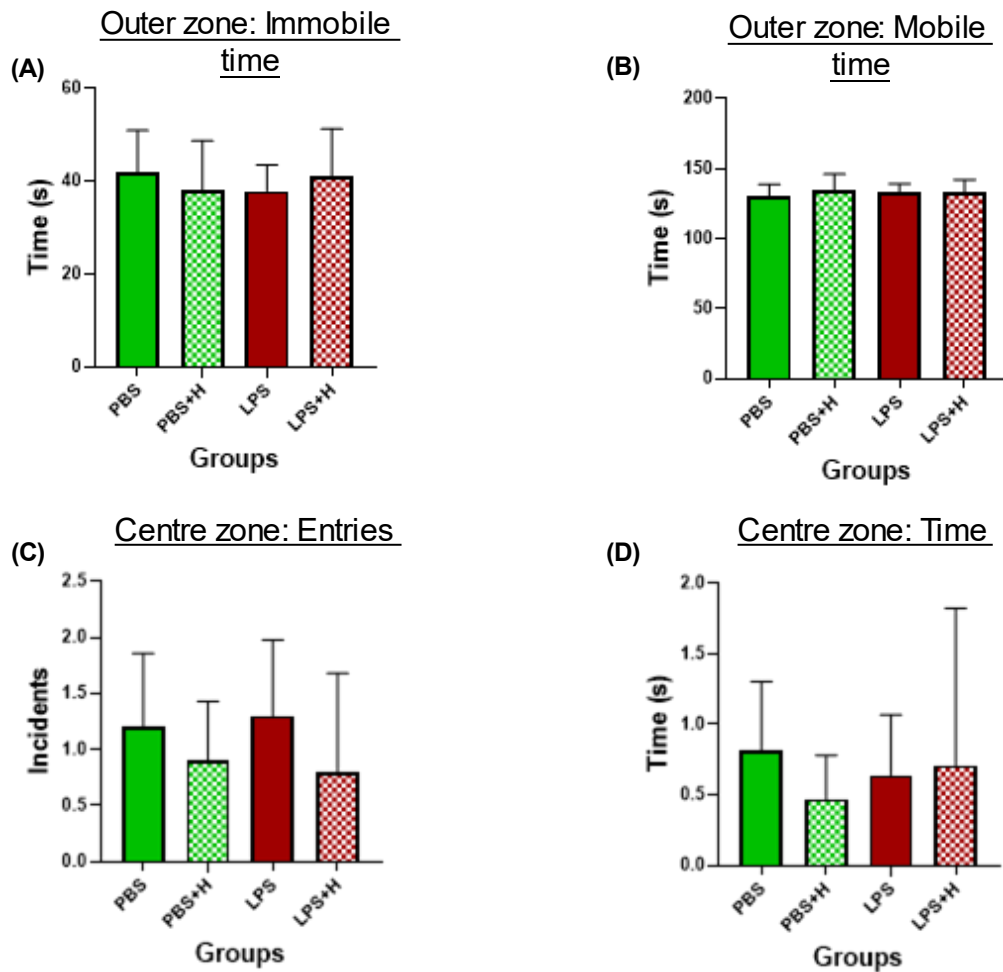
---

When the control groups were compared to the experimental groups, the study found no significant differences in distance travelled, mean speed, mobile time and immobile time. The data is illustrated in Figure 4.1.



**Figure 4.1: Open field test control and experimental group mobile profiles-** The Open field test was conducted and these float bars represent the following: distance, mean speed, mobile time, immobile time, consisted of the mobile profile. The study found that the movement mobility, speed, and time of each animal group did not display significant differences. Top line: the maximum value, Middle line: the mean, Bottom line: minimum value.

When the control groups were compared to the experimental groups, the study found no significant differences in outer zone: immobile time, outer zone: mobile time, centre zone: entries and centre zone: time. The mean and 95% confidence interval of each group are graphically displayed in Figure 4.2.



**Figure 4.2: Open field test control and experimental group zone profiles-** The Open field test was conducted and these float bars represented the mean time and entries into the specific zones (outer and centre) travelled by each animal group. The study found that the movements in each zone did not display significant differences. Top line: the maximum value, Middle line: the mean, Bottom line: minimum value.

### 4.3.2 The Novel object recognition test analysis

During the experimental period, the Novel object recognition was conducted on each animal. The following results illustrate data from the first and second trial of the experimental and control groups. The data was compared using a One-Way ANOVA on GraphPad prism 9.0.0 and discovered that there was no statistical difference between the groups and the animals generally did not show significant difference between the two trials. A Two-way ANOVA compared the various categories in trial one and trial two as well as the first and second trial of each individual in all the testing categories. The P-value was calibrated at  $\leq 0.05$ . The data is illustrated in tables 4.4 and 4.5, and figures 4.3.

Table 4.4 documents the One-way ANOVA findings that the experimental and control groups lacked significant differences in their overall mean values in all of the tested criteria.

Table 4.4: Novel object recognition test- Overall group statistical comparisons

<b>Groups</b>	<b>P-value</b>	<b>Significant (yes or no)</b>
<b>PBS vs PBS+H</b>	0,9996	No
<b>PBS vs LPS</b>	0,9994	No
<b>PBS vs LPS+H</b>	>0,9999	No
<b>PBS+H vs LPS</b>	>0,9999	No
<b>PBS+H vs LPS+H</b>	0,9995	No
<b>LPS vs LPS+H</b>	0,9992	No

A Two-way ANOVA was conducted and the experimental and control groups showed no statistical differences in the time spent or entries made into block A or C in both trials as displayed in table 4.5.

Table 4.5: Novel object recognition- Group statistical comparisons

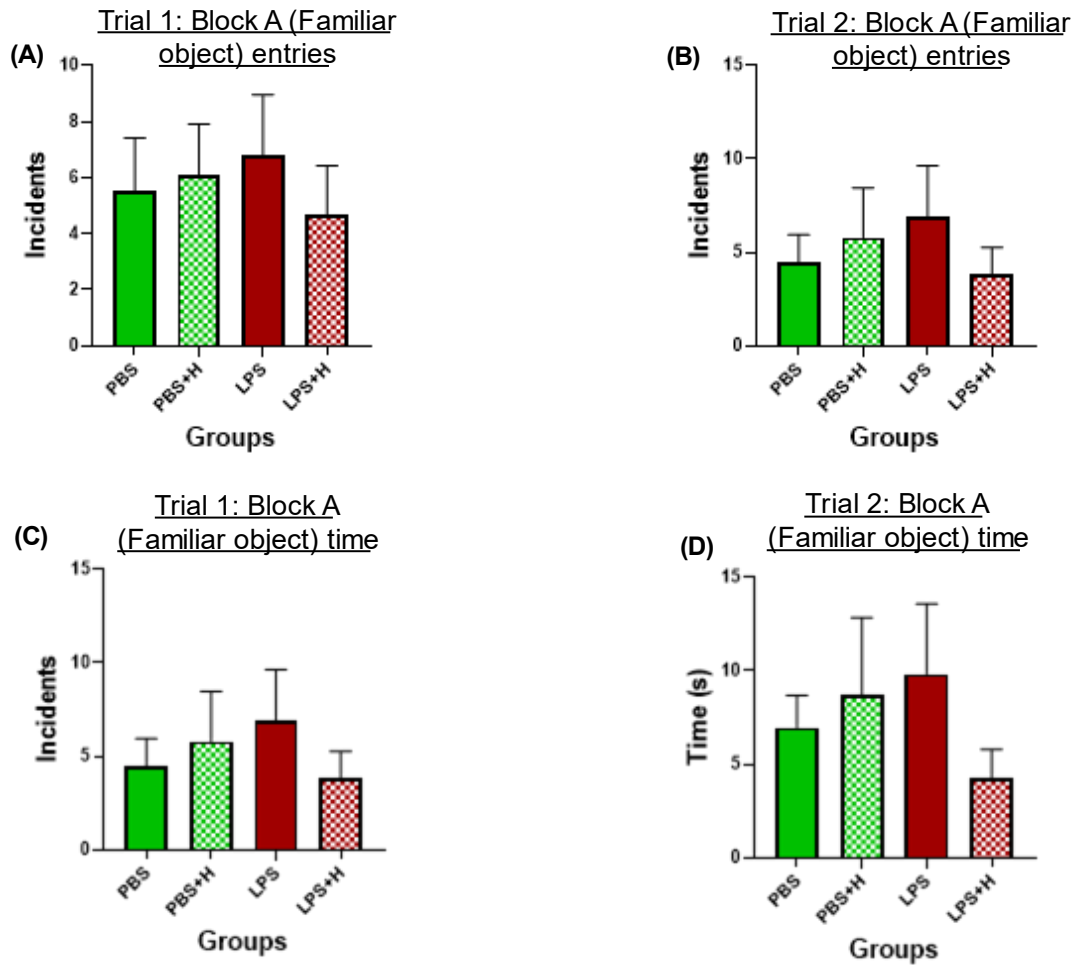
<b>Groups</b>	<b>Category</b>	<b>P-value</b>	<b>Significant (yes/no)</b>
<b>PBS vs PBS+H</b>	<b>Trial 1 Block A: entries</b>	0,9983	No
<b>PBS vs LPS</b>		0,9833	No
<b>PBS vs LPS+H</b>		0,9960	No
<b>PBS+H vs LPS</b>		0,9973	No
<b>PBS+H vs LPS+H</b>		0,9793	No
<b>LPS vs LPS+H</b>		0,9348	No
<b>PBS vs PBS+H</b>	<b>Trial 2 Block A: entries</b>	0,9833	No
<b>PBS vs LPS</b>		0,9064	No
<b>PBS vs LPS+H</b>		0,9973	No
<b>PBS+H vs LPS</b>		0,9897	No
<b>PBS+H vs LPS+H</b>		0,9430	No



LPS vs LPS+H		0,8192	No
PBS vs PBS+H		0,8809	No
PBS vs LPS		0,9805	No
PBS vs LPS+H	<b>Trial 1 Block A: Times</b>	0,9905	No
PBS+H vs LPS		0,9847	No
PBS+H vs LPS+H		0,9717	No
LPS vs LPS+H		0,9998	No
PBS vs PBS+H		0,9639	No
PBS vs LPS		0,8522	No
PBS vs LPS+H	<b>Trial 2 Block A: Times</b>	0,8675	No
PBS+H vs LPS		0,9880	No
PBS+H vs LPS+H		0,5956	No
LPS vs LPS+H		0,3932	No
PBS vs PBS+H		>0,9999	No
PBS vs LPS		0,9696	No
PBS vs LPS+H	<b>Trial 1 Block C: Entries</b>	0,9995	No
PBS+H vs LPS		0,9747	No
PBS+H vs LPS+H		0,9998	No
LPS vs LPS+H		0,9867	No
PBS vs PBS+H		0,9575	No
PBS vs LPS		0,7581	No
PBS vs LPS+H	<b>Trial 2 Block C: Entries</b>	0,9998	No
PBS+H vs LPS		0,9639	No
PBS+H vs LPS+H		0,9747	No
LPS vs LPS+H		0,8046	No
PBS vs PBS+H		0,9908	No
PBS vs LPS	<b>Trial 1 Block C: Time</b>	0,9913	No
PBS vs LPS+H		0,9001	No
PBS+H vs LPS		>0,9999	No

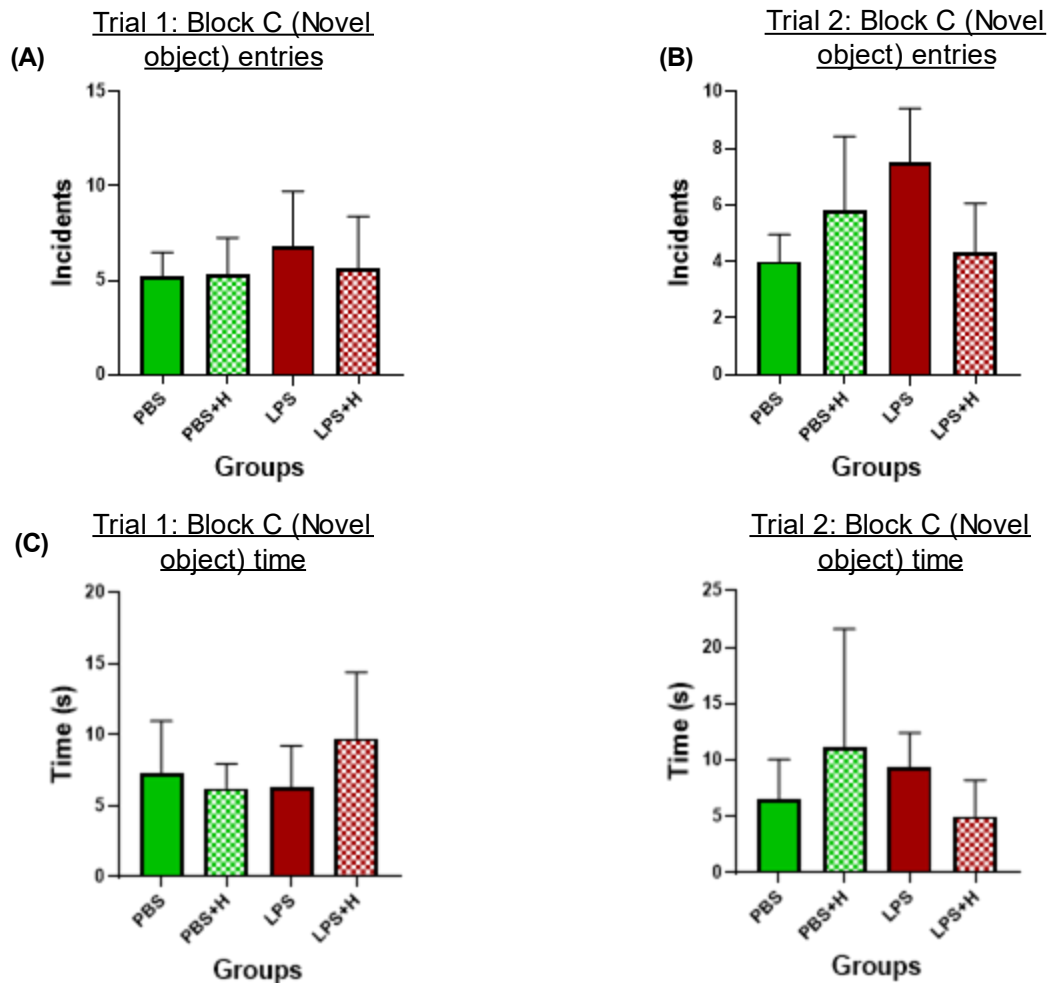
<b>PBS+H vs LPS+H</b>		0,7549	No
<b>LPS vs LPS+H</b>		0,7581	No
<b>PBS vs PBS+H</b>		0,5758	No
<b>PBS vs LPS</b>		0,8675	No
<b>PBS vs LPS+H</b>	<b>Trial 2 Block C: Time</b>	0,9727	No
<b>PBS+H vs LPS</b>		0,9569	No
<b>PBS+H vs LPS+H</b>		0,3173	No
<b>LPS vs LPS+H</b>		0,6243	No
<b>Abbreviations: H: Manuka honey, LPS: Lipopolysaccharide, PBS: Phosphate-buffered saline, SD: Standard deviation</b>			

The experimental and control groups did not show significant differences in the amount of time spent or entries made into block A. The mean and 95% confidence interval of the block A's entries and times are displayed in figure 4.3.



**Figure 4.3: Novel object recognition test trial 1 and 2 Block A (Familiar object) entries and times-** The Novel object recognition test was conducted and the study found that there were no significant differences in the Block A (Familiar object) entries and times between the groups and the trials.

The experimental and control groups did not have significant differences in the entries made and time occupied at block C. The mean and 95% confidence interval of the entries and time passed at block C are illustrated in figure 4.4.



**Figure 4.4: Novel object recognition test trial 1 and 2 block C (Novel object) entries and times-** The Novel object recognition test was conducted and the study found that there were no significant differences in the block C (novel object) entries and times between the groups and the trials.

A Two-way ANOVA was conducted comparing the individual control and experimental groups followed by comparing trial one and two. The test found the results of the control, treated control, experimental and treated experimental group did not improve or worsen in performance thus resulting in no significant difference within the groups between the following categories in trial one and two: block A and C entries and times.

### 4.3.3 The Y-Maze test analysis

The following results document the findings acquired during testing phase. The data was compared using a One-Way ANOVA on GraphPad prism 9.0.0 and discovered that there was no statistical difference between the evaluated testing categories of the control and experimental groups as illustrated in table 4.6. However, upon conducting a Two-way ANOVA,

the time spent in the N arm was statistically different when comparing some of the testing groups. The P-value was  $\leq 0.05$ . Table 4.7 and 4.8 illustrates the F and N arm group comparisons. The data is illustrated in figure 4.5 and 4.6.

**Table 4.6: Y-Maze- Overall comparison of the parameters**

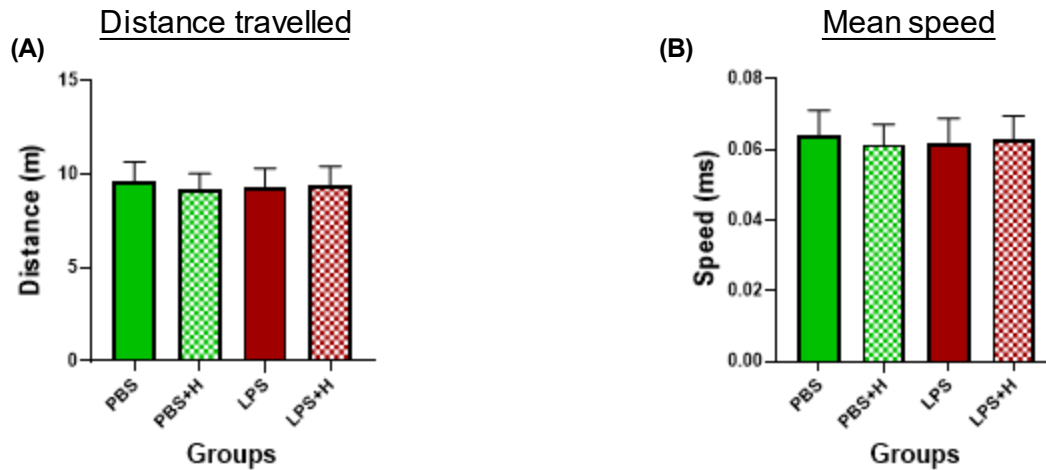
<b>Groups</b>	<b>P-value</b>	<b>Significant (yes or no)</b>
<b>PBS vs PBS+H</b>	>0,9999	No
<b>PBS vs LPS</b>	>0,9999	No
<b>PBS vs LPS+H</b>	>0,9999	No
<b>PBS+H vs LPS</b>	>0,9999	No
<b>PBS+H vs LPS+H</b>	>0,9999	No
<b>LPS vs LPS+H</b>	0,9998	No

A Two-way ANOVA was conducted and the findings are as follows: When comparing the habituation and testing time spent in F arm all the groups showed significant differences. All the animal groups spent less time in the F arms during testing.

**Table 4.7: Y-Maze- Familiar time: Habituation vs testing time comparisons**

<b>Category</b>	<b>Mean difference (s)</b>	<b>P-value</b>	<b>Significant (yes or no)</b>
<b>Testing: Habit arm times vs Habituation Familiar arm time</b>	-47.72	< 0.0001	Yes (****)
<b>Symbols- *: P <math>\leq</math> 0.05, **: P <math>\leq</math> 0.01, ***: P <math>\leq</math> 0.001, **** P <math>\leq</math> 0.0001</b>			

The distance and mean speed (mean and 95% confidence interval) of the control and experimental groups were documented and are illustrated in figure 4.5. After performing a Two-way ANOVA test, the study found that the testing groups showed no significant difference in the distance and the mean speed travelled during the test.



**Figure 4.5: Y-Maze test distance and mean speed-** The Y-Maze test was conducted and the study found that there were no significant differences in the distance and mean speed.

Upon conducting the Two-way ANOVA statistical test, the animal groups displayed no significant differences between the F arm entries. The study found that the vehicle control and two experimental groups showed significant differences for the F arm times. The control group spent significantly less time in the F arm compared to the two experimental groups. While the experimental and the treated experimental group showed significant F arm: time differences. The LPS group also showed significantly less time in the F arm when compared to the treated experimental group. After the other groups were compared to each other there were no significant differences in the time they spent in the F arm as shown in table 4.8. Less time spent in the F arm indicates greater retained short term spatial memory.

**Table 4.8: Familiar arm: times - Group statistical comparisons**

Groups	Mean differences	P-value	Significant (yes or no)
PBS vs PBS+H	-4,420	0,4069	No
PBS vs LPS	0,5000	0,9981	No
PBS vs LPS+H	-7,840	0,0310	Yes (*)
PBS+H vs LPS	4,920	0,3101	No
PBS+H vs LPS+H	-3,420	0,6262	No
LPS vs LPS+H	-8,340	0,0186	Yes (*)

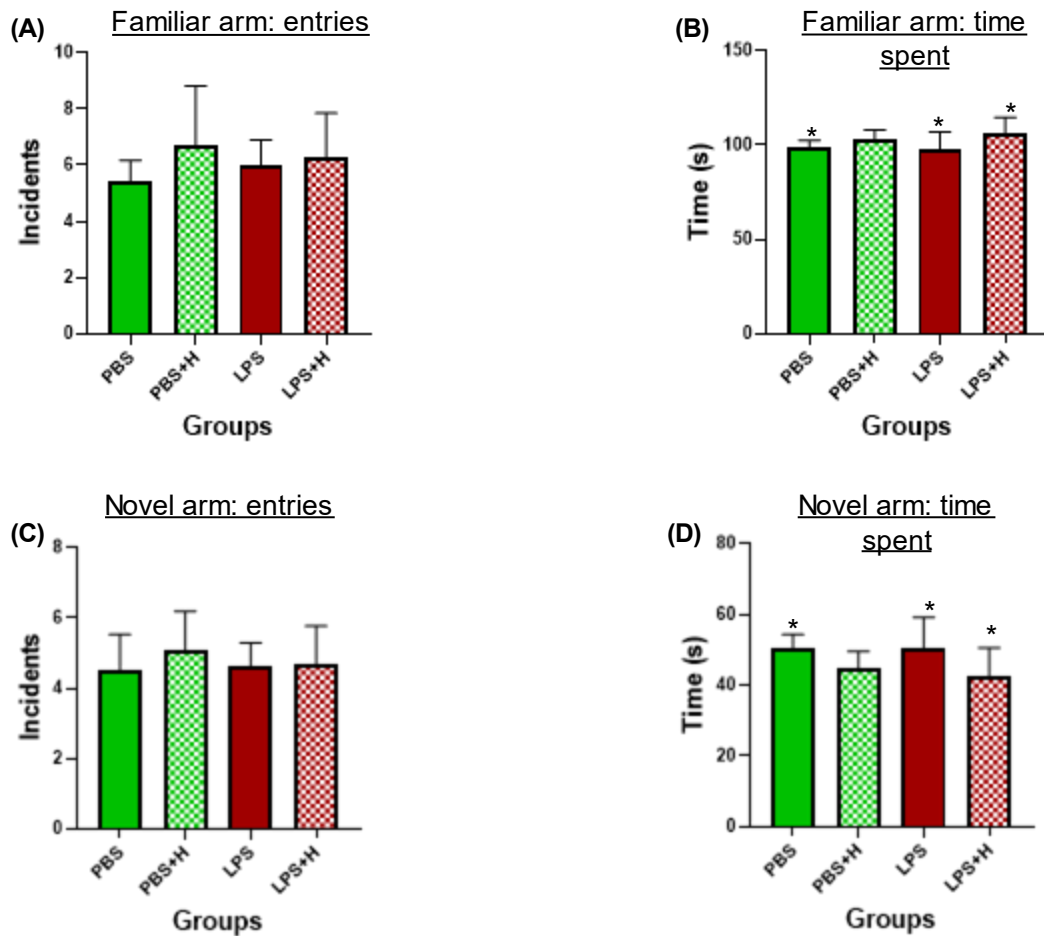
Symbols- \*:  $P \leq 0.05$ , \*\*:  $P \leq 0.01$ , \*\*\*:  $P \leq 0.001$ , \*\*\*\*  $P \leq 0.0001$

The N and F arm entries are illustrated in figure 4.6. The control and experimental groups showed no differences in the entries made into N arm. Although the number of N arm entries is an indication of short-term spatial memory, the time spent in the N arm provides a picture of greater accuracy. Greater time occupied in the N arm indicated greater retained short term spatial memory. When the time spent in the N arm was compared, the following was found, the control and treated experimental group showed a significant difference between them. The control group spent significantly more time in the N arm than the treated experimental group. In addition, the experimental and treated experimental group showed significant difference in the time they occupied the N arm. The experimental group spent significantly more time in the N arm than the treated experimental group. The following is shown in table 4.9.

**Table 4.9: Novel arm: times - Group statistical comparisons**

<b>Groups</b>	<b>Mean differences</b>	<b>P-value</b>	<b>Significant (yes or no)</b>
<b>PBS vs PBS+H</b>	5,590	0,2033	No
<b>PBS vs LPS</b>	-0,06000	>0,9999	No
<b>PBS vs LPS+H</b>	7,970	0,0272	Yes (*)
<b>PBS+H vs LPS</b>	-5,650	0,1952	No
<b>PBS+H vs LPS+H</b>	2,380	0,8373	No
<b>LPS vs LPS+H</b>	8,030	0,0256	Yes (*)

**Symbols- \*: P ≤ 0.05, \*\*: P ≤ 0.01, \*\*\*: P ≤ 0.001, \*\*\*\* P ≤ 0.0001**



**Figure 4.6: Y-Maze familiar and novel arms entries and times-** The Y-Maze test was conducted and the study found significant differences in the time spent in the F and N arm between the control and treated experimental group as well as between the experimental groups.

## 4.4 Discussion

As a consequence neurological LPS exposure results in neuroinflammation, this pathophysiological phenomenon may play a pivotal role in neurodegenerative diseases such as AD aetiology and progression<sup>191,196</sup>. Previous research has discovered the endotoxin resides in the hippocampal and superior temporal lobe neocortex brain lysates of AD patients<sup>191</sup>. The average LPS levels ranged from two-fold neocortex upsurges to three-fold hippocampal upsurges in the age-matched control group, some of the test subjects with advanced AD displayed a 26-fold LPS elevation<sup>191</sup>.

This chapter explored the effects of early LPS exposure on young male rats through performing behavioural analyses to assess anxiety, movement, spatial, short-term and long-term object recognition memory. The groups were compared by averaging the scores each



animal received in the individual parameters by conducting a One-way ANOVA as well as the comparing mean scores the groups had received on a specific parameter using the Two-way ANOVA. The overall comparison between the groups and the specific parameter evaluations allowed for greater precision and specificity.

The Open field test was used to both introduce the animals to the testing environment, and reduce anxiety as a confounding factor in the following tests and it was used to evaluate anxiety levels. No significant differences could be found between the groups when comparing them as a whole or when comparing individual parameters. Therefore, the animals showed the same levels of anxiety. Testing the distance, mean speed, overall mobile time and immobile time also evaluated effects of early LPS exposure on motility (indication of fatigue). The test subjects did not display significant differences in any of the evaluated parameters and thus didn't indicate significant differences in the energy levels. Therefore, early low dose LPS exposure does not elevate or reduce anxiety, or change motility patterns and no conclusive evidence that Manuka honey administration enhanced or reduced the anxiety brought about by LPS. Nevertheless, studies have shown that the release of IL-1 $\beta$  in the central nervous system in response to inflammation and stress is closely related to anxious and depressed behaviour<sup>197-198</sup>. Research suggests that neuro-inflammation and dysfunctional hippocampal autophagy play a key role in the manifestation of anxious-, depressed behaviour and neurodegenerative disease<sup>199-200</sup>. The endotoxin increases microglial activation and reactive oxygen species (ROS) release in all ages<sup>201</sup>. The underlying autophagy and neuro-inflammation regulation resulting in pro-inflammatory cytokine release may result from microglial activation and the elevation of microglial activation levels as a consequence of LPS exposure. The endotoxin may induce anxious-, depressed behaviour and cognitive disease. The present study may show that early low dose LPS exposure does not induce significant microglial activation resulting in insignificant IL-1 $\beta$  release resulting in the insignificant changes in locomotion seen in the experimental and control groups or that they may be an absence microglial activation.

The Novel object recognition data showed that the test subjects typically showed similar interest levels in the novel object. The interest levels showed in Block C in trial one and two did not significantly differ. The trials showed no significant differences to each other, the animals recognised the familiar block and there was no significant difference in the time spent in trial one and two. The test found that the groups showed similar short- and long-term memory. Thus, early low dose LPS exposure did not significantly affect short or long-term memory, and no conclusive evidence showed that Manuka honey administration enhanced or reduced the harmful effects of LPS on short- and long-term object recognition memory. However, a study conducted by Mastinu et al. (2019) documented that LPS induced

hippocampal inflammation without affecting locomotion however, but the test group lost the ability to distinguish the novel object from the familiar object<sup>202</sup>. The present study may show that early low dose LPS exposure does not induce significant amounts of neuroinflammation to induce familiar object recognition impairment. Nevertheless, research shows that long-term memory performance alteration, IL-1 $\beta$  and TNF- $\alpha$  are a consequence of LPS induced interleukin-6 (IL-6) expression<sup>202</sup>. Thus, continual LPS exposure may result in long-term memory deficits.

However, the Y-Maze found that the evaluated groups exhibited a substantial difference in the F arm entries between the habituation and testing indicating an intact working recall memory. The groups also showed no significant difference in the distance travelled and mean speed used during the test. The groups also showed no significant differences between F arm and N arm entries however, the control and treated experimental group showed significant differences in the time spent in the F arm. The control spent significantly less time in the F arm and more time in the N arm compared to the treated experimental group. This signifies that the control group had greater spatial memory than treated the experimental groups. While experimental and treated experimental group showed significant F and N arm time differences. The experimental group also had spent significantly less time in the F arm and more time in the N arm when compared to the treated experimental, indicating that the experimental group had better spatial memory. However, when comparing the experimental group to the control groups no significant differences were found in the time spent in the F and N arm, thus showing similar spatial memory. Therefore, Manuka honey may enhance neurodegenerative capabilities of LPS.

A study conducted Hauss-Wegrzyniak et al. (2000) discovered that after injecting LPS into the fourth ventricle over a 37-day period resulted in fever or seizures as a consequence and the endotoxin impaired spatial memory but did not affect object recognition memory<sup>203</sup>. Spatial memory may be affected before novel object recognition is impaired. The study identified many hippocampal neurons that displayed paired rough endoplasmic reticulum cisternae and other ultrastructural changes to structures such as Golgi apparatus which suggested damaged or reduced cellular protein synthesis with the cytoplasm<sup>203</sup>.

In addition, the treated experimental displayed greater spatial memory impairment indicating greater hippocampal damage as a consequence. Researchers have found that Manuka honey exposure concludes in the release of the following pro-inflammatory cytokines: IL-1  $\beta$ , IL-6 through the TLR-4- dependent mechanism and TNF $\alpha$ , aiding in accelerated wound repair<sup>204</sup>. However, Manuka honey also possesses anti-inflammatory effects that can reduce free radical production. The two work together through the manifestation of a two-pronged mechanism

and although the anti-inflammatory property and pro-inflammatory cytokine release may be an effective wound treatment, it may not be suitable when coupled with LPS exposure<sup>204</sup>. The pro-inflammatory cytokine production of Manuka honey may have elevated neuroinflammation in the hippocampus, thus concluding in greater physiological damage, nevertheless more research needs to be conducted.

The other animal groups showed similar spatial memory properties exhibited in the experimental group indicating that early low dose LPS exposure does not produce fatigue or memory deficits at first. The neuroinflammatory effects of LPS may be subclinical or non-existent. However, inflammatory proteins are elevated in AD patients, years before neurodegeneration begins or signs of illness occur as is seen in the LPS experimental rat group<sup>205</sup>. Nevertheless, research shows that continual LPS exposure eventually produces memory loss<sup>206</sup>.

## **4.5 Conclusion**

The chapter highlighted that early low dose LPS exposure results in no initial memory deficits (spatial, short- and long-term, or novel object recognition memory). Thus, the neurological damage may be subclinical thus producing no noticeable behavioural or memory anomalies or non-existent. In addition, the endotoxin did not affect motility. However, this chapter could not highlight whether or not Manuka honey is a suitable treatment for the neurodegenerative symptoms produced by LPS because early LPS exposure did not produce effects on behaviour or memory. The treatment is seen to enhance spatial memory deterioration induced by LPS and despite its anti-inflammatory properties, the stimulated pro-inflammatory cytokine release may cause the spatial memory deficits seen in the treated experimental group. The next chapters will evaluate the effects of LPS on the following: aortic and cardiac myofibril and mitochondrial structure, CV cellular element morphology (erythrocyte, fibrin network and platelet) temperature, weight. In addition, will evaluate physiological consequence of Manuka honey on the harmful effects of LPS on these parameters.

# **Chapter 5: Body weight and temperature**

## **5.1 Chapter Objectives**

Assess and compare the body temperatures of the experimental, treated experimental, control and treated control group.

Assess and compare the weight gain rates of the experimental, treated experimental, control and treated control group.

## **5.2 Introduction**

The Lipopolysaccharide endotoxin exposure induces sickness behaviours such as weight loss, decreased locomotion, increased anxiety and fever and/or hypothermia<sup>207-208</sup>. As previously stated systemic inflammation may also facilitate weight loss and temperature changes<sup>190</sup>. Weight loss and temperature changes are often the first or only sickness behaviour exhibited by LPS exposed animals, however this is dose dependent<sup>135-136</sup>. A study conducted by Moraes et al. (2017) observed that LPS (dose: 1 mg/kg/day) induced sickness behaviour in rats<sup>136</sup>. In addition, a study conducted by Bison (2009) et al. has shown that significant weight loss observed in animals exposed to varying low doses (0.001, 0.005, 0.015, 0.05, 0.125, and 0.25 mg/kg)<sup>135-136</sup>. Unfortunately, current research fails to explain the mechanisms resulting in LPS induced weight loss, thus further research is required.

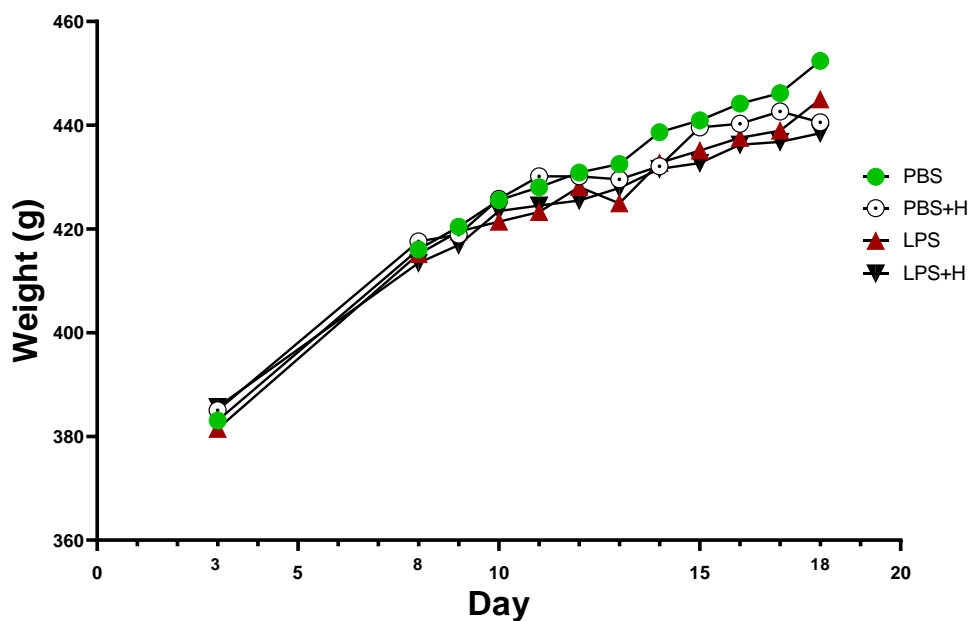
Hypothermia arises in severe systemic inflammatory syndrome cases instead of fever and is an adaptive host mechanism to reduce injury as a result of the inflammatory response induced by the innate immune system<sup>209</sup>. Hypothermia aids in endotoxin elevation, abdominal organ dysfunction, hypotension, and mortality reduction in *E. coli* injected animals<sup>210</sup>. Lipopolysaccharide intraperitoneal (IP) administration results in the dose-dependent fever or hypothermia induction: a low 0.05 to 0.1 mg/kg dose brought about hyperthermia (fever), whereas a high 2.5 mg/kg dose caused hypothermia in mice<sup>211</sup>. Both thermodynamic responses are complementary survival mechanisms and there is limited information on the fever, hypothermia switching mechanism<sup>211</sup>.

The aim of this chapter is to compare the weight and core body temperatures of the control and experimental groups. The chapter explores the development of body- temperature and weight changes upon low dose LPS exposure. Both markers were an indication of the possible severity of the sickness behaviours that LPS induced and Manuka honey was introduced as a treatment.

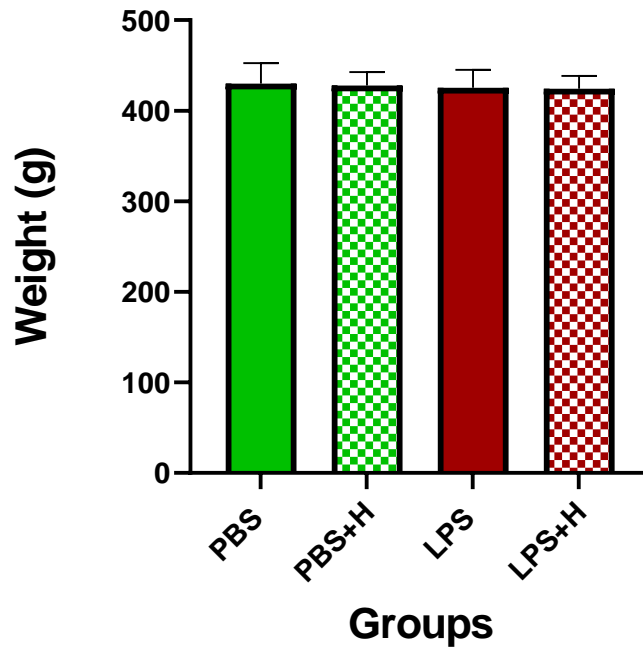
## 5.3 Results

### 5.3.1 Weight analysis

During the experimental period, every test subject was weighed on these specific days, days: three, eight to eighteen as illustrated in figure 5.1 and 5.2. The data was analysed on GraphPad Prism 9.0.0. A One-way ANOVA was conducted and no significant differences in weight between of the experimental, treated experimental, control and treated control group were found. A Two-way ANOVA found that there was no significance between the weight gained on any particular day.



**Figure 5.1: Daily body weight gain-** The weights were taken on day three, eight to eighteen. Significant differences between the control and experimental groups were evaluated at a p-value of  $\leq 0.05$ .



**Figure 5.2: Total mean weight of Sprague Dawley rats-** Displays the mean total weight gain that each testing group attained.

### 5.3.2 Core body temperature analysis

The rectal temperatures of the experimental and control rat groups were measured and documented before termination. The statistical data is illustrated in table 5.1, table 5.2 and figure 5.3. The data was analysed on GraphPad Prism 9.0.0. and a Two-way ANOVA found that there were no significant differences between the temperatures of the experimental, treated experimental control and treated control group.

**Table 5.1: Core temperature- Test groups statistics**

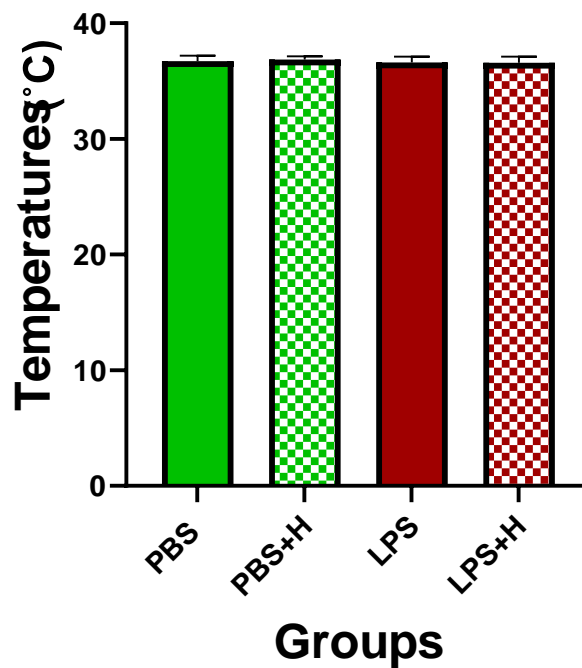
Temperature (°C)		
Group	Median	Mean ± SD
PBS	36,8	36,74 ± 0,65
PBS + H	37	36,85 ± 0,41
LPS	36,8	36,63 ± 0,65
LPS + H	36,9	36,58 ± 0,74

Abbreviations: H: Manuka honey, LPS: Lipopolysaccharide, PBS: Phosphate-buffered saline, SD: Standard deviation

Table 5.2: Core temperature- Group temperature comparisons

Temperature (°C)		
Groups	P-value	Significant (yes/no)
PBS vs PBS+H	0,9264	No
PBS vs LPS	0,9534	No
PBS vs LPS+H	0,9102	No
PBS+H vs. LPS	0,6712	No
PBS+H vs LPS+H	0,5846	No
LPS vs. LPS+H	0,9990	No

Abbreviations: H: Manuka honey, LPS: Lipopolysaccharide, PBS: Phosphate-buffered saline, SD: Standard deviation



**Figure 5.3: Total mean core temperature of Sprague Dawley rats-** This figure displays the mean and 95% confidence interval total of the core temperature of each test group measured in degrees Celsius.



## **5.4 Discussion**

Body weight and core temperature were used as health biomarkers. In addition, core body temperature was used as an immune response indicator, because bacterial infections induce hyperthermia<sup>211</sup>. Lipopolysaccharides induce inflammation as an immune response<sup>211</sup>. In this study, hypothermia was defined as 33.0–34.0 °C and normothermia was defined as 36.99 ± 0.42 °C<sup>212</sup>. In addition, research has found that LPS introduction at significant systemic circulation results in weight loss<sup>207-208</sup>. The present study administered LPS concentration was a low physiological level of 0.05 mg/kg dose (SC injection) studies have found that such a dose would result in a mild chronic systemic inflammation. The dose simulates the dose that humans with loose teeth and/or impaired gastrointestinal tight junctions may have in their CV circulation<sup>20</sup>.

After ten days of LPS exposure, there were no significant changes in the body weight- and temperatures of the control, treated control, experimental and treated experimental group. A steady weight increase comparable to the control groups was observed in the experimental groups. While a rectal temperature that resembled the control rat groups was observed in the experimental rat groups. The experimental groups experienced low systemic inflammation levels that resulted in an insignificant thermo-generation, thermo-reduction and weight decline. Significant mitochondrial dysfunction in the form of mitochondrial uncoupling may not have occurred. There was no significant difference in the body- weight and temperature of the treated experimental group and the experimental group. Although within normothermia criterion, the experimental groups had lower mean temperatures than the control rat groups. Previous studies have documented that, low LPS doses result in hyperthermia, however lowered body temperatures may be a consequence of LPS induced hippocampal damage, both cannot be concluded in this study<sup>203</sup>. In addition, the Manuka honey treated experimental group presented with mean temperature that were lower than the experimental group however, the results were inconclusive and thus it could not be determined if Manuka honey is an effective or ineffective treatment. Nevertheless, both experimental groups test subjects remained seemingly as healthy as the control group during early LPS exposure.

## **5.5 Conclusion**

As a consequence, it is unknown if chronic systemic inflammation experienced by the LPS exposed animals or if the lack of symptoms stems from an insignificant immune response however, physicians cannot use weight loss and body temperature as biomarkers for LPS exposure. Studies have found that low dose LPS exposure results in low grade chronic

systemic inflammation however, this study documents that the inflammation does not result in thermo-dysfunction or weight loss in the initial stages. The following chapters will explore whether LPS induces significant damage to the individual CV cellular elements (erythrocyte, fibrin network and platelet morphology investigation), cardiomyocyte damage, and total cholesterol elevation or reduction. In addition, perhaps upon further exposure, the experimental animals may have displayed significant loss weight and temperature elevation or reduction when compared to the control groups. Such information would be vital for diagnostic purposes in a follow up study.

# **Chapter 6: Investigating the histology of the cardiovascular system**

## **6.1 Chapter Objectives**

Investigate the ultrastructural morphology of aortic and cardiac muscle cells of the experimental and control rat groups using transmission electron microscopy. The aim was to study the elastic fibre morphology of the aorta in both groups by utilizing the Verhoeff-Van Gieson staining technique using light microscopy.

In addition, study possible general cardiac muscle cell abnormalities in the tissue fibres of the groups by making use of the Haematoxylin and Eosin staining technique using light microscopy.

Lastly, to study cardiac tissue fibre polysaccharide content of the groups using Periodic Acid-Schiff staining technique using light microscopy.

## **6.2 Introduction**

The CV system plays a vital role in blood oxygenation and immunity<sup>213</sup>. This chapter aims to investigate cardiac and aortic tissue histology and compare the experimental and control rat tissue.

The heart consists of long branched single or multiple nuclei cardiomyocytes with a sarcoplasm that contain an abundance of mitochondrial and glycogen as well as some lipofuscin pigment. Cardiomyocytes are arranged into atrial and ventricular components<sup>214</sup>. These atrial and ventricular components allow for the heart muscle to contract, propelling blood throughout the body. However, tight junctions exist between well-arranged cardiomyocyte structures resulting in optimal cardiac performance<sup>38</sup>. This arrangement concludes in electrical and mechanical communication between cells, in addition, the cardiac muscle presents as striations and Z-lines. Available nutrients allow cardiomyocytes to contain large mitochondria numbers which are in close contact with the muscle fibrils. These mitochondria efficiently power the cardiac muscle fibres which form complete units with cell membranes regardless of their branching and interdigitated nature<sup>215</sup>. When one muscle fibre ends another begins. Each fibre's cell membrane lies parallel to the other resulting in a series of folds<sup>215</sup>. These areas occur at the Z-disk and are called intercalated disks. These disks provide a strong union between the muscle fibres, maintain constant cell-to-cell communication<sup>215</sup>. In addition to the intercalated disks, which result in the interconnectedness of the heart, are gap junctions that are electrical connections between cardiomyocytes that which act as low-resistance bridges<sup>215</sup>. These bridges spread signals from one fibre to the next permitting the cardiac muscle fibres to beat concurrently with one another even though protoplasmic bridges between the cardiomyocytes are absent<sup>215</sup>. However, pathology can

inhibit cardiac functioning. Cardiomyocyte autophagy is a consequence of LPS exposure and hypoperfusion may occur as a result<sup>216</sup>.

Normally cardiac structures allow optimal contraction while the blood vessels form the ideal transport structure<sup>38</sup>. As a result of the presence of blood vessels in all organs and tissues, cardiac or vascular disease are not restricted to a small range of signs and symptoms which makes diagnosis formulation difficult<sup>217</sup>. For that reason, all organs are potential targets of injury when vascular disease occurs<sup>217</sup>. The CV pathology may result in symptoms indicative to injury to a specific organ or tissue a result of a diminished nutrient or oxygen supply resulting in further pathogenesis<sup>217</sup>.

Blood vessel diseases are a burden on modern society and upon exposure researchers have found that LPS has atherosclerotic effects that may be the result of elastin depletion or damage<sup>115</sup>. Potentially contributing to or resulting in vascular disease. Elastin is produced by perivascular smooth muscle cells that form the tunica media elastic lamellae<sup>172</sup>. The blood vessel walls of large arteries consist of epithelial tissue, connective tissue and smooth muscle. Collagen fibres are distributed between the smooth muscle layers and the epithelium<sup>218</sup>. In addition, Elastin is a major component<sup>172,218</sup>. The elastin is organised into concentric fenestrated lamellae rings that are between myocyte layers allowing these fibres to stretch up to 50% of their length before recoiling to their original length. This is a vital characteristic that allows elastin within the arteries tunica media to facilitate blood flow pressure wave propagation specifically in elastic blood vessels such as the pulmonary arteries and the aorta<sup>172</sup>. This phenomenon is known as the Windkessel effect and it allows the maintenance of uniform arterial blood pressure, despite pulsatile blood flow, the stiffening of these vessels may disrupt this uniform flow<sup>172</sup>.

As stated above, it has been proven that LPS shed from gram-negative bacteria causes systemic inflammation that may have the ability to exacerbate the development of various CV illnesses<sup>21,143,219</sup>. The heart and blood vessels would be the organs that are in closest contact with the toxin as it circulates through the body. This study has investigated the effects of LPS on the following: ultrastructural and elastic fibre morphology, mitotic phase abnormalities, cardio muscular and mitochondrial abnormalities, using light microscopy and transmission electron microscopy.

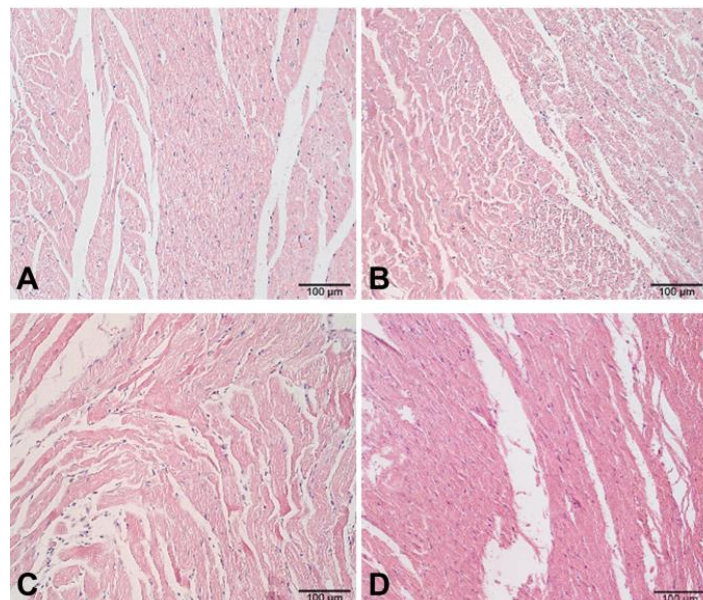
The aim of this chapter was to investigate the cardiac and aortic morphological differences between the control and experimental groups, this will show the various effects that LPS may have on the CV system.

## **6.3 Results**

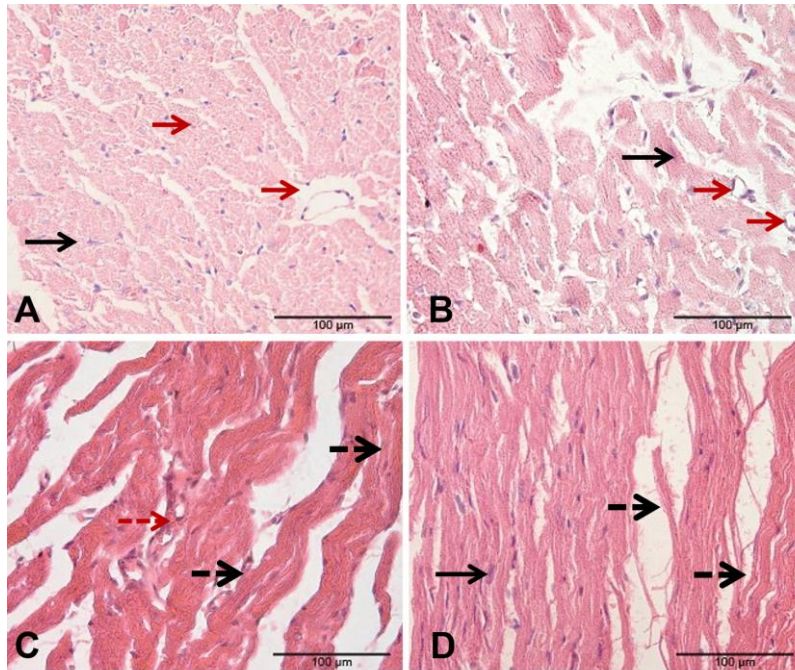
### **6.3.1 Light microscopy: Lipopolysaccharides effect on cardiac and aortic tissue and exploring Manuka honey as a treatment**

#### **Cardiac muscle**

Haematoxylin and Eosin allowed for the identification and documentation of normal or pathological cardiomyocyte and aortic cell morphology. The findings of both the control and experimental groups are documented in figure 6.1 and figure 6.2 which displays a general overview of the myofibrils of the control and experimental groups, while the figure 6.2 provides a magnified image allowing for the detailed examination. The myofibrils displayed by the control and treated control group (figures 6.1 A and B) were normal neatly arranged myofibrils at low magnification. While at high magnification (figures 6.1 A and B) both the myofibrils of the control and treated control group displayed oval and centralised nuclei that contained blood vessels and capillaries. Both the experimental and treated experimental group displayed oval nuclei. However, the experimental group displayed in figures 6.1 and 6.2 C myofibril damage and erythrocyte extravasation. In addition, the treated experimental group showed myofibril damage.

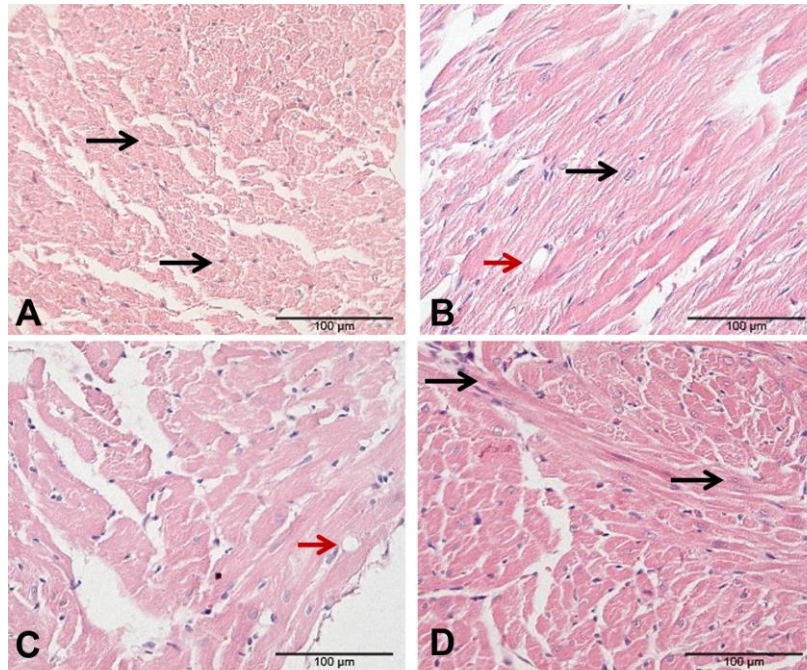


**Figure 6.1: Haematoxylin and Eosin cardiac muscle 20x sections-** Figure A (control), Figure B (treated control), Figure C (experimental), Figure D (treated experimental). The images display a general overview of the cardiovascular tissue found in each group. The images were captured at 20 x magnification. (Scale bar: 100 µm)



**Figure 6.2: Haematoxylin and Eosin cardiac muscle 40x sections-** Figure A (control), Figure B (treated control), Figure C (experimental), Figure D (treated experimental). The images display a detailed image of the common condition of the cardiovascular tissue found in each group. The images were captured at 40 x magnification. Black arrow: Oval and centrally located nuclei, Black dashed arrow: Myofibril damage. Red arrow: Blood vessel and capillaries. Red dashed arrow: Erythrocyte extravasation (Scale bar: 100 µm)

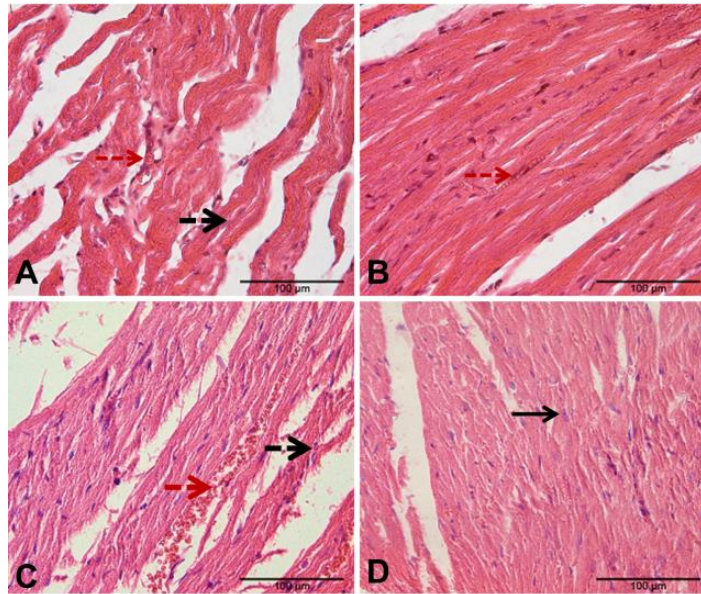
Figure 6.3 displays the H and E cardiac muscle variations found in the control (figure 6.3 A and B) and treated control group (Figure 6.3 C and D).



**Figure 6.3: Haematoxylin and Eosin cardiac muscle sections for the control and treated control group-** Figure A and B (control), Figure C and D (treated control). The images display a magnified image of the cardiovascular tissue found in the control and treated control group in which the control groups cardiomyocyte morphologies were compared. The images were captured at 40 x magnification. Black arrow: Oval and centrally located nuclei, Black dashed arrow: Myofibril damage. Red arrow: Blood vessel and capillaries. Red dashed arrow: Erythrocyte extravasation. (Scale bar: 100 µm)

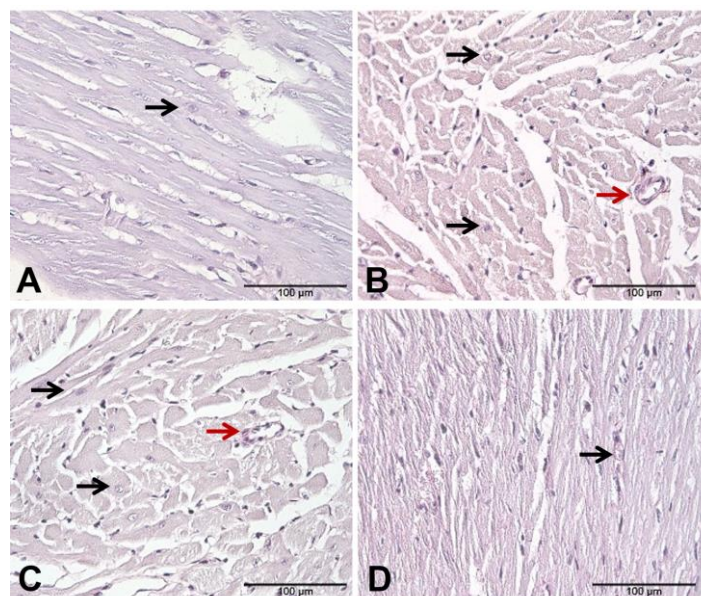
The myofibrils of the experimental and treated experimental groups displayed both oval nuclei and normal, healthy elongated myofibril stands however some muscle area's showed tissue damage and erythrocyte extravasation in both groups as seen in figure 6.4.





**Figure 6.4: Haematoxylin and Eosin cardiac muscle sections for the experimental and treated experimental group-** Figure A and B (experimental), Figure C and D (treated experimental). The images display a magnified image of the cardiovascular tissue found in the experimental and treated experimental group. The images were captured at 40 x magnification. Black arrow: Oval and centrally located nuclei, Black dashed arrow: Myofibril damage. Red arrow: Blood vessel and capillaries. Red dashed arrow: Erythrocyte extravasation (Scale bar: 100 µm)

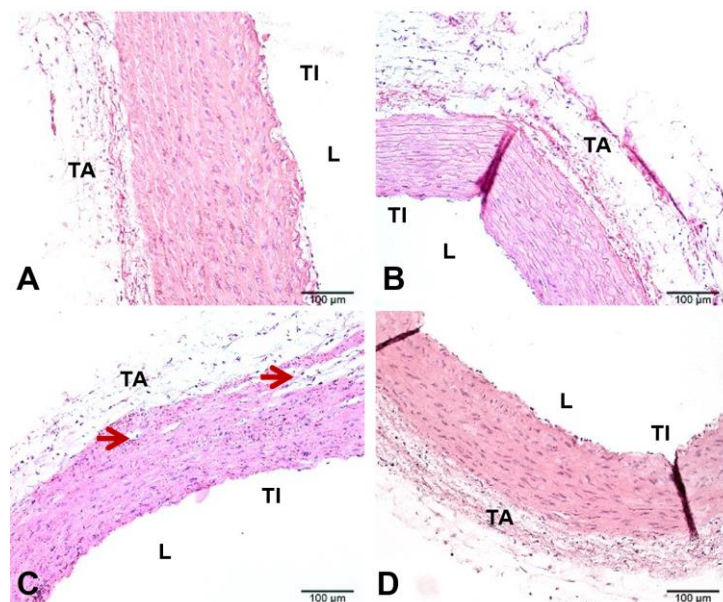
The PAS technique provides display the glycogen content within in the cardiac tissue. The following images are of the control and experimental cardiac tissue specimens. All of the control and experimental specimens (figure 6.5) showed normal glycogen content which is a low glycogen concentration that expresses itself as light purple in colour.



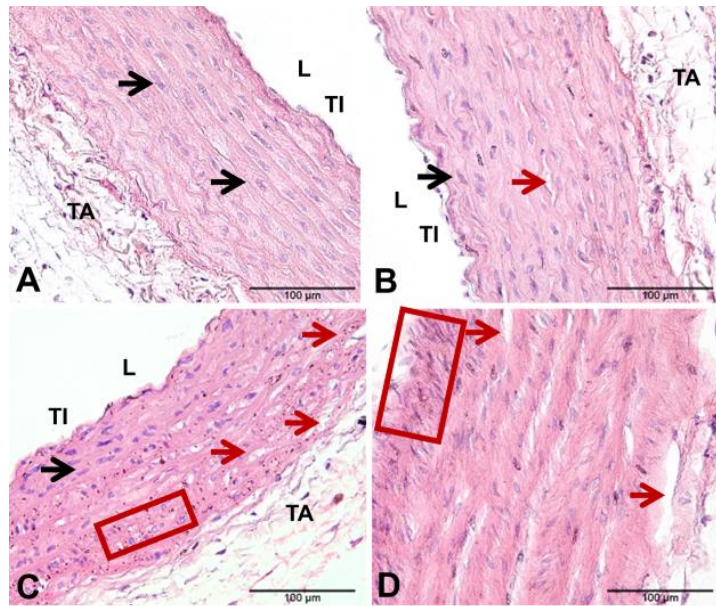
**Figure 6.5: Periodic Acid-Schiff cardiac muscle sections-** Figure A (control), Figure B (control treated), Figure C (experimental), Figure D (experimental treated). The images were captured at 40 x magnification. CM: Cardiac myofibrils. Black arrow: Nucleus. Red arrow: Blood vessel and capillaries (Scale bar: 100 µm)

## Aorta

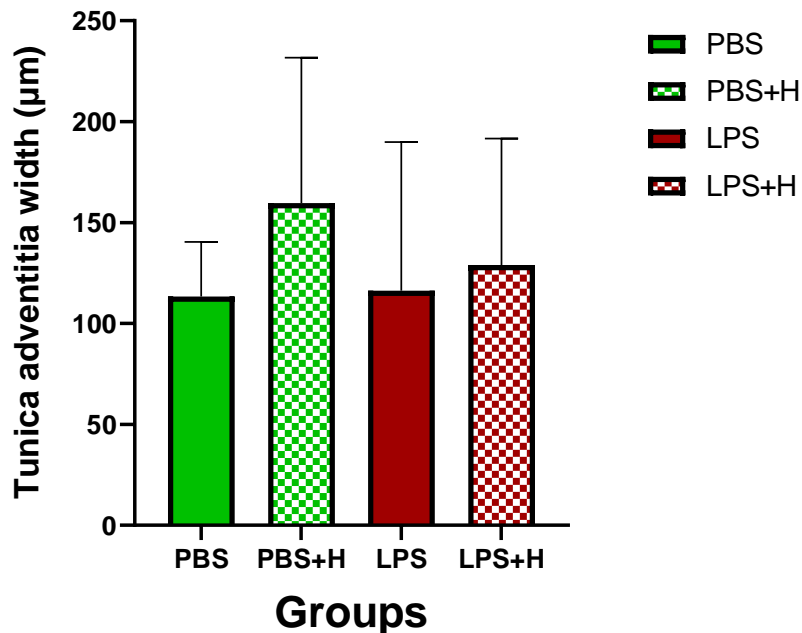
The control and experimental group aortic tissue specimens were stained with the H and E (figure 6.6 to 6.7) and VVG (figure 6.8). Staining allowed for the cellular structure and elastic fibre assessment. Figures 6.6 and 6.7 provide an overview on the structural condition of the aortas found in each group. Upon tissue inspection on low magnification of the aortic tissue of the control and treated control groups, the aorta of the control group displayed normal morphology.. When viewing the tissue on a higher magnification, the aorta of the control and treated control group displayed normal morphology which is described as the following: even aortic wall thickness with oval nuclei with a small amount of perinuclear space. The tunica adventitia sections were measured using the ImageJ software. Upon conducting a One-way ANOVA using GraphPad Prism 9.0.0, the tunica adventitia thickness of the all the test groups did not display a significant difference. The mean and standard deviations of test groups are displayed in figure 6.8. The experimental group showed both normal aortic morphologies however large degrees of tissue destruction in some areas, the destruction can be seen on lower magnification (figure 6.6 C). When viewing the tissue on a higher magnification as seen in figure 6.7 C and D, both the experimental and treated experimental group displayed both an even wall thickness and areas with oval nuclei and widely spread perinuclei while in other areas the nuclei were flattened and clustered together. Meanwhile, the treated experimental group displayed largely intact aortic tissue however upon closer examination cellular tissue destruction in what looks like perforations occurred (figure 6.7 D).



**Figure 6.6: Haematoxylin and Eosin aorta 20x sections-** Figure A (control), Figure B (control treated), Figure C (experimental), Figure D (experimental treated). The images were captured at 20 x magnification. L: Lumen. TA: Tunica Adventitia. TI: Tunica Intima. Red arrow: Changes in tissue structure. (Scale bar: 100 µm)

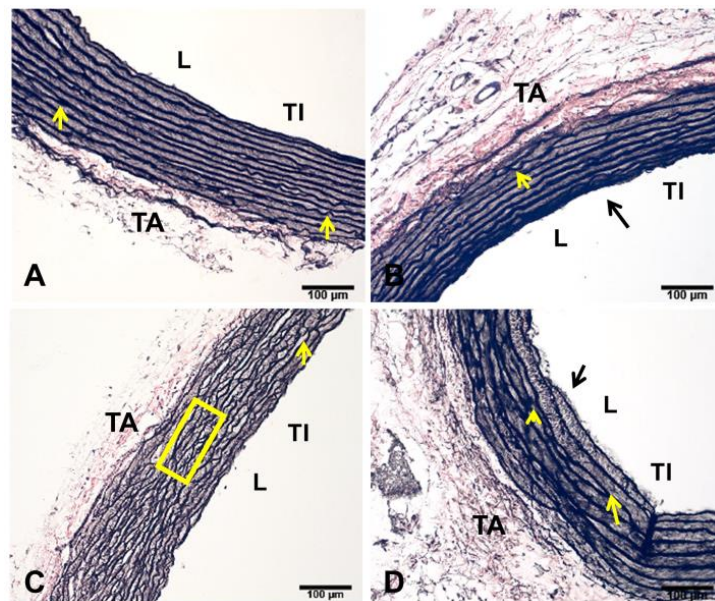


**Figure 6.7: Haematoxylin and Eosin aorta 40x sections-** Figure A (control), Figure B (control treated), Figure C (experimental), Figure D (experimental treated). The images were captured at 20 x magnification. L: Lumen. TA: Tunica Adventitia. TI: Tunica Intima. Red box: Noticeably clustered nuclei, Red arrow: Changes in tissue structure. (Scale bar: 100  $\mu\text{m}$ )



**Figure 6.8: Tunica adventitia width-** The width of the tunica adventitia of the control, treated control, experimental and treated experimental group were measured and compared using a One-way ANOVA. The tunica adventitia width of the groups are not significantly different.

Figure 6.9. displays the aortas of the control, control treated, experimental and treated experimental groups that were stained using the VVG technique. The control and treated control group showed evenly thick, regular arranged purple/black elastin fibres strand that contained interlinkages between the elastic laminae as seen in figures 6.9 A and B. The experimental group displayed elastic fibres that were unevenly thick and contained many interlinkages between the elastic laminae, displaying disordered elastic fibre arrangements as seen in figure 6.9 C. The treated experimental group displayed minor to moderate changes in elastic fibre arrangements and displayed interlinkages between the elastic laminae as seen in figure 6.9 D.



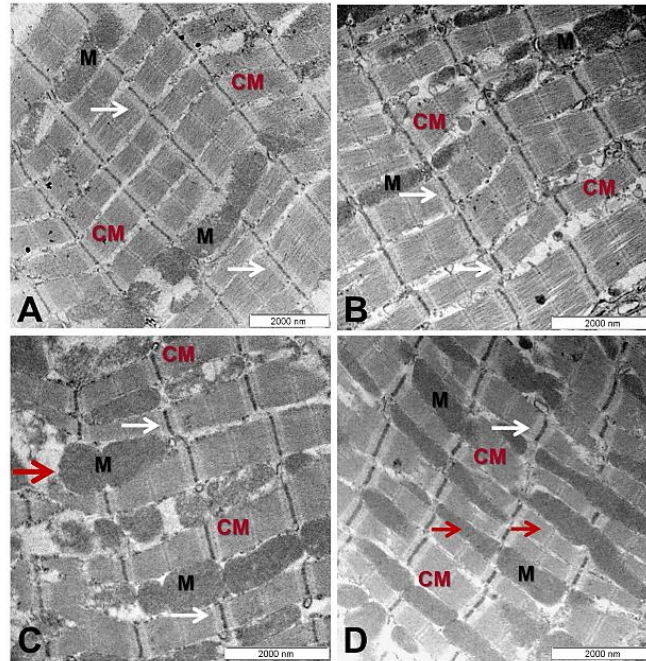
**Figure 6.9: Verhoeff-Van Gieson aorta sections-** Figure A (control), Figure B (control treated), Figure C (experimental), Figure D (experimental treated). The images were captured at 20 x magnification. L: Lumen. TA: Tunica Adventitia. TI: Tunica Intima. Black arrow: Tunica Intima changes. Yellow arrow: Crosslinks between elastic laminae. Yellow box: Major cell layer disruptions in the form of cross links. (Scale bar: 100  $\mu$ m)

### 6.3.2 Transmission electron microscopy: Lipopolysaccharides effect on cardiac and aortic tissue and exploring Manuka honey as a treatment

The following cardiac muscle and aortic samples were viewed on the uranyl acetate and lead citrate-stained copper grids. They were observed and compared between the control and experimental populations. The cardiac muscle mitochondria and myofibrils and the aorta collagen and elastin fibres were viewed. The four testing populations were evaluated and compared.

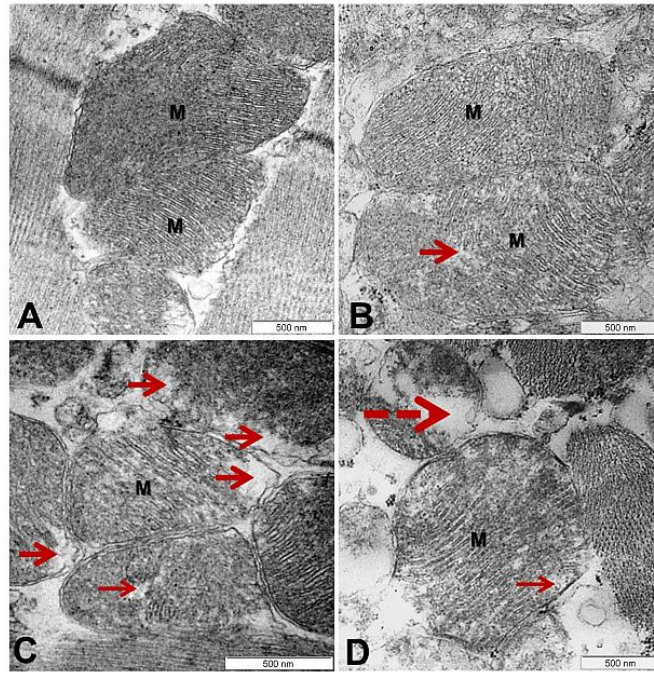
#### Cardiac muscle

Longitudinal cardiac muscle sections allowed for cardiac myofibril ultrastructure observations and comparisons between the control, treated control, experimental and treated experimental groups as seen in figure 6.10 (A-D). Normal ultrastructure with well organised parallel mitochondrial and cardiac fibrils and clear Z lines (white arrows) was exhibited in the control and treated control groups (figure 6.10 A and B). While the experimental groups displayed minor damage and an elevated mitochondrial presence. Both the experimental groups displayed clear Z lines. However, the thinned cardiac myofibrils showed minor damage through Z line interruptions in the presence of enlarged mitochondria between cardiac muscle in both the experimental and treated experimental groups (figures 6.10 C and D). Minor mitochondrial destruction was illustrated as red. None of the groups had a presence of autophagic vacuoles. The experimental group displayed myofibrils that showed moderate damage while the treated experimental group displayed minor cardiac myofibril damage.



**Figure 6.10: Detailed ultrastructure of cardiomyocyte longitudinal sections-** Figure A (control), Figure B (control treated), Figure C (experimental), Figure D (experimental treated). CM: Cardiac myofibrils. M: Mitochondria. White arrow: normal Z-lines. Red arrow: Myofibril thinning and destruction (Scale bars: 2000 nm)

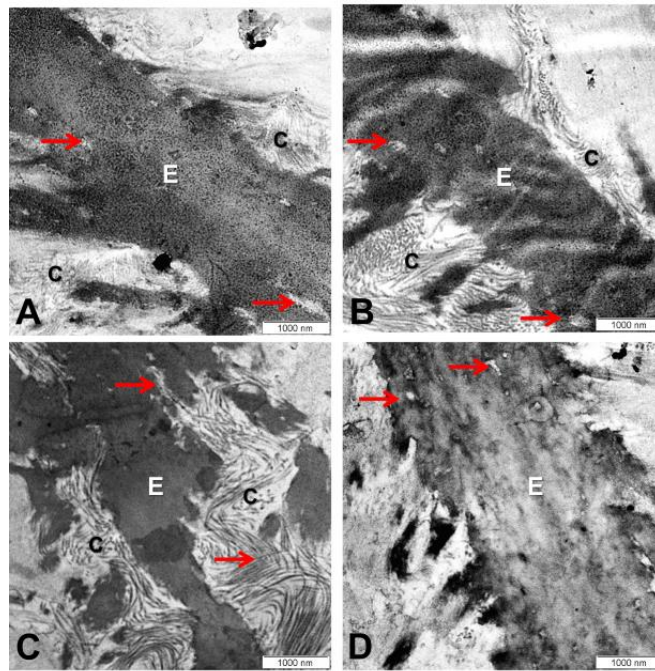
The changes in mitochondrial shape and change are displayed in figure 6.11 (A-D) where the ultrastructure of control and experimental mitochondrial are displayed. The control groups displayed normal and healthy mitochondrial crista that were neatly and densely packed (figure 6.11 A and B), axial tubules are the empty spaces visible in the tissues. Variations to standard cristae morphology to occur in the control groups but were rarities. While the experimental group presented less densely packed and neatly organised mitochondria in figures 6.11 C and D. The groups illustrated a variety of mitochondrial morphologies such minor damage as seen in figures 6.11 C and D.



**Figure 6.11: Detailed ultrastructure of cardiomyocyte transverse sections displaying mitochondria-** Figure A (control), Figure B (control treated), Figure C (experimental), Figure D (experimental treated). M: Mitochondria. Red arrow: Cristae destruction. Red dashed arrow: Large amount of cristae destruction (Scale bar: 500 nm)

## Aorta

Following cardiac myofibril observations and comparisons the aortas of the control and experimental groups were conducted. Figures 6.12 A-D provides a general elastic and collagen fibres overview shown in the control and experimental groups. The control groups showed solid elastic fibres with minor fragmentation following neighbouring collagen depositions. Larger elastic fibre fragmentation and alterations to the standard structure did occur however these were infrequent and minor. While the experimental groups displayed abundant elastin fibre fragmentation and collagen deposition. Elastin fibre fragmentation signified elastic fibre destruction. In areas where elastin is destroyed collagen was deposited. Nevertheless, the remaining elastin fibre fragments retained their density. The treated experimental group displayed a standard solid elastin fibre with reduced density. Although, the group displayed a lessened degree of elastin fibre fragmentation and collagen deposition, less collagen fibres were observed around the elastic fibres (figure 6.12 D).



**Figure 6.12: Detailed ultrastructure of aortic transverse sections-** Figure A (control), Figure B (control treated), Figure C (experimental), Figure D (experimental treated). C: Collagen fibres, E: Elastic fibre. Red arrow: Elastin fibre fragmentation (Scale bars: 1000 nm)

## 6.4 Discussion

A consequence of continual LPS exposure brings about cardiac injury through cardiomyocyte autophagy<sup>20</sup>. Excessive autophagy can cause disease and autophagic cell death. Research has discovered that LPS-induced autophagy participates in a multitude of biological processes such as liver autophagy, osteoclastogenesis and vascular endothelial cell autophagy, thus concluding in widespread pathogenesis in various bodily systems<sup>39,49-50</sup>. In cardiac muscle, LPS exposure induces pathogenic autophagy and hypertrophy that concludes in a cardiomyocyte viability reduction<sup>39,216</sup>. A study conducted by Jianjun et al. (2018) found that LPS changed cardiomyocytes resulting in a swollen appearance, transverse striation loss, and a greater influx of inflammatory cells<sup>220</sup>. In addition, the group observed that LPS elevated the levels of the following pro-apoptotic cytokines: BAX (no abbreviation), cytochrome c, cleaved-caspase 3, cleave-caspase 9, and Poly (ADP-ribose) polymerase (PARP)<sup>220</sup>. Thus, endotoxin exposure can result in apoptosis. In addition, there is increasing evidence that ROS are secondary messengers in the instigation and amplification of various biological processes such as apoptosis, cell growth, inflammation and cellular oxidative stress<sup>221</sup>. The oxidation-anti-oxidation imbalance is a consequence of a ROS imbalance and results in an elevation in oxidative stress causing oxidative damage in macromolecules e.g deoxyribonucleic acid (DNA), lipids and proteins<sup>222</sup>. It produces inflammation through the nuclear factor kappa-light-



chain-enhancer of activated B cell (NF- $\kappa$ B) pathway increasing the IL-1 $\beta$ , IL-6 and TNF $\alpha$  sensitivity<sup>223</sup>. Upon LPS exposure, the innate immune system release the TLR-4 inflammatory cytokine<sup>224</sup>. In addition the elevated IL-1 $\beta$ , IL-6, Nitric oxide (NO), ROS, TNF $\alpha$ , and elevated primary human peripheral blood mononuclear cells (PBMC) pro-inflammatory cytokine release concludes in inflammation<sup>189,225</sup>. Reactive oxidative species signal induces apoptosis through the following pathway: the elevation of mitochondrial membrane permeability through the BAX elevation and BCL-2 reduction results in cytochrome C release thus causing caspase 9 activation enhancement which concludes in apoptosis complex formation<sup>226-227</sup>.

Researchers have postulated that vascular hypo-responsiveness concluding in abnormal tissue perforation is a likely consequence of pro-inflammatory mediators and ROS exposure<sup>225</sup>. The exact mechanism of LPS induced vascular dysfunction is unknown<sup>225</sup>. However, systemic inflammation and ROS exposure may trigger vascular dysfunction affecting heart rate modulation concluding in hypo-tissue perfusion<sup>225</sup>.

This chapter investigates the cardiac and aortic structure of the control, control treated, experimental and treated experimental groups and explores Manuka honey's effectiveness as a treatment. Manuka honey possesses anti-inflammatory, anti-hypertensive and anti-oxidant properties, moreover it stimulates angiogenesis and may be an effective natural treatment<sup>23,146</sup>.

The anti-inflammatory and anti-oxidant qualities of Manuka honey may prevent the induction of the following: oxidative cardiac mitochondrial damage, cell abnormalities, elastin fragmentation and structural anomalies, cardiomyocyte autophagy, and glycogen accumulation indicative of hypoxia that maybe a consequence of LPS exposure.

The present study documented the following when conducting the H and E technique on the aortic and cardiac tissue of the control and treated control group, both groups displayed normal cellular morphology. However, when comparing cardiac tissue of the experimental and treated experimental groups to both the control and control treated groups, both groups displayed a standard healthy cardiac myofibril arrangements and obvious cardiac myofibril damage as seen in figure 6.2. In areas with damaged cardiac myofibrils, both groups displayed moderate to severe cardiac myofibril damage and erythrocyte extravasation which is a histological characteristic associated with vascular leakage that is a consequence of endothelial damage<sup>228</sup>. Lipopolysaccharides induce endothelial and cardiac myofibril toxicity through inflammation and the ROS elevation concluding in apoptosis through the TLR-4/ NADPH oxidase (NOX) inflammatory pathway in cardiomyocytes<sup>229</sup>. The homolog NADPH oxidase-4 (NOX-4) produces ROS and is highly expressed in cardiomyocytes, the homolog may be inducing ROS production in the cardiac myofibrils of the experimental and treated

experimental group following LPS exposure<sup>230</sup>. NADPH oxidase-4 and TLR-4 expression are closely associated with TNF $\alpha$  secretion concluding in a reduction in cardiac performance<sup>231</sup>. This study has found that early low dose LPS exposure results in viable cardiac myofibril damage, however the exact pathway needs to be investigated.

The PAS staining technique showed no significant difference to the glycogen concentrations in the control, treated control, experimental and treated experimental groups, thus displaying that early low dose LPS exposure does not result in glycogen accumulation which occurs during hypoxia. Thus, the cardiac cells were not hypoxic.

Upon investigation of the TEM images found that the cardiac myofibrils of the control and treated control groups presented with clear Z-lines and normal ultrastructure. However, cardiac myofibrils of the experimental group presented with moderate myofibril damage nevertheless when compared to the treated experimental group, the treated experimental group presented with only minor cardiac myofibril damage. Both groups displayed less dense mitochondrial cristae when compared to the cristae of the control and treated control groups thus illustrating mitochondrial damage caused by LPS. Still, these findings show that Manuka honey prevent cardiac myofibril destruction as a consequence of LPS exposure to a minor to moderate degree. However, the treatment could not neutralise the mitochondrial destruction induced by LPS.

A study conducted by Haileselassie et al. (2019) discovered that LPS treated group appeared to display elevated mitochondrial cristae destruction and if continued may result in decreased mitochondrial respiration concluding in an upsurge in mitochondrial oxidative stress and a reduction in membrane potential<sup>232</sup>. Early LPS exposure results in the early mitochondrial cristae destruction potentially reducing mitochondrial respiration, however the levels at which that occurs still need to be investigated.

In addition, with regards to aortic tissue, the present study documented the following: upon conducting the H and E technique the control and treated control groups displayed normal even elastic layers consistent with normal aortic cell histology. When comparing the aortic tissue of the experimental group to the control group, the study found that early LPS exposure results in varying tissue disruption in the form of nuclei clustering and flattening as well as what appears to be perforations in some aortic wall areas. In contrast, when comparing the treated experimental group to control group, the group presented with the same flattened and overly clustered nuclei found in the experimental group however, perforations could only be upon closer magnification. Manuka honey had neutralised some of the cellular aortic destruction caused by LPS. When comparing the tunica adventitia of the control, treated

control, experimental and treated experimental did not display a significant difference in thickness.

The VVG staining technique elaborates on the effect that LPS has on aortic tissue by providing a clear image of the elastic layers. With regards to the elastic tissue of the control and treated control groups, the animals display normal evenly thick and well-arranged elastin fibres with a minimal number of crosslinks between elastic laminae. However, when comparing the elastic fibres of the control and experimental groups, the elastic fibre disruption that was displayed as a disordered arrangement of fibres and many elastic laminae crosslinks. When compared to the experimental group, the treated experimental group displayed elastic fibres that displayed greater organisation.

When examining the elastin and collagen structures using TEM, it was documented that early low dose LPS exposure caused elastin fibre fragmentation and collagen deposition. When comparing elastin and collagen structures of the control and treated control groups had insignificant differences between them. Both groups presented with compact elastic fibres that had minor peripheral fragmentation that were filled with neighbouring collagen deposits. Upon comparing the elastic and collagen structures of the control and experimental groups substantial elastin fibre fragmentation and collagen deposition between the fragmented elastin structures were found. In contrast, when comparing aortic tissue of the control and treated experimental groups it was discovered that the groups presented with standard solid elastin fibres that had reduced density. When comparing the elastic and collagen fibres of the experimental and treated experimental groups, it could be observed that the treated experimental group had less elastin fibre fragmentation and collagen deposition. However, when comparing the treated experimental group to the control group an unexplained depletion of collagen fibres was observed.

The study showed that early LPS exposure may later induce cardiac and vascular dysfunction through cardiac myofibril as well as mitochondrial damage, elastin fibre fragmentation and collagen deposition which may result in CV pathogenesis later in life. Elastin is an ECM protein that determines a vessels mechanical strength at low pressure<sup>233</sup>. Vascular remodelling may conclude in pathological vascular disorders such as atherosclerosis and hypertension<sup>234-235</sup>. Lipopolysaccharides result in arteriolar stiffening through elastin depletion and fragmentation as well as collagen deposition. Depletions in elastin conclude in arterial stiffness through delegating the blood propulsion to the collagen fibres which possess a greater structural rigidity when compared to elastin fibres<sup>234</sup>. Decreased elastin content contributes to CV disease and is found in older individuals with hypertension<sup>234</sup>. Although Manuka honey administration mitigated the effects of LPS, some cardiac myofibril damage was observed in

the treated experimental group. In addition, a reduction of elastin density and a reduction in collagen deposits was observed in this treated experimental group when it was compared to the control group. A reduction in elastin density results in vascular rigidity while collagen fibre depletions result in a reduction in rigidity possibly counteracting effects of rigidity however reducing the presence of a healthy aortic structure<sup>234</sup>. Some rigidity is vital in the aorta's structure and function; thus, the treated experimental group may maintain its elastic recoil but lose the rigidity required to maintain the aortas' structure result in future aortic destruction. Nevertheless, these findings prove that Manuka honey protects the aortic tissue from some of the elastin fragmentation caused by early LPS exposure, however not perfectly. Although Manuka honey neutralised some of the harmful effects of LPS.

## **6.5 Conclusion**

Early LPS exposure results in cardiac myofibril destruction and disrupted aortic elastic fibre organisation. Upon closer examination it is observed that LPS induces cardiac myofibril and mitochondria cristae destruction as well as elastin fibre fragmentation and collagen deposition. Both occurrences may conclude in future cardiac hypoxia and aortic elevations in rigidity thus resulting in hypoperfusion potentially concluding in widespread organ dysfunction, however further study is needed. Manuka honey was used as a treatment in this study and the following was observed, the natural therapeutic mitigated some of the effects of LPS by substantially reducing cardiac myofibril destruction and elastic fibre disorganisation. Upon closer examination the evaluated therapeutic, displayed a minor neutralisation of the LPS produced cardiac myofibril injury, however failed to prevent the resulting harm caused to the mitochondrial cristae. Manuka honey prevented elastin fibre fragmentation however, the elastic fibres displayed a density reduction and a depletion of collagen fibres was observed. The cardiac and aortic damage shows that early LPS exposure may directly affect CV health. Overall, although Manuka honey has shown promising results although it fails to completely neutralise the cardiac and aortic destruction produced by LPS. The following chapters will further investigate the effect of early LPS exposure on total cholesterol levels and the CV system cellular elements (erythrocytes, fibrin networks and platelets) while exploring Manuka honey as a treatment.

# **Chapter 7: Total cholesterol levels**

## **7.1 Chapter Objective**

Determine CV health by measuring the total cholesterol concentrations of the experimental, treated experimental, control and treated control group using a sandwich ELISA assay.

## **7.2 Introduction**

The total cholesterol concentration consists of high density lipoprotein cholesterol (HDL), intermediate- density lipoprotein cholesterol (IDL), LDL and very low density lipoprotein cholesterol (VLDL)<sup>236</sup>. Studies have shown that long-term intake of a fat rich diet specifically impairs the hepatic cholesterol pathway, for this reason, the animals used in the current study were fed a low-fat diet in order to definitively conclude the effects of LPS on the CV total cholesterol level<sup>237</sup>.

A high LDL cholesterol level results in negative physiological results, while a high HDL level indicates positive physiological results<sup>236</sup>. High density lipoprotein cholesterol has a strong inverse relationship with CV disease and has been identified as being a CV protective factor<sup>238</sup>. While LDL is suspected to play a contributing factor to heart failure, however studies have found that there is no association between heart failure risk and increased LDL cholesterol level<sup>239</sup>. Nevertheless, LDL cholesterol does increase the likelihood of CV injury and atherosclerosis<sup>240</sup>. In addition, an elevated non-fasting triglyceride level (the non-fasting triglyceride level is the level of triglycerides that can be measured when an individual is in the non-fasting state) is associated with a higher heart failure risk<sup>239</sup>. Lipopolysaccharide induced inflammation is known to elevate serum cholesterol levels through the downregulation of genes such as Low-Density Lipoprotein Receptor (LDLR) which plays an important role in low density lipoprotein uptake<sup>241</sup>. Thus, low-density lipoprotein uptake disruption would potentially induce or aggravate CV complications.

The elderly population have a significant risk of developing CV complications and LPS may intensify the development of these complications. Hypercholesteremia is associated with an elevated CV dysfunction<sup>242</sup>. Artherosclerosis is induced by an inflammatory process that is characterised by oxidised LDL deposition, endothelial cell injury and vascular wall plaque accretion<sup>243</sup>. In addition, Experimental studies have also shown that gut-derived LPS are proatherogenic and may therefore further enhance the negative effects of elevated LDL cholesterol levels. Lipopolysaccharides may alter the components of the total cholesterol, potentially lowering HDL levels while elevating LDL levels<sup>87</sup>. Furthermore, researchers discovered that animals that are exposed to LPS developed vulnerable plaques that were characterised by thrombi and intraplaque haemorrhages<sup>87</sup>. Moreover, the study found that a

possible platelet response amplification also occurred, LPS may prompt hypercoagulability which would further increase the likelihood of CV system complications.

A total cholesterol sandwich ELISA test was conducted with the aim to evaluate the total cholesterol level differences between the experimental and control test groups. The total cholesterol ELISA test used did not require that the animals remain in a fasting state<sup>236</sup>. The total cholesterol test was used as a CV health indicator. Considering all the evidence, this study used a biochemical test in order to produce results of greater reliability and accuracy to confirm physiological total cholesterol levels.

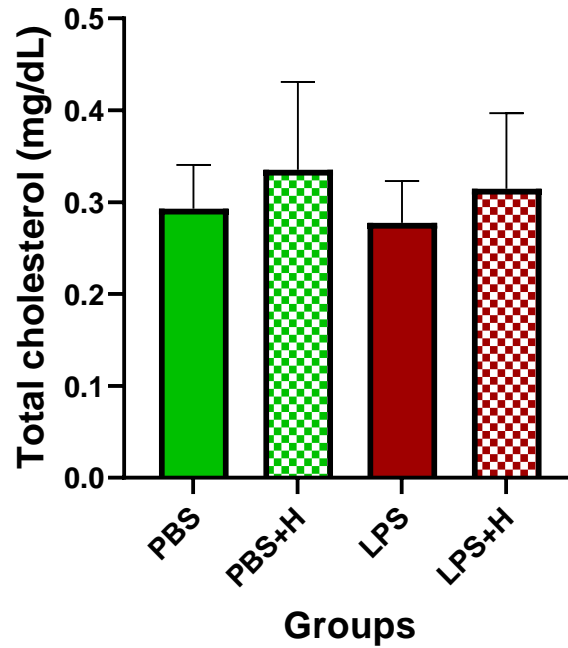
### **7.3 Results**

The total cholesterol level of each group was analysed using GraphPad Prism 9.0.0. A One-way ANOVA was conducted which compared the mean total cholesterol levels of each testing population. The test found that the total cholesterol levels of the control, treated control, experimental and treated experimental group showed no significant differences. The data is displayed in table 7.1 and figure 7.1.

**Table 7.1: Total cholesterol levels- Test groups statistics**

<b>Total cholesterol (mg/dl)</b>				
<b>Group</b>	<b>Mean ± SD</b>	<b>Median</b>	<b>P-value</b>	<b>Significant (yes/no)</b>
<b>PBS</b>	0,293 ± 0,049	0,289	0,5571	No
<b>PBS + H</b>	0,335 ± 0,090	0,316		
<b>LPS</b>	0,277 ± 0,040	0,270		
<b>LPS + H</b>	0,318 ± 0,067	0,332		

**Abbreviations: H: Manuka honey, LPS: Lipopolysaccharide, PBS: Phosphate-buffered saline, SD: Standard deviation**



**Figure 7.1: Mean total cholesterol of the control and experimental rat groups-** Displays the mean and 95% confidence interval total of the total cholesterol of each test group measured in mg/dL.

Table 7.2 documents the control, treated control, experimental and treated experimental rat group individual comparisons between each group. The comparison definitively displays that the total cholesterol of the control group shows no statistical significance with the treated control, experimental and treated experimental group. In addition, the other test groups did not display statistical differences to one another.

Table 7.2: Total cholesterol concentration- Group temperature comparisons

Total cholesterol (mg/dL)			
Groups	Mean difference	P-value	Significant (yes/no)
PBS vs PBS+H	-0,04229	0,8500	No
PBS vs LPS	0,01563	0,9376	No
PBS vs LPS+H	-0,02172	0,9376	No
PBS+H vs. LPS	0,05791	0,7182	No
PBS+H vs LPS+H	0,02056	0,9376	No
LPS vs. LPS+H	-0,03735	0,8643	No



---

**Abbreviations: H: Manuka honey, LPS: Lipopolysaccharide, PBS: Phosphate-buffered saline, SD: Standard deviation**

---

## **7.4 Discussion**

Research has found that HDL produces an anti-inflammatory response and results in the clearance and neutralisation of LPS<sup>244</sup>. Exposure to a significant amount of the lipoprotein concludes in corticosterone production coupled with leukocyte recruitment during sepsis<sup>244</sup>. High density lipoprotein cholesterol administration in LPS exposed animals improves cardiac function, reduces pro-inflammatory cytokine production providing a better prognosis<sup>245</sup>.

In contrast, lipid saturated macrophages (foam cells) are a consequence of abnormal oxidised LDL accumulation and hyperlipidaemia. A cholesterol imbalance results in a disruption in cholesterol homeostasis contributing to foam cell formation through LDL induced lipid macrophage deposition<sup>246-247</sup>. Foam cell formation is associated with atherosclerosis development and plays a key role in the inflammation-associated immune response<sup>248</sup>. The foam cells release a variety of pro-inflammatory cytokines such as IL-1 and interleukin-2 (IL-2) that result in inflammation that aggravates atherosclerosis pathogenesis<sup>246</sup>. Inflammation both results in macrophage activation and foam cell formation, while disproportionately elevating ROS production<sup>246</sup>. Both phenomena encourage foam cell apoptosis which concludes in the plaque formation found in an atherosclerotic lesion thus significantly negatively impacting CV health<sup>246</sup>.

Chronic inflammation significantly elevates the CV disease risk<sup>249</sup>. The present study investigated the effect of early LPS exposure on total cholesterol levels, thus providing an indicator of CV health by evaluating the cholesterol homeostasis. The findings are as follows: early low LPS exposure not reduce or elevate the total cholesterol blood concentrations.

Although the total cholesterol of the LPS group did not present a significant change, chapter six documents the effect that early low dose LPS exposure has on the aortic and cardiac tissue. The LPS results in elastin fibre fragmentation, general cell destruction beginning at the tunica intima. Together the chapters describe that early LPS exposure results in CV tissue damage thus directly negatively impacting CV health. However, additional research is needed to conclude the effect of early LPS exposure on HDL, LDL levels and LDL receptor mRNA expression on macrophages.

## **7.5 Conclusion**

Total cholesterol, TEM imaging of the aorta and cardiac muscle were used to investigate CV health. Although, early LPS exposure results in ultrastructural damage of the heart and the

aorta, it does not produce an elevation or reduction in total cholesterol levels and thus does not affect cholesterol homeostasis. Therefore, total cholesterol cannot be used as one of the early indicators of the effects of LPS or low-grade systemic inflammation. Furthermore, the effect of Manuka honey on the impact of LPS on total cholesterol was explored however, no significant differences between the groups was found thus the results were inconclusive. Chapter eight will explore the effect of LPS on erythrocyte, fibrin network and platelet morphology in order to conclude if early exposure to low LPS dose may result in morphological disruptions and therefore future physiological complications.

# **Chapter 8: Ultrastructural** **blood analysis**

## **8.1 Chapter Objective**

Study the morphology of erythrocytes, platelets and fibrin network structure of the experimental, treated experimental and control, treated control groups using SEM.

## **8.2 Introduction**

Erythrocytes, platelets, and fibrin networks play a vital role in maintaining haemostasis. A mature erythrocyte has a stable yet complex plasma membrane that is composed of an intact specialised lipid bilayer that comes into contact with integral membrane protein through protein interactions<sup>66</sup>. When the asymmetry of the bilayer is disrupted by the eryptosis cascade, the cells structural integrity is compromised resulting in erythrocyte aging and CV system clearance<sup>66</sup>. In addition, pathogenic exterior eryptotic signals may induce eryptosis, resulting in the premature clearance of the cell<sup>58</sup>. Inflammatory lipases formed throughout the inflammatory process conclude in accelerated erythrocyte aging<sup>73</sup>. Toxic substances such as LPS, induce a significant increase in haemolysis possibly resulting from a reduction in the erythrocyte membrane integrity, thus affecting one or more of the internal proteins of the cell<sup>79</sup>. The endotoxin can change the membrane integrity by inserting itself into the cell membrane through the cholesterol or sphingomyelin domains thus destabilizing the membrane<sup>250</sup>. In the same way that erythrocytes are affected by the endotoxin, platelets play a vital role in the coagulation cascade and are sensitive to external cytokine contact<sup>88</sup>. The haemostatic process consists of the following steps: vessel injury, vasoconstriction, platelet activation, coagulation cascade and fibrinolysis as described in Chapter 2. Bacterial or bacterial metabolite contact may result in GP Ib receptor hyperactivation through cytokine overstimulation that leads to unintended initiation of the coagulation cascade in the absence of a wound and can conclude in pathology<sup>251</sup>. There is an overwhelming amount of information that proves that LPS causes systemic inflammation<sup>20,79,88</sup>. The endotoxin may trigger platelet activation, aggregation, granule release or platelet leukocyte formation<sup>86</sup>. Normal platelet activation refers to a series of overlapping events that are triggered by platelet subendothelial tissue exposure. These events include platelet shape change, adhesiveness, aggregation and various release reactions resulting in haemostatic plug formation. However, when the process occurs in the absence of a wound could be indicative of inflammation and platelet hyperactivation<sup>21</sup>. An alteration in blood coagulation factor expression also occurs inducing thrombin upregulation as a result of systemic inflammation thus producing pronounced procoagulant effects<sup>252</sup>. These procoagulant effects act via key cell protease activated receptors which are expressed in arterial vessel walls concluding in thrombin inducing proatherogenic actions that lead to the further activation of inflammatory pathways<sup>252</sup>. Platelets play an important role in

atherosclerosis development and thus the investigation of platelets prothrombotic states can be extended to investigating the atherosclerotic risk<sup>87</sup>. Research suggests that LPS adds an additional atherosclerotic burden on patients resulting from the inflammatory properties of the toxin concluding in plaque formation<sup>87</sup>. In addition, a study conducted by Nunes et al. (2020) documented that LPS may interact with fibrin resulting in thick fibres and abnormal clot structures<sup>253</sup>.

This study used SEM to investigate the ultrastructural erythrocyte, platelet and fibrin network changes that may occur from early LPS exposure while investigating Manuka honey as a possible treatment. Thus, resulting in an increase in the body of information regarding the effect of LPS on the CV cellular components.

The aim of this chapter was to compare the morphology through the ultrastructural analysis of both the control and experimental populations to determine the effect of LPS on each CV cellular component.

## **8.3 Results**

### **8.3.1 The effect of lipopolysaccharides on blood haemostasis and exploring Manuka honey as a treatment**

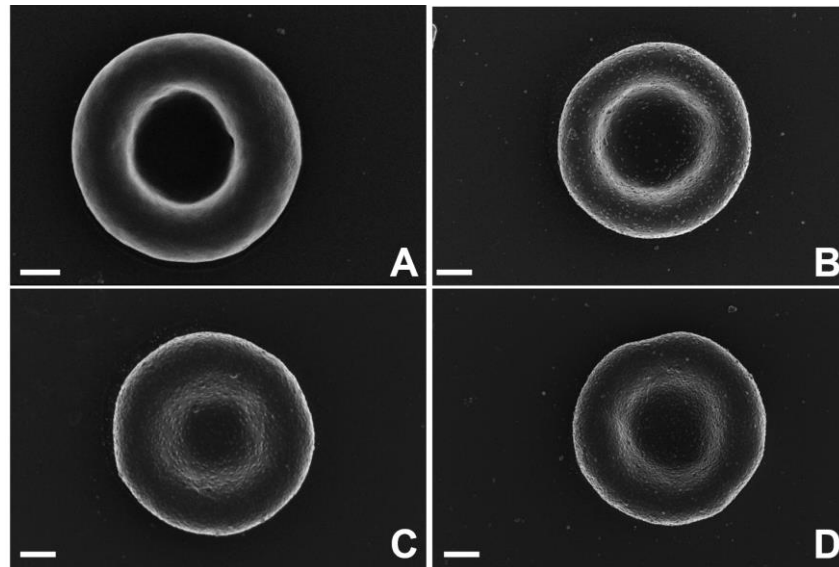
In this study a low LPS dose (0.1 mg/ml at a volume of 0.05 mg/kg) was administered to the treated experimental and experimental population. The comparison and evaluation of the platelet and fibrin network structure of each population investigated whether the administered LPS dose created a sufficient inflammatory response that resulted in a constant prothrombotic state. Excessive platelet spreading and a dense disorganised fibrin network structure are a consequence of a prothrombotic state<sup>88</sup>. Highly activated platelets produce many pseudopodia and spread outwards (figure 3.8 C-D) while mildly activated platelets maintain a circular shape with a reduced pseudopodia number (1 or 2) (figure 3.8 A and B). Normal fibrin networks produce thin and thick regularly arranged fibrin networks as seen in figure 3.9 A, while an abnormal fibrin network produces a dense network with thick strands (figure 3.9 B-D)<sup>176</sup>.

#### **Erythrocytes**

Whole blood samples were collected and placed into sodium citrate tubes, following that, SEM micrographs were created. The following blood samples were viewed: Figures 8.2-8.7 are representative images of each control and experimental group.

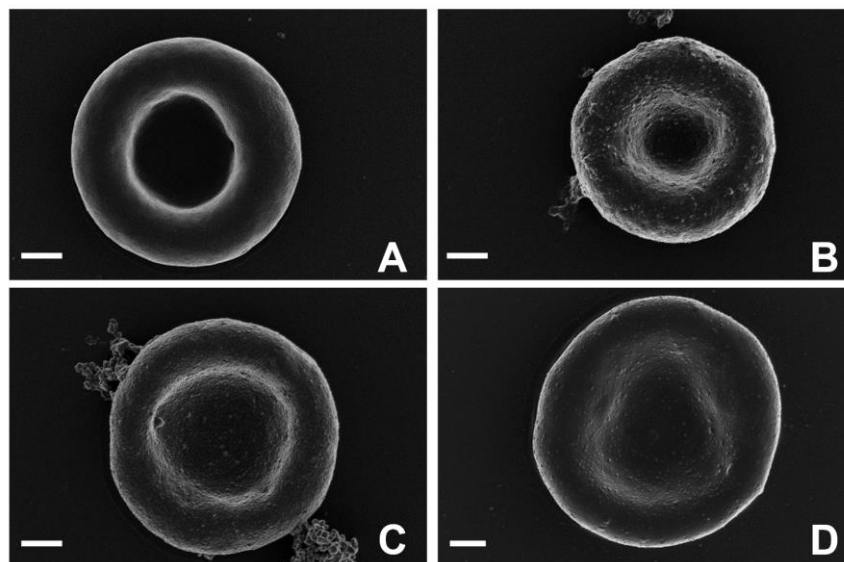
Figure 8.1 represents the erythrocyte morphologies of the control and experimental groups. The micrographs were compiled for the purpose of group comparison. In figure 8.2 normal

erythrocyte morphology can be seen in every group. While, figures 8.3-8.6 display the erythrocyte morphology in greater detail.



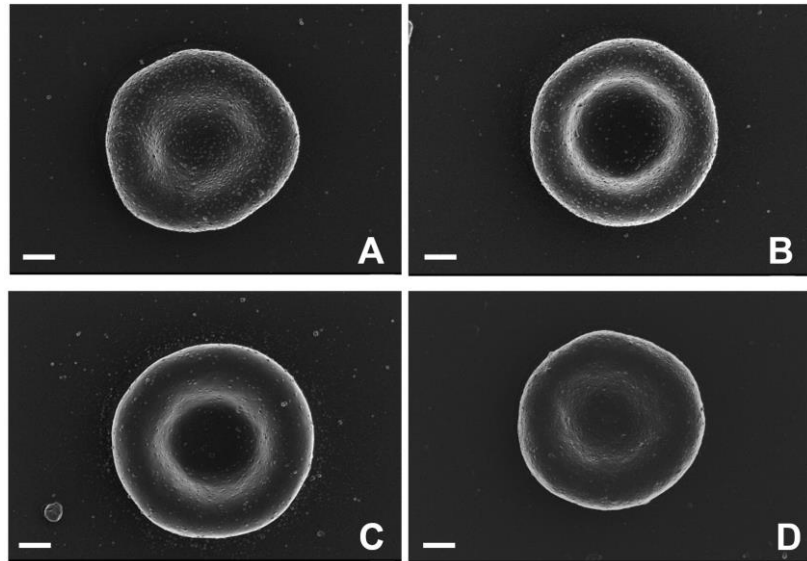
**Figure 8.1: The SEM micrographs displaying the predominant erythrocyte structure found in the control and experimental group-** Figure A (control), Figure B (control treated), Figure C (experimental), Figure D (experimental treated) depict the biconcave erythrocyte structure. (Scale bars: 1  $\mu\text{m}$ )

Figure 8.2 illustrates the normal erythrocyte biconcave structure found in the PBS control group. The majority of erythrocytes possessed the standard biconcave structure.



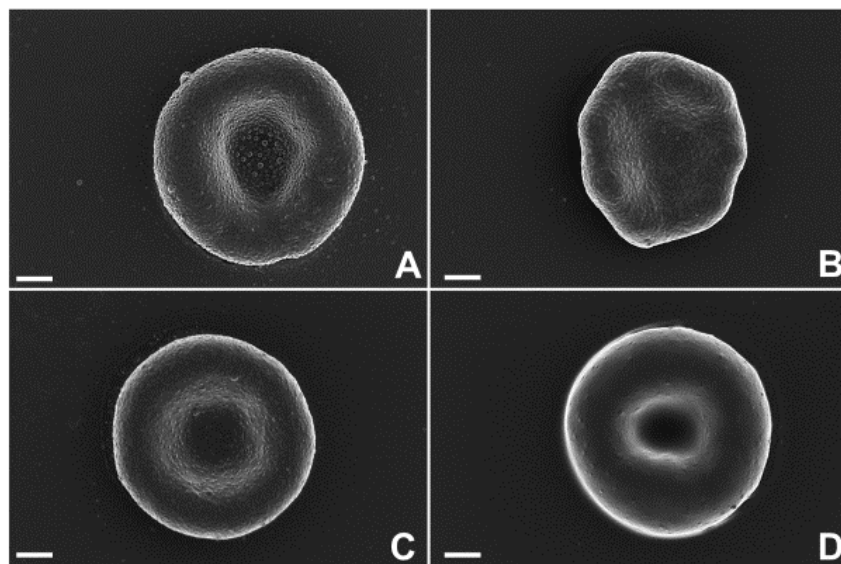
**Figure 8.2: SEM micrographs displaying PBS control group erythrocyte morphology-** Figure A-D depict the biconcave erythrocyte structure within the CV system of the control rat group. (Scale bars: 1  $\mu\text{m}$ )

The Manuka honey treated control group showed a biconcave erythrocyte structure as displayed in figure 8.3.



**Figure 8.3: SEM micrographs displaying treated control group erythrocyte morphology-** Figure A-D are representative images of the biconcave erythrocyte structure present within the CV system of the treated control group. (Scale bars: 1  $\mu\text{m}$ )

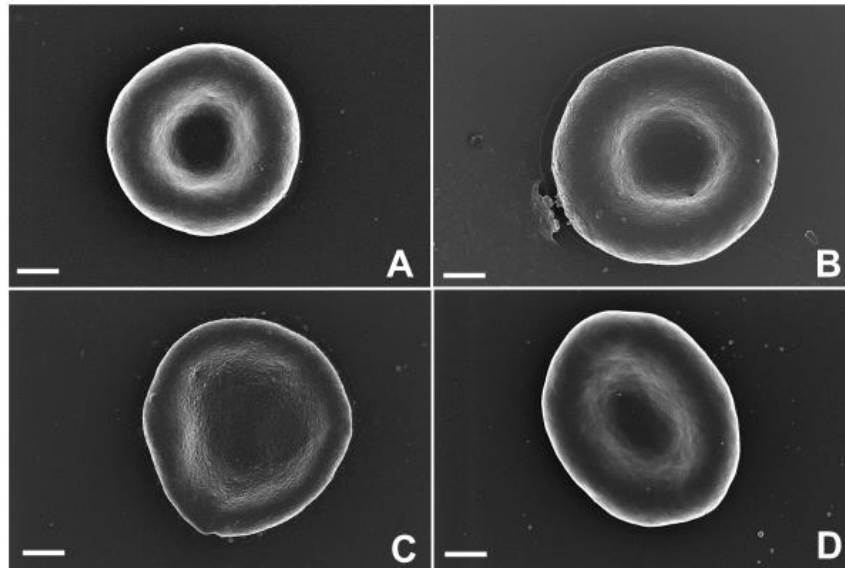
Figure 8.4 displays that the general erythrocyte structure that was observed in the experimental group had a biconcave structure as displayed in figure 8.4 C and D, however, some cells displayed structural differences to the typical biconcave structure as seen in figure 8.4 A. An elevation of early elliptocyte formation (as seen in figure 8.4 B) was observed in the samples of the LPS group.



**Figure 8.4: SEM micrographs displaying experimental group erythrocyte morphology-** Figures A-D represent erythrocyte shapes that the LPS experimental group presented. Figure A, C, D – Illustrate a biconcave erythrocyte with minor morphological alterations. Figure B- Illustrates early elliptocyte formation. The micrographs generally displayed biconcave erythrocytes with commonly observed cell morphologies. (Scale bars: 2  $\mu\text{m}$ )

Figure 8.5 displays that the LPS and manuka honey experimental and control rat groups had biconcave erythrocytes. While figure D displays an erythrocyte in early elliptocyte formation.

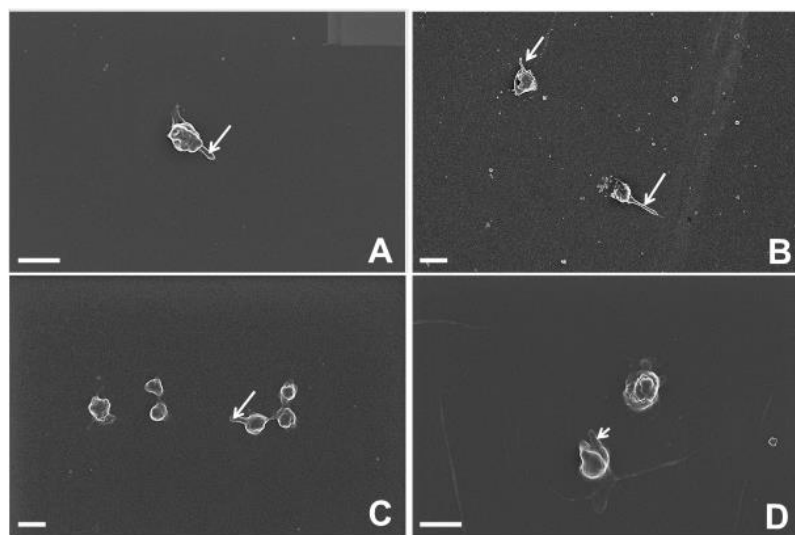




**Figure 8.5: SEM micrographs displaying treated experimental group erythrocyte morphology-** Figures A-D are erythrocyte morphologies found in the LPS and Manuka honey experimental group. Figure A and B- Display biconcave erythrocytes. Figure C and D- Commonly observed erythrocyte morphologies; D- Illustrates early elliptocyte formation. The micrographs generally displayed biconcave erythrocytes. (Scale bars: 1  $\mu\text{m}$ )

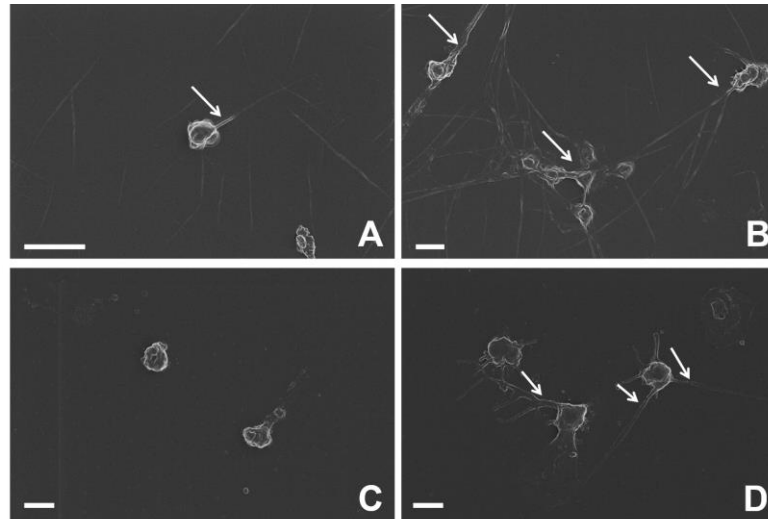
### Platelet morphology

The following micrographs (figures 8.6 and 8.7) are representative of platelet micrographs of the control and experimental groups. The control and treated control groups are displayed in figure 8.6 (A and B) and showed normal platelet spreading with minimal shape changes and pseudopodia. Figure 8.7 (C and D) displays the platelets of the experimental and treated experimental group, these platelets display minimal shape changes and pseudopodia.



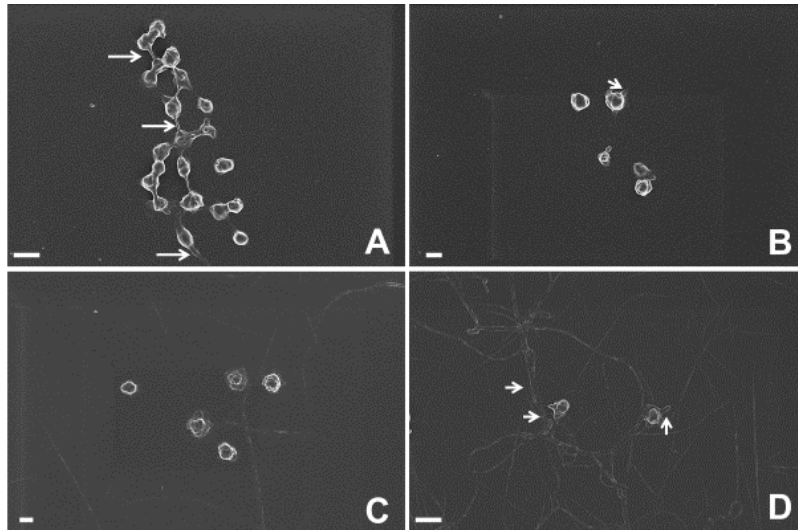
**Figure 8.6: SEM thrombin exposed samples displaying the platelets of the control and experimental rat group-** Figure A (control), Figure B (treated control), Figure C (experimental), Figure D (treated experimental). The white arrows identify the pseudopodia (Scale bars: 2  $\mu\text{m}$ )

The platelets of the control group are displayed in figure 8.7 A and B. The control group displayed platelets with minor activation as well as display platelet-platelet interactions which are defined as collections of two or more platelets. The treated control groups displayed minor platelet spreading and a minimal degree of platelet-platelet interaction as seen in figure 8.7 C and D.



**Figure 8.7: SEM thrombin exposed samples displaying the platelets of the control and treated control group-** Figure A and B display the platelets of the control group and Figure C and D depict the platelets of the treated control group. The white arrows identify the pseudopodia (Figure A Scale bar: 3  $\mu\text{m}$ ) (Figure B-D: 2  $\mu\text{m}$ )

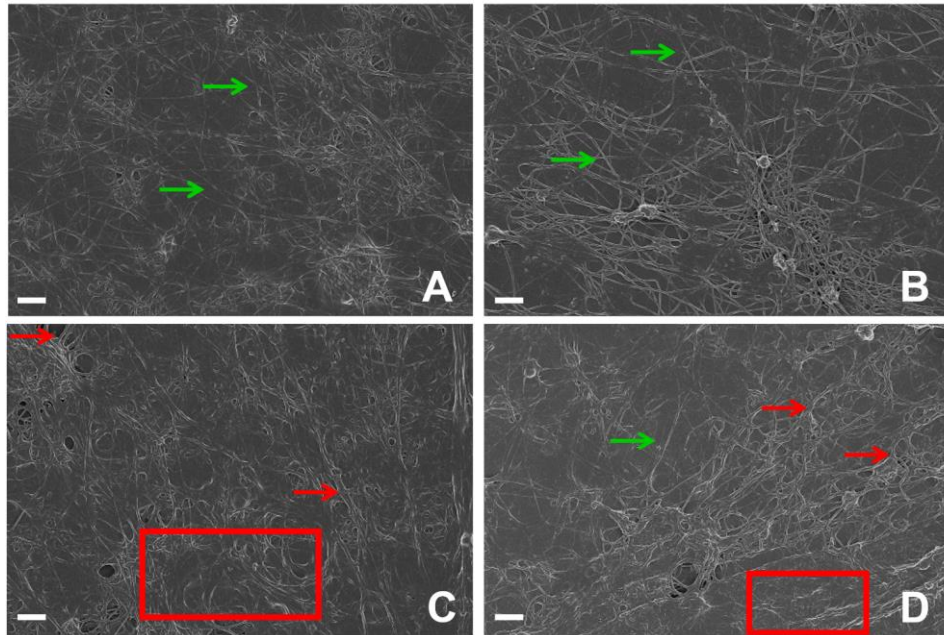
Figure 8.8 illustrates the platelet morphology of the experimental and treated experimental groups. The experimental group displayed few pseudopodia and morphological changes as seen in figure 8.8 B, and minor platelet spreading. Platelet-platelet interactions are identified seen in figure 8.8 A and D. Both groups showed mostly minor (figure 8.8 C) to moderate (figure 8.8 D) pseudopodia formation. The platelets display minor spreading as seen in figure 8.8 D.



**Figure 8.8: SEM thrombin exposed samples displaying the platelets of the experimental and treated experimental group-** Figure A and B- LPS experimental rat group, Figure C and D- LPS and Manuka honey group. The white arrows identify the pseudopodia (Figure A and D- Scale bar: 2 $\mu$ m, Figure B and C- 1 $\mu$ m)

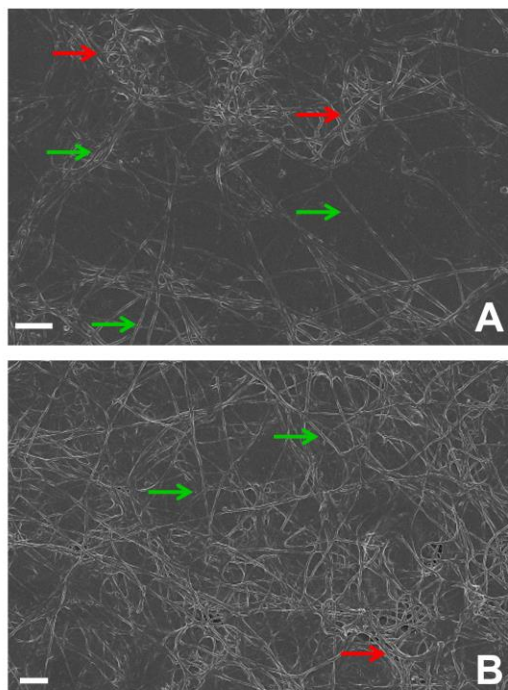
### Fibrin fibre structure

An evaluation of the thrombin exposed samples of the control and treated control groups (Figures 8.9 A and B) revealed a normal fibrin network architecture in which the individual fibres that varied in thickness and in some cases creating an overlapping fibrin mesh. In addition, open spaces were evenly distributed throughout the sample. However, there were some observable fibrin networks that appeared to be denser, fused and thick in the experimental group, while the treated experimental group displayed fibrin fibres that appeared to be denser and fused fibrin however the fibres later formulated a normal network.



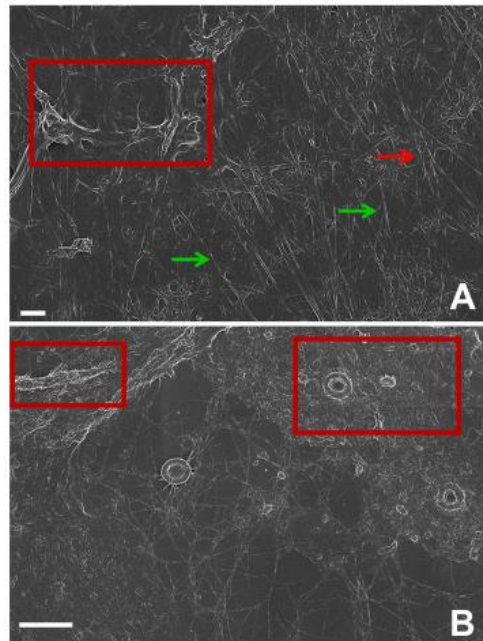
**Figure 8.9: SEM thrombin exposed samples prepared fibrin networks of the control and experimental rat group-** micrograph A (control), micrograph B (control treated), micrograph (experimental), micrograph (experimental treated). Green arrows: Thin fibrin fibers; Red arrows: Thick fibrin fibers, Red block: Fused fibrin fibers (Scale bars: 2 $\mu$ m)

The control and treated control groups displayed thin and thick fibrin networks that are found in normal fibrin networks as displayed in figure 8.10.



**Figure 8.10: SEM micrographs prepared from fibrin networks of the control group-** micrograph A- PBS, micrograph B- PBS and honey. Green arrows: Thin fibers (Micrographs A and B- Scale bars: 2 $\mu$ m)

The experimental group appeared to display fused and thick fibrin fibres as displayed in figure 8.11 A. Figure 8.11 B, displays a representative image found in the treated experimental group. The treated experimental group produced normal fibrin networks with both thin and thick fibres with areas that appeared to contain fused thick meshes. However, the overall mesh presented with a heterogeneity as seen in figure 8.11 B.



**Figure 8.11: SEM samples prepared from fibrin networks of experimental groups-** micrographs A- LPS, micrographs B- LPS and honey. (Micrographs A and B- Scale bars: 2µm; micrograph B: 10µm)

A summary of the WB SEM analysis is presented in table 8.1 and the table contains a summary of the effects of LPS on erythrocyte, fibrin network and platelet morphologies as well as the effect of manuka honey as a potential treatment.

Table 8.1: Summary of Whole blood SEM analysis

Groups	Erythrocyte	Platelets	
	Altered morphology	Altered morphology	Spread appearance
PBS	-	-	-
PBS + H	-	-	-
LPS	-	-	-
LPS + H	-	-	-
Groups	Fibrin network		

<b>Altered fibre morphology</b>		<b>Dense-like network appearance</b>	
<b>PBS</b>	-	-	-
<b>PBS + H</b>	-	-	-
<b>LPS</b>	++	++	++
<b>LPS + H</b>	++	++	++

<b>No or minimal change</b>	<b>Mild</b>	<b>Moderate</b>	<b>Severe</b>
-	+	++	+++

## **8.4 Discussion**

The effect of LPS on the CV system and its cellular elements (e.g erythrocyte, fibrin network structure, and platelets) are well documented in literature and is well described in chapter 2<sup>58,79,87</sup>. In this study, the low physiological endotoxin dose simulated what may occur in LPS exposure patients due the previously mentioned modes of entry. Scanning electron microscopy was utilised to investigate the effects of LPS on the erythrocyte, fibrin network and platelet morphological structures and the following was documented:

When comparing the erythrocyte morphology of the control and experimental groups no significant differences were found. One of the aims of this study was to explore the effect of LPS on erythrocyte morphology the study has found that early low dose of LPS exposure over a short period resulting in insignificant morphological changes<sup>73,79</sup>

The platelets of the control and experimental groups were compared and spreading were not significantly different. All the evaluated platelets exhibited normal morphology and platelet-platelet interactions. A study conducted by Zhang et. al. (2009) discovered that platelets that were directly exposed to LPS levels lower than 100 µg/ml, do not aggregate<sup>254</sup>. Following the direct LPS exposure, a significant amount of platelet adenosine triphosphate (ATP) is released which induced dense granule secretion<sup>254</sup>. Nevertheless, the ATP quantity released through LPS induction is lower than the quantity secreted through a platelet agonist (e.g thrombin) stimulation. Although thrombin does enhance the effects of LPS, the platelets of the experimental and treated experimental groups did not show any significant difference to the control and treated control groups which is dependent on the dose that the platelets were exposed to *in vivo*. The low SC release may have resulted in underexposure or an insignificant exposure period that did not produce a significant comparable chronic platelet activation response. When the micrograph preparation occurred all of the platelets were exposed to thrombin which induced platelet activation. The LPS dose may have contributed an additional, but insignificant secretion of ATP resulting in the lack of significant differences between the platelets of the control, treated control, experimental and treat experimental groups. However, although no morphological differences between the groups has been found previous studies have found that low LPS dose exposure results in low-grade systemic inflammation<sup>88</sup>.

When the fibrin networks experimental and treated experimental groups were compared, it was found that the treated experimental and experimental groups produced fibrin network structures that appeared to be significantly denser fibrin networks than the control and control treated groups. The fibrin fibre samples from the two control groups manifested normal fibrin networks in which individual fibres were of varying thickness and in most cases overlay to produce a fibrin mesh. Significant differences between the two control groups could not be

found. Fibrin network properties are largely altered by environmental factors. It is well documented that LPS induces blood clots that are denser in nature and contain amyloid marker traces<sup>21,255</sup>. The treated experimental group displayed fibrin network structures that appeared to produce thin, thick and fused fibres that were heterogenous compared to those found in the experimental group. The experimental group mostly displayed fibrin network structures that appeared to consist of thick and fused fibres.

Abnormal fibrin formation concludes in a thrombotic risk and patients present with fibrin clots that resist fibrinolysis<sup>256</sup>. Blood clots that are resistant to fibrinolysis are prone to cause thrombotic events in patients. Denser fibrin networks have been verified in arterial hypertension, heart failure, renal insufficiency, myocardial infarction, and type 2 diabetes mellitus<sup>257</sup>. It is well documented that LPS causes hypercoagulation and that prothrombotic and antifibrinolytic states are a consequence of persistent systemic inflammation which is a hypercoagulability hallmark<sup>258-259</sup>. This study shows that LPS causes significantly denser fibrin networks in low doses indicating a hypercoagulative state however, more research is needed.

In contrast, previous research has discovered that Manuka honey has anti-inflammatory, antibacterial and antimicrobial properties<sup>23,146,204</sup>. The compound is utilised for infection treatment in burns, abscesses, surgical and traumatic injury wounds<sup>23,204</sup>. In addition, the Manuka factor initiates both pro-inflammatory and anti-inflammatory processes to promote wound healing<sup>204,260</sup>. The wound healing time after administration is significantly reduced by preventing a prolonged inflammatory response at the injury site through: firstly, suppression of inflammatory cell (macrophages and lymphocytes) production and propagation, neutrophil migration. Neutrophils facilitate a inflammatory response resulting in the second phase while killing bacteria through phagocytosis, ROS, cytokine, chemokine, matrix-degrading enzyme release<sup>260</sup>. The second phase consists of the simulation of inflammatory response. Pro-inflammatory cytokine release and fibroblast and epithelial cell proliferation concluding in accelerated wound healing<sup>204</sup>. Researchers have found that Manuka honey exposure concludes in the following pro-inflammatory cytokine release of: IL-1  $\beta$ , IL-6 through the TLR-4- dependent mechanism and TNF $\alpha$  at the injury site<sup>204</sup>. A study by Minden-Birkenmaier et al. (2020) discovered that the simulation of pro-inflammatory and anti-inflammatory cytokine expression after Manuka honey solution exposure to a wound site, is dose dependent<sup>260</sup>. A 0.5% Manuka honey solution exposure induces the simulation of both pro-inflammatory and anti-inflammatory cytokines. While exposure to a 3% Manuka honey solution results in the increase of TNF- $\alpha$  and IL-8 release<sup>260</sup>. The anti-inflammatory effects are facilitated by neutrophils exposed to Manuka honey resulting in the decreases inflammatory free-radical damage, therefore preventing tissue necrosis in deep wounds<sup>204</sup>.



In this study, there were some observable fused fibres in the experimental and Manuka honey treated experimental groups, however the treated experimental group presented with both dense and fused fibrin fibres and normal networks that are comparable to the control fibrin fibres.

When comparing the fibrin network structure of the experimental and treated experimental groups, it is observed that LPS exposure resulted in the fused and thick aggregated fibrin mesh production that seldom displayed thin fibrin fibres. The Manuka honey treated experimental group produced a wide assortment of fibrin fibres that were fused, thick and thin in nature. The nature of the fibrin structures created by each experimental group would cause an elevation in coagulability possibly concluding in thrombotic events. However, the experimental group may produce a dense, but stable clot in comparison to the clots created by the treated control group. Although ingesting Manuka honey neutralised some of the harmful hypercoagulative effects that were a consequence of LPS exposure, resulting in the presentation of a normal network presentation in some areas. The treated experimental group presented with fibrin networks that were uneven in thickness that could result in the formation of unstable clots with greater porosity and may conclude in an elevation of bleed incidents. Although the dense blood clots that are found in the experimental group would result in thrombosis in any case.

Low doses of LPS exposure elevates the risk of thrombosis thus elevating the CV pathology risk. Patients with AF were found to be in a hypercoagulable state with denser fibrin networks<sup>261</sup>. Impaired fibrinolysis is associated with ischaemic stroke and bleeding complications<sup>256,261</sup>. Lipopolysaccharide exposure would raise that risk. Atrial fibrillation is more prevalent in men and these patients elevated subclinical or silent stroke incidence and a greater dementia risk (including AD) as a consequence<sup>95-98,102</sup>.

## **8.5 Conclusion**

Lipopolysaccharides elevate thrombotic risk as a consequence of a hypercoagulative state. Early exposure to low LPS doses results in insignificant erythrocyte and platelet morphological changes as well as inducing substantial alterations in clot structure. Denser fibrin network formation was a consequence of endotoxin exposure and may elevate the thrombotic and CV disease risk. In addition, although the Manuka factor produces anti- bacterial and - inflammatory effects, Manuka honey presented as an inadequate treatment. While ministering the treatment bought about the reduction of the hypercoagulative state produced by LPS in the form of thick and fused fibrin fibres, the treated experimental group produced dense and

uneven fibrin networks<sup>23</sup>. Although Manuka honey possess many beneficial properties such as the ability to reduce inflammation during in the wound healing process, it does not fully neutralise the pro-coagulative effects of the endotoxin. Thus, it is an insufficient treatment for the prevention of hypercoagulability with LPS exposure. However, further research would provide a deeper understanding to the molecular mechanisms of the therapeutic effects of Manuka honey and why it failed to completely neutralize the pro-coagulative effects of LPS.

# **Chapter 9: Conclusion**

## **9.1 Introduction**

Many sub-Saharan countries like South Africa are experiencing elevations in urbanisation resulting in lifestyle changes. As a consequence, an epidemiological shift from infectious disease to lifestyle diseases such as CV disease is being observed<sup>262</sup>. An increase in diabetes, hypertension and obesity are contributing factors however, CV disease are not a sub-Saharan public health priority<sup>262</sup>. Therefore, many individuals may live with undiagnosed CV disease as a consequence. A study conducted by Hamid et al. (2018) discovered that hypertension is a major risk condition consequentially individuals with undiagnosed and thus untreated CV disease are at an increased risk of developing other CV diseases<sup>122</sup>. In addition, these individuals, who are often in a lower income bracket, are less likely to be diagnosed with chronic systemic inflammation or LPS endotoxin exposure, due to the failing public health systems found in the region. Sixty-six percent of South Africa is urbanised and the country contains an elderly population of eight percent<sup>263</sup>. Coupled with the elevated CV disease prevalence in the region, LPS exposure may result in a greater undiagnosed CV disease risk. As a consequence, placing further strain on already ailing sub-Saharan health systems.

In this study, ten-week-old, male Sprague dawley rats were used to explore the effects of early (ten days) endotoxin exposure on the general population as well as in young males. The study reviewed if early exposure would induce dementia type behaviour and cognitive deficits as well as produce CV changes. Meanwhile, Manuka honey was administered as a possible treatment to prevent behavioural, cognitive or CV changes that may have resulted as a consequence of LPS exposure. This study showed that early LPS exposure at a low physiological dose has damaging results on the CV system while Manuka honey was an incomplete treatment for the effects of LPS exposure.

## **9.2 Key findings**

A Sprague dawley rat model was successfully designed and implemented over a 19-day period. The study investigated the effect of a low SC LPS (at 0.1 mg/ml at a volume of 0.05 mg/kg of the rat) dose on behaviour and memory, core body temperature (thermogenesis) and weight, and the CV system. As described in chapter four, the experimental group presented with anxiety behaviour, short- and long-term familiar object recognition, and short-term spatial memory that was similar to that of the control groups. While the treated experimental presented with only anxiety behaviour and short- and long-term familiar object recognition memory that were similar to the control and treated control group. The treated experimental group showed a significant decline short-term spatial memory when compared to the control

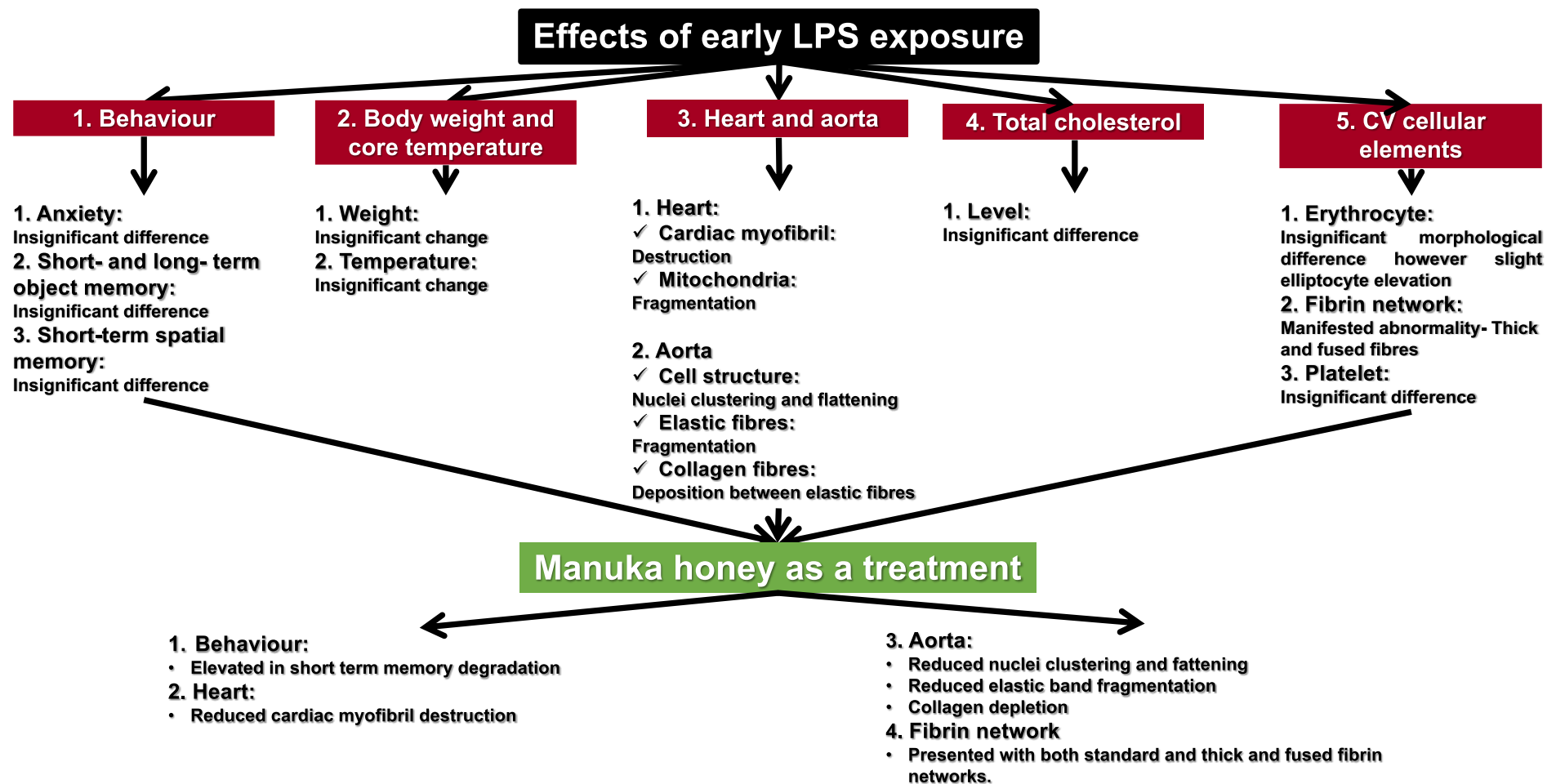
and experimental group. However, the group presented with no significant change in spatial memory than the treated control group. Fructose exposure coupled with LPS exposure may result in a greater spatial memory degeneration. A study conducted by Fierros-Campuzano have found that a high fructose diet is associated with a deficit in the hippocampal cognitive functions, which may provide a possible explanation for the findings in this study<sup>264</sup>. Although, honey contains a substantial amount of sugar e.g fructose, chapter five indicated the weight of the experimental and treated experimental group showed a steady increase similar to the control groups<sup>145</sup>. In addition, the experimental groups presented with similar core body temperatures to the control populations.

The aortic and cardiac tissue were evaluated in chapter six. Upon evaluating the cardiac tissue using H and E, the cardiac muscle of the animals exposed to LPS presented with visible cardiac myofibril damage and erythrocyte extravasation associated to vascular leakage as a consequence of endothelial damage in some areas<sup>228</sup>. While other areas presented with normal cardiac histology. However, when investigating glycogen accumulation as an indicator of cardiac hypoxia using Periodic acid-Schiff the experimental groups displayed a lack of glycogen accumulation when compared to the control groups. Therefore, all of the test groups displayed no visible signs of hypoxia. With the in-depth TEM investigation, the LPS treated groups presented with moderate myofibril damage while the addition of the LPS and Manuka honey group presented with reduced myofibril damage. Endotoxin exposure produced mild mitochondrial cristae damage. Meanwhile, Manuka honey administration failed to counteract the mechanisms involved in the destruction of mitochondria cristae.

When evaluating the aorta using H and E, varying tissue disruption in the form of nuclei clustering and flattening in some area was a consequence of endotoxin exposure. In contrast, Manuka honey only presented with aortic tissue damage that presented as perforations that could be observed upon closer magnification, thus neutralising some of the harmful effects of LPS. When evaluating the elastin layers using VVG. LPS caused elastic fibre disruption that was displayed as disordered fibre arrangements and a large number of elastic laminae crosslinks. Manuka honey exposure concluded in a reduction in the elastic fibre disruption caused by the endotoxin. Upon elastin and collagen inspection using TEM, endotoxin administration concludes in elastin fragmentation and collagen deposition. In contrast, Manuka honey prevents the fragmentation of elastin to a significant degree however, as a consequence the treatment results in collagen depletion.

Following the blood analyses, it was concluded that early LPS exposure does not disrupt cholesterol homeostasis or significantly alter erythrocyte and platelet morphology. However, exposure dose may increase the elliptocyte presence in the circulating erythrocyte population.

In contrast, endotoxin exposure resulted in the thickening and fusion of fibrin fibres. Still, the therapeutic treatment partly countervailed the effects of the endotoxin thus resulting in the restoration of normal fibrin fibre structure in some areas while producing fused and thick fibres in other areas. Nevertheless, Manuka honey is not effective as a treatment for systemic inflammation or LPS exposure since the treatment failed to fully counteract the harmful effects of the endotoxin.



**Figure 9.1: Study summary-** Endotoxin exposure resulted in the following: cardiac myofibril destruction, mitochondrial damage, aortic cell disruption, elastin fibre fragmentation, abnormal collagen deposition, and abnormal fibrin network in the form of thick and fused fibres. The therapeutic agent, Manuka honey reduced cardiac myofibril destruction, reduced aortic destruction, elastin fibre fragmentation and in CV circulation counteracted some of fibrin thickening effects of the endotoxin. However, the treatment elevated short term memory degradation and resulted in aortic collagen depletion.

### **9.3 Relevance of the findings**

Lipopolysaccharides is widely used to investigate the effects of fever and sepsis on the human body. However, the present study provided preliminary data on the early effects of the LPS endotoxin on behaviour, cognition, the CV system, thermogenesis and weight. The study identified that the endotoxin presents with CV damage in the form of cardio myofibril and aortic damage that may result in accelerated CV aging and increased risk to CV disease. In addition the observed mitochondrial cristae destruction may result in a reduction in mitochondrial respiration leading to an upsurge in mitochondrial oxidative stress and a reduction in membrane potential<sup>232</sup>. Continued LPS exposure may result in further mitochondrial cristae destruction that may conclude in widespread oxidative stress overtime resulting in the apoptosis of many cardiomyocytes potentially leading to CV complications. Elastin depletion may result in the vasculature stiffening resulting in hypertension and impaired blood flow to vital areas such as the brain, heart, liver and lungs. However, initially individuals do not present with temperature, weight or total cholesterol alterations, thus rendering identification and diagnosis difficult. In addition, the study has identified the need for further investigation the area of LPS early exposure symptom identification as well as the need for a readily accessible and effective treatment. Although, Manuka honey has a variety of therapeutic uses such as wound healing acceleration, it cannot be used as a treatment for LPS exposure or low-grade systemic inflammation it fails to fully prevent the harmful effects of LPS exposure and results in aortic collagen depletion. Collagen depletion compromises the structural integrity of the aorta thus resulting in vascular pathology. The study confirmed the relevance of an animal model on the effects of early LPS exposure.

### **9.4 Limitations of the study and future recommendations**

Although this study added to existing literature on the topic, it did present with limitations such as the range of biological tests that were utilised as well as the endotoxin exposure duration. An increase in the number of days from ten days to perhaps 15 days may allow for distinguishable differences between the control and experimental groups concluding in clear descriptions of the effects of a low LPS dose on behaviour, cognition, the CV system, thermogenesis and weight. Further linking the endotoxin to early neurodegenerative disease pathogenesis. Future studies may need to increase the number of rats, as well as evaluate rats of both the male and female sex. The elevation in rat number would increase the statistical power of the results obtained. Evaluating both sexes would allow for the evaluation of how gonadal hormones may contribute to cardiac protection or degradation. Studies have found that pre-menopausal women display a greater level of cardiac hypertrophy protection when



compared to their male counterparts<sup>265</sup>. In addition, oestrogen counteracts pro-hypotrophy signals however, this protection is non-existent following menopause and is incompletely regained after the commencement of oestrogen replacement therapy<sup>265</sup>. Thus, oestrogen provides cardiac protection that cannot be overlooked when conducting a study regarding CV health. In addition, male and females manifest behavioural and cognitive pathological symptoms differently. A wholistic view on the effect of gonadal hormones on the harmful effects of LPS may widen the stream of knowledge available on the external presentation that women and men display in the early onset of a neurodegenerative disease.

In addition, TEM and SEM only provide qualitative and not quantitative data. A future study should evaluate beats per minute, blood pressure, and cardiac troponin-I since the endotoxin exposure presents with CV myocardial injury that could show significant cardiac troponin-I, systolic and diastolic pressure differences even after a short duration of endotoxin exposure. The cardiac troponin-I test would evaluate cardiac myofibril specific injury. The aortic destruction evaluated in this study would need to be further investigated and the next phase would be to investigate its effect on CV pressure. Beats per minute may provide another quantitative marker on the effect of LPS on cardiac contraction. An investigation into LDL, HDL and LDL receptor mRNA expression on macrophages would broaden the amount information on the effect of the endotoxin on cholesterol homeostasis and if it corresponds to macrophage foam cell formation.

Regarding blood cellular element analysis, thromboelastography (TEG<sup>®</sup>) would be vital in comparing the clot strength of both the control, and experimental groups. The test would investigate the efficiency of blood coagulation in exposed and control individuals. Creating clots from the blood of the control and experimental groups then fracturing the respective clots opposed to coating on a coverslip would provide a superior indication of clot formation in blood i.e., the CV system. Therefore, this would assist in the identification of the interactions between clotting factors with one another. Thus, expanding on the information of the variety of thrombotic events that LPS exposed individuals are likely to manifest. In addition, Amyloid  $\beta$  and tau protein are two hallmark proteins for AD since it is thought that amyloid  $\beta$  oligomers followed by downstream tau protein dysfunction, may conclude in AD<sup>266</sup>. Amyloid  $\beta$  and tau protein evaluation using ELISA would definitively link LPS to AD allowing for the strengthening of its association with AD. In addition, data shows that vascular factors are important AD risk contributors and the first AD change is a reduction in cerebral blood flow<sup>267</sup>. An investigation of the vasculature of both cardiac and cerebral would investigate cerebral and cardiac blood flow, and amyloid  $\beta$  and tau protein level quantification would provide detailed image of disease aetiology.

Lastly, future studies may need to obtain the Manuka factor (methylglyoxal) extract from Manuka honey and utilise it as a treatment in the place of the raw material. Using the methylglyoxal extract would provide a greater concentrated anti-inflammatory agent thus potentially providing better results without the counteractive pro-inflammatory and hippocampal degenerative effects of fructose<sup>23,268</sup>. For the reason that, lowering the Manuka honey dose to prevent the effects of fructose would result in an even greater inability of the treatment to counteract the injurious effects of LPS.

In conclusion, LPS are readily available in our environment and thus CV entry resulting in subclinical physiological changes may occur. A greater body of information is vital as a notable elevation in CV disease prevalence found in sub-Saharan Africa may further be elevated due untreated endotoxin exposure. Thus, may result in the further elevation of the risk of neurodegeneration. Natural anti-inflammatory agents on the continent and abroad may assist in the fight against low-grade systemic inflammation or LPS exposure. Once the identification of the early symptoms of LPS exposure and natural cost effective therapeutic's occur, treatment of affected individuals of all socioeconomic backgrounds can begin, resulting in the prevention of LPS induced CV disease and possible neurological degradation.

# **Chapter 10: Appendixes**

## 10.1 Appendix A

### 10.1.1 Materials and chemicals

- 10 mm Coverslips
- 24-well plates
- Absolute Ethanol (Manufacturer: Illovo, catalogue number: 1170) (used: all light microscopy test (which include: H and E, VVG, and MT), and TEM)
- Beakers
- Blood vacuum tubes: (Sodium citrate vacucare (2.7 ml) (use: SEM), Serum vacucare tube (5 ml) (use: Total cholesterol ELISA kit)
- Colour stickers to easily identify the different groups
- Coverslips (22 mm x 40 mm x 100/pcs (Manufacturer: Lasec)
- Elastic staining kit (Manufacturer: Sigma-Aldrich, catalogue number: HT25A-1KT)
- Entellan® mounting medium (Manufacturer: Merck, catalogue number: HX68664361)
- F10 SC veterinary disinfectant (Manufacturer: Health and Hygiene (Pty) LTD) (use: Disinfecting surfaces between behavioural tests)
- Fixative (4% formaldehyde made before getting to University of the Witwatersrand CAS unit and taken there) (use: Light microscopy and TEM)
- Forceps
- Formaldehyde (Manufacturer: Merck, catalogue number: F8773-25ml)
- Glass tubes for TEM and LM samples (ALS, B793, 10 ml glass vials)
- Gloves (M/L)
- H and E stain (Manufacturer: Sigma-Aldrich, Haematoxylin catalogue number: H9627-25G, Eosin catalogue number: 230251-25G) (use: H and E)
- HMDS (Manufacturer: Merck, catalogue number: 440191-1L) (use: SEM)
- Manuka honey (Sourced from: Ample Resources South Africa)
- Micropipettes (use: SEM prep)
- Organs: heart and aorta
- Papers with 1 mm<sup>3</sup> blocks on to indicate the size of the TEM samples to cut
- Paraffin white wax pellets (Manufacturer: Merck, catalogue number: 76242)
- Pasteur plastic pipettes
- Periodic acid-Schiff staining system kit (Manufacturer: Sigma-Aldrich, catalogue number: 395B-1KT)
- Petri dishes

- Phosphate Buffer Solution (made before getting to the University of the Witwatersrand CAS unit and taken there) (use: rat experimental group dosing, Cholesterol ELISA kit test, SEM and TEM)
- Pipette tips
- Secondary Fixative (4% Osmium tetroxide (Manufacturer: Merck, catalogue number: 75632-5 ml)) (Manufacturer: SPI Suppliers) (made up the day before termination) (use: SEM and TEM)
- Shandon MB DynaSharp microtome blades 34°/80 mm (manufacturer: Thermo Election Corporation)
- Single edge blades (Manufacturer: SPI Suppliers)
- Slide Boxes (Manufacturer: ALS)
- Star select- Frosted Glass slides (Manufacturer: Lasec catalogue number: 3000F-02-1009) (use: Light microscopy)
- Stickers for labelling tubes (this is done before arrival at University of the Witwatersrand CAS unit)
- Thrombin (use: blood prep)
- Xylene (Manufacturer: Sigma-Aldrich, catalogue number: 534064-4L) (use: Light microscopy)

## **10.2 Appendix B**


### **10.2.1 Link for test raw data**

Please find the link for the raw data acquired during the behavioural study (Open field, Novel object recognition, The Y-maze novelty preference test), body weight, core body temperature and total cholesterol ELISA test:

<https://drive.google.com/drive/folders/1vLrEHOAJq0nt-cfZDv9UjwdSWlqfajJE?usp=sharing>

## 10.3 Appendix C

### 10.3.1 University of Pretoria: Animal ethics committee approval

  
UNIVERSITEIT VAN PRETORIA  
UNIVERSITY OF PRETORIA  
YUNIBESITHI YA PRETORIA

Faculty of Veterinary Science  
Animal Ethics Committee

3 August 2020

**Approval Certificate with Conditions  
New Application**

**AEC Reference No.:** 171/2020  
**Title:** The effect of systemic lipopolysaccharides on the cardiovascular system in Sprague-Dawley rats  
**Researcher:** Miss GI Tambwe  
**Student's Supervisor:** Dr S Alummootti

Dear Miss GI Tambwe,

The **New Application** as supported by documents received between 2020-06-15 and 2020-07-27 for your research, was approved by the Animal Ethics Committee on its quorate meeting of 2020-07-27.

Please note the following about your **CONDITIONAL** ethics approval:

- Approval is prospective only and does not cover any data collected before the 6<sup>th</sup> of July 2020 i.e. no retrospective data may be used as part of this approval.
- The committee has decided, that this project will be inspected since it is outside of a UP managed facility. Please provide the committee for the starting dates of the project so that an inspection can be arranged.

1. The use of species is approved:

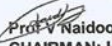
Species and Samples	Number
Rats	60

- Ethics Approval is valid for 1 year and needs to be renewed annually by 2021-08-03.
- Please remember to use your protocol number (171/2020) on any documents or correspondence with the AEC regarding your research.
- Please note that the AEC may ask further questions, seek additional information, require further modification, monitor the conduct of your research, or suspend or withdraw ethics approval.

**Ethics approval is subject to the following:**

- The ethics approval is conditional on the research being conducted as stipulated by the details of all documents submitted to the Committee. In the event that a further need arises to change who the investigators are, the methods or any other aspect, such changes must be submitted as an Amendment for approval by the Committee.

We wish you the best with your research.  
Yours sincerely

  
Prof V Naidoo  
CHAIRMAN: UP-Animal Ethics Committee

---

Room 6-13, Arnold Theiler Building, Onderstepoort  
Private Bag X04, Onderstepoort 0110, South Africa  
Tel +27 12 529 8483  
Fax +27 12 529 8321  
Email [aec@up.ac.za](mailto:aec@up.ac.za)  
[www.up.ac.za](http://www.up.ac.za)

Fakulteit Veeartsenykunde  
Lefapha la Diseanse tša Bongakadiruiwa

### 10.3.1 University of Pretoria: Faculty of health sciences research ethics committee approval

Please find the link for the Faculty of health sciences research ethics renewal:

<https://drive.google.com/drive/folders/1vLrEHOAJq0nt-cfZDv9UjwdSWlqfajJE?usp=sharing>



10.3.2 University of the Witwatersrand: Animal research ethics committee approval

UNIVERSITY OF THE  
WITWATERSRAND  
JOHANNESBURG



**STRICTLY CONFIDENTIAL**

**ANIMAL RESEARCH ETHICS COMMITTEE (AREC)**

**CLEARANCE CERTIFICATE NO.** 2019/07/44/C

**APPLICANT:** Prof W Daniels

**SCHOOL:** Physiology

**DEPARTMENT:**

**LOCATION:**

**PROJECT TITLE:** Investigating lipopolysaccharide-induced hypercoagulability in Sprague-Dawley rats with Alzheimer's type neuroinflammation

Number and Species

75X male 10 weeks old wild-type Sprague-Dawley Rats

Approval was given for the use of animals for the project described above at an AREC meeting held on 2019/07/30. This approval remains valid until 2021/09/30.

Unreported changes to the application may invalidate the clearance given by the AREC.

An annual progress report must be provided.

The use of these animals is subject to AREC guidelines for the use and care of animals, is limited to the procedures described in the application form and is subject to any additional conditions listed below:

Signed: \_\_\_\_\_  
(Chairperson, AREC)

Date: 1<sup>ST</sup> OCTOBER 2019

I am satisfied that the persons listed in this application are competent to perform the procedures therein, in terms of Section 23 (1) (c) of the Veterinary and Para-Veterinary Professions Act (19 of 1982)

Signed: \_\_\_\_\_  
(Registered Veterinarian)

Date: 01 October 2019

cc: Supervisor: N/A  
Director: CAS

Works 2000/ain0015/AESCcert.wps

# **Chapter 11: References**

1. Todd D., Gould DTD, Colleen E. Kovacsics CE. The open field test. Mood and anxiety related phenotypes in mice. Humana Press, Totowa, NJ; 2009. p. 1-20.
2. Langford DJ, Bailey AL, Chanda ML, Clarke SE, Drummond TE, Echols S, et al. Coding of facial expressions of pain in the laboratory mouse. *Nature methods*. 2010; 7(6):447-9.
3. World health organisation [Internet] Cardiovascular diseases World health organisation; 2017 [updated 17/05/2021; cited 2021 21/05/2021].
4. Steven S, Frenis K, Oelze M, Kalinovic S, Kuntic M, Bayo Jimenez MT, et al. Vascular inflammation and oxidative stress: Major triggers for cardiovascular disease. *Oxidative medicine and cellular longevity*. 2019; 2019.
5. Daiber A, Steven S, Weber A, Shuvaev VV, Muzykantov VR, Laher I, et al. Targeting vascular (endothelial) dysfunction. *British journal of pharmacology*. 2017; 174(12):1591-619.
6. Jeon YJ, Jung SJ, Kim HC. Does serum vitamin d level affect the association between cardiovascular health and cognition? Results of the cardiovascular and metabolic diseases etiology research center (cmerec) study. *European Journal of Neurology*. 2021; 28(1):48-55.
7. Katsumoto A, Takeuchi H, Takahashi K, Tanaka F. Microglia in alzheimer's disease: Risk factors and inflammation. *Frontiers in neurology*. 2018; 9:978.
8. Blossom CM, Stephan SLH, Keage HAD, Babateen D, Robinson L, Siervo M. Cardiovascular disease, the nitric oxide pathway and risk of cognitive impairment and dementia. *Current Cardiology Reports volume* 2017; 19(87).
9. Furman D, Campisi J, Verdin E, Carrera-Bastos P, Targ S, Franceschi C, et al. Chronic inflammation in the etiology of disease across the life span. *Nature medicine*. 2019; 25(12):1822-32.
10. Netea MG, Balkwill F, Chonchol M, Cominelli F, Donath MY, Giamarellos-Bourboulis EJ, et al. A guiding map for inflammation. *Nature immunology*. 2017; 18(8):826-31.
11. Fleming TP, Watkins AJ, Velazquez MA, Mathers JC, Prentice AM, Stephenson J, et al. Origins of lifetime health around the time of conception: Causes and consequences. *The Lancet*. 2018; 391(10132):1842-52.
12. Almeida AJPOd, Ribeiro TP, Medeiros IAd. Aging: Molecular pathways and implications on the cardiovascular system. *Oxidative Medicine and Cellular Longevity*. 2017; 2017:7941563.
13. Adamo L, Rocha-Resende C, Prabhu SD, Mann DL. Reappraising the role of inflammation in heart failure. *Nature Reviews Cardiology*. 2020; 17(5):269-85.
14. Zhu Y, Xian X, Wang Z, Bi Y, Chen Q, Han X, et al. Research progress on the relationship between atherosclerosis and inflammation. *Biomolecules*. 2018; 8(3):80.

15. Raggi P, Genest J, Giles JT, Rayner KJ, Dwivedi G, Beanlands J et al. Role of inflammation in the pathogenesis of atherosclerosis and therapeutic interventions. *Atherosclerosis*. 2018; 276:98-108
16. Ma Z-G, Yuan Y-P, Wu H-M, Zhang X, Tang Q-Z. Cardiac fibrosis: New insights into the pathogenesis. *International journal of biological sciences*. 2018; 14(12):1645.
17. Potashkin JASaJA. The impact of disease comorbidities in alzheimer's disease. *Frontiers in aging neuroscience*. 2021.
18. Lu C-HZ, Han Z, Yao X-L. Irhom2 is involved in lipopolysaccharide-induced cardiac injury in vivo and in vitro through regulating inflammation response. *Biomedicine & Pharmacotherapy*. 2017; 86:645-53.
19. Zhan X, Stamova B, Sharp FR. Lipopolysaccharide associates with amyloid plaques, neurons and oligodendrocytes in alzheimer's disease brain: A review. *Frontiers in Aging Neuroscience*. 2018; 10:42.
20. Carnevale R, Nocella C, Petrozza V, Cammisotto V, Pacini L, Sorrentino V, et al. Localization of lipopolysaccharide from escherichia coli into human atherosclerotic plaque. *Scientific Reports*. 2018; 8(3598):1-8.
21. Bester J, Soma P, Kell DB, Pretorius E. Viscoelastic and ultrastructural characteristics of whole blood and plasma in alzheimer-type dementia, and the possible role of bacterial lipopolysaccharides (lps). *Oncotarget*. 2015; 6(34):35284.
22. Benjamin A. Minden-Birkenmaier MBM, Kasyap Cherukuri, Matthew P. Smeltzer, Richard A. Smith, Marko Z. Radic, Gary L. Bowlin. Manuka honey modulates the release profile of a dhl-60 neutrophil model under anti-inflammatory stimulation. *Journal of Tissue Viability*. 2020; 29(2):91-9.
23. Hixon KR, Bogner SJ, Ronning-Arnesen G, Janowiak BE, Sell SA. Investigating manuka honey antibacterial properties when incorporated into cryogel, hydrogel, and electrospun tissue engineering scaffolds. *Cryogelation and Cryogels*. 2019; 5(2):1-16.
24. Silverthorn DU. Cardiovascular physiology. *Human physiology: An intergrated approach* Edinburgh Gate, Harlow: Pearson education limited 2014. p. 489-535.
25. Mohrman DE, Heller LJ. Overview of the cardiovascular system. *Cardiovascular physiology*, 9e. New York, NY: McGraw-Hill Education; 2018.
26. Bos MHA, van 't Veer C, Reitsma PH. Molecular biology and biochemistry of the coagulation factors and pathways of hemostasis. In: Kaushansky K, Lichtman MA, Prchal JT, Levi MM, Press OW, Burns LJ, et al., editors. *Williams hematology*, 9e. New York, NY: McGraw-Hill Education; 2015.
27. Brønnum H, Kalluri R. Cardiac fibrosis: Cellular and molecular determinants. In: Elsevier, editor. *Muscle: Fundamental biology and mechanisms of disease*. 2012. p. 389-404.

28. Mohrman DE, Heller LJ. The heart pump. *Cardiovascular physiology*, 9e. New York, NY: McGraw-Hill Education; 2018.
29. Gillette M, Morneau K, Hoang V, Virani S, Jneid H. Antiplatelet management for coronary heart disease: Advances and challenges. *Current atherosclerosis reports*. 2016; 18(6):35.
30. Pinti M, Appay V, Campisi J, Frasca D, Fülöp T, Sauce D, et al. Aging of the immune system: Focus on inflammation and vaccination. *European journal of immunology*. 2016; 46(10):2286-301.
31. Linthout SV, Tschope C. Inflammation – cause or consequence of heart failure or both? *Current Heart Failure Reports*. 2017; 14:251–65.
32. Wei Y, Du W, Xiong X, He X, Yi P, Deng Y, et al. Prenatal exposure to lipopolysaccharide results in myocardial remodelling in adult murine offspring. *Journal of inflammation*. 2013; 10(1):35.
33. Zettl M, Adrain C, Strisovsky K, Lastun V, Freeman M. Rhomboid family pseudoproteases use the er quality control machinery to regulate intercellular signaling. *Cell*. 2011; 145(1):79-91.
34. Freeman M. Rhomboid proteases and their biological functions. *Annual review of genetics*. 2008; 42:191-210.
35. Adrain C, Zettl M, Christova Y, Taylor N, Freeman M. Tumor necrosis factor signaling requires irhom2 to promote trafficking and activation of tace. *Science*. 2012; 335(6065):225-8.
36. Scott D, Kingsley G. Tumor necrosis factor inhibitors for rheumatoid arthritis. *New England Journal of Medicine*. 2006; 355(7):704-12.
37. Miller DV. Cardiovascular system Rosai and ackerman's surgical pathology: Elsevier; 2018. p. 1916-45.
38. Mescher AL. Muscle tissue. *Junqueira's basic histology: Text and atlas*, 15e. New York, NY: McGraw-Hill Education; 2018.
39. Li X, Liu J, Wang J, Zhang D. Luteolin suppresses lipopolysaccharide-induced cardiomyocyte hypertrophy and autophagy in vitro. *Molecular medicine reports*. 2019; 19(3):1551-60.
40. Viau DM, Sala-Mercado JA, Spranger MD, O'Leary DS, Levy PD. The pathophysiology of hypertensive acute heart failure. *Heart*. 2015; 101(23):1861-7.
41. Cui S, Cui Y, Li Y, Zhang Y, Wang H, Qin W, et al. Inhibition of cardiac hypertrophy by aromadendrin through down-regulating nfat and mapks pathways. *Biochemical and biophysical research communications*. 2018; 506(4):805-11.
42. Lee Y-M, Cheng P-Y, Chim L-S, Kung C-W, Ka S-M, Chung M-T, et al. Baicalein, an active component of *scutellaria baicalensis georgi*, improves cardiac contractile function in

endotoxaemic rats via induction of heme oxygenase-1 and suppression of inflammatory responses. *Journal of ethnopharmacology*. 2011; 135(1):179-85.

43. Timmers L, Sluijter JP, van Keulen JK, Hoefler IE, Nederhoff MG, Goumans M-J, et al. Toll-like receptor 4 mediates maladaptive left ventricular remodeling and impairs cardiac function after myocardial infarction. *Circulation research*. 2008; 102(2):257-64.

44. Levine B, Mizushima N, Virgin HW. Autophagy in immunity and inflammation. *Nature*. 2011; 469(7330):323-35.

45. Mizushima N, Komatsu M. Autophagy: Renovation of cells and tissues. *Cell*. 2011; 147(4):728-41.

46. Mizushima N. Autophagy: Process and function. *Genes & development*. 2007; 21(22):2861-73.

47. Iida T, Onodera K, Nakase H. Role of autophagy in the pathogenesis of inflammatory bowel disease. *World journal of gastroenterology*. 2017; 23(11):1944.

48. Kizilarlanoglu MC, Ülger Z. Role of autophagy in the pathogenesis of alzheimer disease. *Turkish journal of medical sciences*. 2015; 45(5):998-1003.

49. Sul O-J, Park H-J, Son H-J, Choi H-S. Lipopolysaccharide (Lps)-induced autophagy is responsible for enhanced osteoclastogenesis. *Molecules and cells*. 2017; 40(11):880.

50. Chung KW, Kim KM, Choi YJ, An HJ, Lee B, Kim DH, et al. The critical role played by endotoxin-induced liver autophagy in the maintenance of lipid metabolism during sepsis. *Autophagy*. 2017; 13(7):1113-29.

51. Azizad-Pinto P, Tapson VF. Rheumatologic disease and the cardiovascular system In: Fuster V, Harrington RA, Narula J, Eapen ZJ, editors. *Hurst's the heart*, 14e. New York, NY: McGraw-Hill Education; 2017.

52. Lukiw WJ. *Bacteroides fragilis* lipopolysaccharide and inflammatory signaling in alzheimer's disease. *Frontiers in microbiology*. 2016; 7:1544.

53. Chan MY, Andreotti F, Becker RC. Hypercoagulable states in cardiovascular disease. *Circulation*. 2008; 118(22):2286-97.

54. Kawaguchi S, Okada M, Ijiri E, Koga D, Watanabe T, Hayashi K, et al. B3-adrenergic receptor blockade reduces mortality in endotoxin-induced heart failure by suppressing induced nitric oxide synthase and saving cardiac metabolism. *American Journal of Physiology-Heart and Circulatory Physiology*. 2020; 318(2):H283-H94.

55. Saramago EA, Borges SG, Singolani-Jr CG, Nogueiraa JE, Soriano RN, Cárnio EC, Branco LGS. Molecular hydrogen potentiates hypothermia and prevents hypotension and fever in Lps-induced systemic inflammation. *Brain, behaviour and immunity*. 2019; 75:119-28.

56. Roher AE, Debbins JP, Malek-Ahmadi M, Chen K, Pipe JG, Maze S, et al. Cerebral blood flow in alzheimer's disease. *Vascular health and risk management*. 2012; 8:599.

57. Cattaneo A, Cattane N, Galluzzi S, Provasi S, Lopizzo N, Festari C, et al. Association of brain amyloidosis with pro-inflammatory gut bacterial taxa and peripheral inflammation markers in cognitively impaired elderly. *Neurobiology of aging*. 2017; 49:60-8.
58. Pretorius E, Bester J, Mbotwa S, Robinson C, Kell DB. Acute induction of anomalous blood clotting by molecular amplification of highly substoichiometric levels of bacterial lipopolysaccharide (lps). *BioRxiv*. 2016:053538.
59. Liu L. Haemostasis. *Basics of anesthesia*. 7th ed. 2018. p. 377-94.
60. Silverthorn DU. *Blood. Human physiology 6ed*: Pearson; 2014. p. 559.
61. MD LRC. *Imaging and laboratory diagnosis. Caplan's stroke*,. 4 ed: Saunders; 2009. p. 87-145.
62. Hogg K, Weitz JI. Blood coagulation and anticoagulant, fibrinolytic, and antiplatelet drugs. In: Brunton LL, Hilal-Dandan R, Knollmann BC, editors. *Goodman & Gilman's: The pharmacological basis of therapeutics*, 13e. New York, NY: McGraw-Hill Education; 2017.
63. Hall JE. Hemostasis and blood coagulation. *Guyton and Hall textbook of medical physiology*: Elsevier; 2016. p. 483-94.
64. Mescher AL. *Blood. Junqueira's basic histology: Text and atlas*, 15e. New York, NY: McGraw-Hill Education; 2018.
65. Page MJ, Bester J, Pretorius E. The inflammatory effects of  $\text{tnf-}\alpha$  and complement component 3 on coagulation. *Scientific reports*. 2018; 8(1):1-9.
66. Pretorius E, du Plooy JN, Bester J. A comprehensive review on eryptosis. *Cellular Physiology and Biochemistry*. 2016; 39(5):1977-2000.
67. Sirachainan N, Thongsad J, Pakakasama S, Hongeng S, Chuansumrit A, Kadegasem P, et al. Normalized coagulation markers and anticoagulation proteins in children with severe  $\beta$ -thalassemia disease after stem cell transplantation. *Thrombosis research*. 2012; 129(6):765-70.
68. Weiss E, Cytlak UM, Rees DC, Osei A, Gibson JS. Deoxygenation-induced and  $\text{ca}^{2+}$  dependent phosphatidylserine externalisation in red blood cells from normal individuals and sickle cell patients. *Cell calcium*. 2012; 51(1):51-6.
69. Pomorski T, Menon A. Lipid flippases and their biological functions. *Cellular and Molecular Life Sciences CMLS*. 2006; 63(24):2908-21.
70. Devaux PF, Herrmann A, Ohlwein N, Kozlov MM. How lipid flippases can modulate membrane structure. *Biochimica et Biophysica Acta (BBA)-Biomembranes*. 2008; 1778(7-8):1591-600.
71. Litvinov RI, Weisel JW. Role of red blood cells in haemostasis and thrombosis. *ISBT Science Series*. 2017; 12(1):176-83.
72. Flamm MH, Diamond SL. Multiscale systems biology and physics of thrombosis under flow. *Annals of Biomedical Engineering*. 2012; 40(11):2355-64.

73. Dinkla S, van Eijk LT, Fuchs B, Schiller J, Joosten I, Brock R, et al. Inflammation-associated changes in lipid composition and the organization of the erythrocyte membrane. *BBA clinical*. 2016; 5:186-92.
74. Bosman GJ. The proteome of the red blood cell: An auspicious source of new insights into membrane-centered regulation of homeostasis. *Proteomes*. 2016; 4(4):35.
75. D'Alessandro A, Kriebardis AG, Rinalducci S, Antonelou MH, Hansen KC, Papassideri IS, et al. An update on red blood cell storage lesions, as gleaned through biochemistry and omics technologies. *Transfusion*. 2015; 55(1):205-19.
76. Willekens F, Bosch F, Roerdinkholder-Stoelwinder B, Groenen-Döpp Y, Werre J. Quantification of loss of haemoglobin components from the circulating red blood cell in vivo. *European journal of haematology*. 1997; 58(4):246-50.
77. Wang Y, Cui H, Niu F, Liu S-L, Li Y, Zhang LM et al. Effect of resveratrol on blood rheological properties in Ips-challenged rats. *Frontiers in Physiology* 2018; 9(1202):1-7.
78. Bester J, Buys A, Lipinski B, Kell DB, Pretorius E. High ferritin levels have major effects on the morphology of erythrocytes in alzheimer's disease. *Frontiers in aging neuroscience*. 2013; 5:88.
79. Peters AL, Kunanayagam RK, van Bruggen R, de Korte D, Juffermans NP, Vlaar APJ . Transfusion of 35-day stored red blood cells does not result in increase of plasma non-transferrin bound iron in human endotoxemia. *the Journal of AABB*. 2016; 57(1):53-9.
80. Pretorius E, Bester J, Kell DB. A bacterial component to alzheimer's-type dementia seen via a systems biology approach that links iron dysregulation and inflammagen shedding to disease. *Journal of Alzheimer's Disease*. 2016; 53(4):1237-56.
81. Xiong Q, Shuai W, Zhou C-I, Dong W. Circulating bilirubin level is determined by both erythrocyte amounts and the proportion of aged erythrocytes in ageing and cardiovascular diseases. *Biomedicine & Pharmacotherapy*. 2020; 123:109744.
82. Andersen CBF, Stødkilde K, Sæderup KL, Kuhlee A, Raunser S, Graversen JH, et al. Haptoglobin. *Antioxidants & redox signaling*. 2017; 26(14):814-31.
83. Liu L. Patient blood management: Coagulation. In: Elsevier, editor. *Miller's anesthesia*. 9th ed. 2020; 1579-602.
84. Deppermann C, Kubes P. Start a fire, kill the bug: The role of platelets in inflammation and infection. *Sage journal*. 2018; 24:335-48
85. Mason JC. Rheumatic diseases and the cardiovascular system. *Braunwald's heart disease: A textbook of cardiovascular medicine: Elsevier* 2019. p. 94, 1847-65.
86. Fejes AV, Best MG, van der Heijden WA, Vancura A, Verschuere H, Q. Mast Q et al. . Impact of escherichia coli k12 and o18:K1 on human platelets: Differential effects on platelet activation, rnas and proteins. *Scientific Reports*. 2018; 8.



87. Jaw JE, Tsuruta M, Oh Y, Schipilow J, Hirano Y, Ngan DA, et al. Lung exposure to lipopolysaccharide causes atherosclerotic plaque destabilisation. *European Respiratory Journal*. 2016; 48(1):205-15.
88. Bakogiannis C, Sachse M, Stamatelopoulos K, Stellos K. Platelet-derived chemokines in inflammation and atherosclerosis. *Cytokine*. 2019; 122:154157.
89. Libby P, Ridker PM, Maseri A. Inflammation and atherosclerosis. *Circulation*. 2002; 105(9):1135-43.
90. Zernecke A, Weber C. Chemokines in atherosclerosis: Proceedings resumed. *Arteriosclerosis, thrombosis, and vascular biology*. 2014; 34(4):742-50.
91. Gawaz M, Langer H, May AE. Platelets in inflammation and atherogenesis. *The Journal of clinical investigation*. 2005; 115(12):3378-84.
92. Antoniadou C, Bakogiannis C, Tousoulis D, Antonopoulos AS, Stefanadis C. The cd40/cd40 ligand system: Linking inflammation with atherothrombosis. *Journal of the American College of Cardiology*. 2009; 54(8):669-77.
93. Stellos K, Seizer P, Bigalke B, Daub K, Geisler T, Gawaz M. Platelet aggregates-induced human cd34+ progenitor cell proliferation and differentiation to macrophages and foam cells is mediated by stromal cell derived factor 1 in vitro. *Seminars in thrombosis and hemostasis*; 2010: © Thieme Medical Publishers.
94. May AE, Kälsch T, Massberg S, Herouy Y, Schmidt R, Gawaz M. Engagement of glycoprotein iib/iii (αiibβ3) on platelets upregulates cd40l and triggers cd40l-dependent matrix degradation by endothelial cells. *Circulation*. 2002; 106(16):2111-7.
95. Shaw LJ, Merz CNB, Pepine CJ, Reis SE, Bittner V, Kelsey SF, et al. Insights from the nhlbi-sponsored women's ischemia syndrome evaluation (wise) study: Part i: Gender differences in traditional and novel risk factors, symptom evaluation, and gender-optimized diagnostic strategies. *Journal of the American College of Cardiology*. 2006; 47(3 Supplement):S4-S20.
96. Chugh SS, Havmoeller R, Narayanan K, Singh D, Rienstra M, Benjamin EJ, et al. Worldwide epidemiology of atrial fibrillation: A global burden of disease 2010 study. *Circulation*. 2014; 129(8):837-47.
97. Albrektsen G, Heuch I, Løchen M-L, Thelle DS, Wilsgaard T, Njølstad I, et al. Lifelong gender gap in risk of incident myocardial infarction: The tromsø study. *JAMA internal medicine*. 2016; 176(11):1673-9.
98. Bleumink GS, Knetsch AM, Sturkenboom MC, Straus SM, Hofman A, Deckers JW, et al. Quantifying the heart failure epidemic: Prevalence, incidence rate, lifetime risk and prognosis of heart failure: The rotterdam study. *European heart journal*. 2004; 25(18):1614-9.
99. Go AS, Hylek EM, Phillips KA, Chang Y, Henault LE, Selby JV, et al. Prevalence of diagnosed atrial fibrillation in adults: National implications for rhythm management and stroke

prevention: The anticoagulation and risk factors in atrial fibrillation (atria) study. *Jama*. 2001; 285(18):2370-5.

100. Asbach S, Olschewski M, Faber TS, Zehender M, Bode C, Brunner M. Mortality in patients with atrial fibrillation has significantly decreased during the last three decades: 35 years of follow-up in 1627 pacemaker patients. *Europace*. 2008; 10(4):391-4.

101. Schnabel RB, Yin X, Gona P, Larson MG, Beiser AS, McManus DD, et al. 50 year trends in atrial fibrillation prevalence, incidence, risk factors, and mortality in the framingham heart study: A cohort study. *The Lancet*. 2015; 386(9989):154-62.

102. Bunch TJ, Galenko O, Graves KG, Jacobs V, May HT. Atrial fibrillation and dementia: Exploring the association, defining risks and improving outcomes. *Arrhythmia & electrophysiology review*. 2019; 8(1):8.

103. Bangen KJ, Nation DA, Delano-Wood L, Weissberger GH, Hansen LA, Galasko DR, et al. Aggregate effects of vascular risk factors on cerebrovascular changes in autopsy-confirmed alzheimer's disease. *Alzheimer's & Dementia*. 2015; 11(4):394-403. e1.

104. Graves KG, May HT, Jacobs V, Bair TL, Stevens SM, Woller SC, et al. Atrial fibrillation incrementally increases dementia risk across all chads2 and cha2ds2vasc strata in patients receiving long-term warfarin. *American heart journal*. 2017; 188:93-8.

105. Thacker EL, McKnight B, Psaty BM, Longstreth W, Sitlani CM, Dublin S, et al. Atrial fibrillation and cognitive decline: A longitudinal cohort study. *Neurology*. 2013; 81(2):119-25.

106. Huang W, Wu X, Xue Y, Zhou Y, Xiang H, Yang W, et al. MicroRNA-3614 regulates inflammatory response via targeting traf6-mediated mapks and nf-kb signaling in the epicardial adipose tissue with coronary artery disease. *International Journal of Cardiology*. 2020.

107. Opstal TS, Hoogeveen RM, Fiolet AT, Silvis MJ, The SH, Bax WA, et al. Colchicine attenuates inflammation beyond the inflammasome in chronic coronary artery disease: A lodoco2 proteomic substudy. *Circulation*. 2020.

108. Horseman M, Surani S, Bowman J. Endotoxin, toll-like receptor-4, and atherosclerotic heart disease. *Current cardiology reviews*. 2017; 13(2):86-93.

109. Vianello E, Dozio E, Arnaboldi F, Marazzi M, Martinelli C, Lamont J, et al. Epicardial adipocyte hypertrophy: Association with m1-polarization and toll-like receptor pathways in coronary artery disease patients. *Nutrition, Metabolism and Cardiovascular Diseases*. 2016; 26(3):246-53.

110. Wu C, Su Z, Lin M, Ou J, Zhao W, Cui J, et al. Nlrp11 attenuates toll-like receptor signalling by targeting traf6 for degradation via the ubiquitin ligase rnf19a. *Nature communications*. 2017; 8(1):1-15.

111. Ben J, Jiang B, Wang D, Liu Q, Zhang Y, Qi Y, et al. Major vault protein suppresses obesity and atherosclerosis through inhibiting ikk–nf-kb signaling mediated inflammation. *Nature communications*. 2019; 10(1):1-15.

112. Troncone L, Luciani M, Coggins M, Wilker EH, Ho C-Y, Codispoti KE, et al. A $\beta$  amyloid pathology affects the hearts of patients with alzheimer's disease: Mind the heart. *Journal of the American College of Cardiology*. 2016; 68(22):2395-407.
113. Tan M-S, Yu J-T, Tan L. Bridging integrator 1 (bin1): Form, function, and alzheimer's disease. *Trends in molecular medicine*. 2013; 19(10):594-603.
114. Elliott P, Andersson B, Arbustini E, Bilinska Z, Cecchi F, Charron F, et al. Classification of the cardiomyopathies: A position statement from the european society of cardiology working group on myocardial and pericardial diseases. *European heart journal*. 2008; 29(2):270 -6.
115. Subramanian K, Gianni D, Balla C, Assenza GE, Joshi M, Semigran MJ, et al. Cofilin-2 phosphorylation and sequestration in myocardial aggregates: Novel pathogenetic mechanisms for idiopathic dilated cardiomyopathy. *Journal of the American College of Cardiology*. 2015; 65(12):1199-214.
116. Tublin JM, Adelstein JM, del Monte F, Combs CK, Wold LE. Getting to the heart of alzheimer disease. *Circulation research*. 2019; 124(1):142-9.
117. Schultheiss H-P, Fairweather D, Caforio AL, Escher F, Hershberger RE, Lipshultz SE, et al. Dilated cardiomyopathy. *Nature reviews Disease primers*. 2019; 5(1):1-19.
118. Pastori D, Carnevale R, Nocella C, Novo M, Santulli M, Cammisotto V, et al. Gut-derived serum lipopolysaccharide is associated with enhanced risk of major adverse cardiovascular events in atrial fibrillation: Effect of adherence to mediterranean diet. *Journal of the American Heart Association*. 2017; 6(6):e005784.
119. Derrien M, van Hylckama Vlieg JET. Fate, activity, and impact of ingested bacteria within the human gut microbiota. *Trends in Microbiology*. 2015; 23(6):355-66.
120. Shen L, Liu L, Ji H-F. Alzheimer's disease histological and behavioral manifestations in transgenic mice correlate with specific gut microbiome state. *Journal of Alzheimer's Disease*. 2017; 56(1):385-90.
121. Jansen VL, Gerdes VE, Middeldorp S, van Mens TE. Gut microbiota and their metabolites in cardiovascular disease. *Best Practice & Research Clinical Endocrinology & Metabolism*. 2021:101492.
122. Cifuentes D, Poittevin M, Dere E, Broquères-You D, Bonnin P, Benessiano J, et al. Hypertension accelerates the progression of alzheimer-like pathology in a mouse model of the disease. *Hypertension*. 2015; 65(1):218-24.
123. Wopereis H, Oozeer R, Knipping K, Belzer C, Knol J. The first thousand days—intestinal microbiology of early life: Establishing a symbiosis. *Pediatric Allergy and Immunology*. 2014; 25(5):428-38.
124. Raetz CR, Reynolds CM, Trent MS, Bishop RE. Lipid a modification systems in gram-negative bacteria. *Annu. Rev. Biochem*. 2007; 76:295-329.

125. Steimle A, Autenrieth IB, Frick J-S. Structure and function: Lipid a modifications in commensals and pathogens. *International Journal of Medical Microbiology*. 2016; 306(5):290-301.
126. Silipo A, Leone MR, Lanzetta R, Parrilli M, Lackner G, Busch B, et al. Structural characterization of two lipopolysaccharide o-antigens produced by the endofungal bacterium burkholderia sp. Hki-402 (b4). *Carbohydrate research*. 2012; 347(1):95-8.
127. Alexander C, Rietschel ET. Invited review: Bacterial lipopolysaccharides and innate immunity. *Journal of endotoxin research*. 2001; 7(3):167-202.
128. Akira S, Takeda K. Toll-like receptor signalling. *Nature reviews immunology*. 2004; 4(7):499-511.
129. Netea MG, van Deuren M, Kullberg BJ, Cavaiillon J-M, Van der Meer JW. Does the shape of lipid a determine the interaction of lps with toll-like receptors? *Trends in immunology*. 2002; 23(3):135-9.
130. Werheim ER, Senior KG, Shaffer CA, Cuadra GA. Oral pathogen porphyromonas gingivalis can escape phagocytosis of mammalian macrophages. *Microorganisms*. 2020; 8(9):1432.
131. Nikkari S, McLaughlin IJ, Bi W, Dodge DE, Relman DA. Does blood of healthy subjects contain bacterial ribosomal DNA? *Journal of Clinical Microbiology*. 2001; 39(5):1956-9.
132. Sato J, Kanazawa A, Ikeda F, Yoshihara T, Goto H, Abe H, et al. Gut dysbiosis and detection of “live gut bacteria” in blood of japanese patients with type 2 diabetes. *American Diabetes Association*. 2014; 37(8):2343-50.
133. Potgieter M, Bester J, Kell DB, Pretorius E. The dormant blood microbiome in chronic, inflammatory diseases. *FEMS Microbiology Reviews*. 2015; 39(4):567-91.
134. Ghosh S, Lertwattanak R, Garduño JdJ, Galeana JJ, Li J, Zamarripa F, et al. Elevated muscle tlr4 expression and metabolic endotoxemia in human aging. *Journals of Gerontology Series A: Biomedical Sciences and Medical Sciences*. 2014; 70(2):232-46.
135. Bison S, Carbon L, Arban R, Bate S, Gerrard P, Razzoli M. Differential behavioral, physiological, and hormonal sensitivity to lps challenge in rats. *International Journal of Interferon, Cytokine and Mediator Research*. 2009; 1:1-13.
136. Moraes MM, Galvão MC, Cabral D, Coelho CP, Queiroz-Hazarbassanov N, Martins MF, et al. Propentofylline prevents sickness behavior and depressive-like behavior induced by lipopolysaccharide in rats via neuroinflammatory pathway. *PLoS One*. 2017; 12(1):e0169446.
137. Mi W, Li Y, Yoon SH, Ernst RK, Walz T, Liao M. Structural basis of msba-mediated lipopolysaccharide transport. *Nature*. 2017; 549(7671):233-7.
138. De Waal GM, Engelbrecht L, Davis T, De Villiers WJ, Kell DB, Pretorius E. Correlative light-electron microscopy detects lipopolysaccharide and its association with fibrin fibres in

parkinson's disease, alzheimer's disease and type 2 diabetes mellitus. *Scientific reports*. 2018; 8(1):1-12.

139. Newby DE, Grubb NR, Bradbury A. *Cardiology Davidson's principles and practice of medicine*: Elsevier; 2018. p. 441-544.

140. MR Pereira MR, Leite PEC. The involvement of parasympathetic and sympathetic nerve in the inflammatory reflex. *Journal of Cellular Physiology* 2016; (213):1862-9.

141. MR Pereira MR, Leite PEC. The involvement of parasympathetic and sympathetic nerve in the inflammatory reflex. *Journal of Cellular Physiology* 2016; (213):1862-9.

142. Zila I, Mokra D, Kopincova J, Kolomaznik M, Javorka M, Calkovska A. Heart rate variability and inflammatory response in rats with lipopolysaccharide-induced endotoxemia. *Physiological research*. 2015; 64:S669.

143. Samokhvalov V, Jamieson KL, Darwesh AM, Keshavarz-Bahaghighat H, Lee TYT, et al. Deficiency of soluble epoxide hydrolase protects cardiac function impaired by lps-induced acute inflammation. *frontiers in pharmacology*. 2019; 9(1572):1-16.

144. Bogdanov S, Jurendic T, Sieber R, Gallmann P. Honey for nutrition and health: A review. *Journal of the American College of Nutrition*. 2008; 27(6):677-89.

145. Roberts AEL, Brown HL, Jenkins RE. On the antibacterial effects of manuka honey: Mechanistic insights. *Research and Reports in Biology*. 2015; 6:215-24.

146. Erejuwa OO, Sulaiman SA, Ab Wahab MS. Honey: A novel antioxidant. *Molecules*. 2012; 17(4):4400-23.

147. Ryan KJ. *Enterobacteriaceae*. *Sherris medical microbiology*, 7e. New York, NY: McGraw-Hill Education; 2017.

148. Ellenbroek B, Youn J. Rodent models in neuroscience research: Is it a rat race? *Disease models & mechanisms*. 2016; 9(10):1079-87.

149. Snyder JS, Choe JS, Clifford MA, Jeurling SI, Hurley P, Brown A, et al. Adult-born hippocampal neurons are more numerous, faster maturing, and more involved in behavior in rats than in mice. *Journal of Neuroscience*. 2009; 29(46):14484-95.

150. Lazarov O, Hollands C. Hippocampal neurogenesis: Learning to remember. *Progress in neurobiology*. 2016; 138:1-18.

151. Jaramillo S, Zador AM. Mice and rats achieve similar levels of performance in an adaptive decision-making task. *Frontiers in systems neuroscience*. 2014; 8:173.

152. Colacicco G, Welzl H, Lipp H-P, Würbel H. Attentional set-shifting in mice: Modification of a rat paradigm, and evidence for strain-dependent variation. *Behavioural brain research*. 2002; 132(1):95-102.

153. Sengupta P. The laboratory rat: Relating its age with human's. *International journal of preventive medicine*. 2013; 4(6):624.

154. Lakatta EG, Levy D. Arterial and cardiac aging: Major shareholders in cardiovascular disease enterprises: Part ii: The aging heart in health: Links to heart disease. *Circulation*. 2003; 107(2):346-54.
155. Capitanio D, Leone R, Fania C, Torretta E, Gelfi C. Sprague dawley rats: A model of successful heart aging. *EuPA open proteomics*. 2016; 12:22-30.
156. Akintola T, Ravier C, Studlack P, Uddin O, Masri R, Keller A. The grimace scale reliably assesses chronic pain in a rodent model of trigeminal neuropathic pain. *Neurobiology of pain*. 2017; 2:13-7.
157. Zimcikova E, Simko J, Karesova I, Kremlacek J, Malakova J. Behavioral effects of antiepileptic drugs in rats: Are the effects on mood and behavior detectable in open-field test? *Seizure*. 2017; 52:35-40.
158. Marmendal M, Eriksson CJP, Fahlke C. Early deprivation increases exploration and locomotion in adult male wistar offspring. *Pharmacol Biochem Behav*. 2006; 85:535-44.
159. Kuniishia H, Satoshi I, Yamamotoa M, Ikubob N, Matsudaa S, Futorab E, et al. Early deprivation increases high-leaning behavior, a novel anxiety-like behavior, in the open field test in rats. *Neuroscience research*. 2017; 123:27-35.
160. Grayson B, Leger M, Piercy C, Adamson L, Harte M, Neill JC. Assessment of disease-related cognitive impairments using the novel object recognition (nor) task in rodents. *Behavioural brain research*. 2015; 285:176-93.
161. Pan X, Jiang T, Zhang L, Zheng H, Luo J, Hu X. Physical exercise promotes novel object recognition memory in spontaneously hypertensive rats after ischemic stroke by promoting neural plasticity in the entorhinal cortex. *Frontiers in behavioral neuroscience*. 2017; 11:185.
162. Ennaceur A, Delacour J. A new one-trial test for neurobiological studies of memory in rats. 1: Behavioral data. *Behavioural brain research*. 1988; 31(1):47-59.
163. Sangüesa G, Cascales M, Griñán C, Sánchez RM, Roglans N, Pallàs M, et al. Impairment of novel object recognition memory and brain insulin signaling in fructose-but not glucose-drinking female rats. *Molecular neurobiology*. 2018; 55(8):6984-99.
164. Narayanan R, Gilbert B, Ravichandran S, Bhuvaneshwari K. Psychopharmacological characterization of effects of ferula asafoetida linn. Formulation in mouse on a y-maze, epm, and open field apparatus. *International Journal of Basic & Clinical Pharmacology*. 2017; 6(9):2254-8.
165. Aydin S. A short history, principles, and types of elisa, and our laboratory experience with peptide/protein analyses using elisa. *Peptides*. 2015; 72:4-15.
166. Varadhachary GR, Raber MN, Abbruzzese JL. Carcinoma of unknown primary. In: Livingstone C, editor. *Abeloff's clinical oncology*: Churchill Livingstone; 2014. p. 1792-803.

167. G.R Hunt. Techniques in nephropathology. In: S.S. IS, editor. Histochemistry in pathologic diagnosis: New York: Marcel Dekker; 1987.
168. Bancroft C. Carbohydrates. Bancroft's theory and practice of histological techniques: Elsevier; 2019. p. 176-97.
169. Szymańska E, Szymańska S, Truszkowska G, Ciara E, Pronicki M, Shin YS, et al. Variable clinical presentation of glycogen storage disease type iv: From severe hepatosplenomegaly to cardiac insufficiency. Some discrepancies in genetic and biochemical abnormalities. Archives of medical science: AMS. 2018; 14(1):237.
170. Percival K, Radi Z. A modified verhoeff-van gieson elastin histochemical stain to enable pulmonary arterial hypertension model characterization. European journal of histochemistry: EJH. 2016; 60(1).
171. Kazlouskaya V, Malhotra S,, Lambe J, Idriss MH, Elston D, Andres C. The utility of elastic verhoeff-van gieson staining in dermatopathology. Journal of Cutaneous Pathology. 2012; 40(2):211-25.
172. Meghan A. Piccinin JS. Histology, verhoeff stain. StatPearls. 2018.
173. Maurice P, Blaise S, Gayral S, Debelle L, Laffargue M, Hornebeck W, et al. Elastin fragmentation and atherosclerosis progression: The elastokine concept. Trends in cardiovascular medicine. 2013; 23(6):211-21.
174. Lillie RD. Histopathologic technic and practical histochemistry McGraw-Hill, editor. New York1965.
175. Mescher AL. Histology & its methods of study. Junqueira's basic histology: Text and atlas, 15e. New York, NY: McGraw-Hill Education; 2018.
176. Venter C, Oberholzer HM, Bester J, Van Rooy M-J, Bester MJ. Ultrastructural, confocal and viscoelastic characteristics of whole blood and plasma after exposure to cadmium and chromium alone and in combination: An ex vivo study. Cellular Physiology and Biochemistry. 2017; 43(3):1288-300.
177. Stirling W. Transmission electron microscopy. Bancroft's theory and practice of histological techniques: Elsevier; 2019. p. 434-75.
178. Lim YY, Kalinowski P, Pietrzak RH, Laws SM, Burnham SC, Ames D, et al. Association of  $\beta$ -amyloid and apolipoprotein e  $\epsilon$ 4 with memory decline in preclinical alzheimer disease. JAMA neurology. 2018; 75(4):488-94.
179. Hill JM, Lukiw WJ. Microbial-generated amyloids and alzheimer's disease (ad). Frontiers in aging neuroscience. 2015; 7:9.
180. Canobbio I, Abubaker AA, Visconte C, Torti M, Pula G. Role of amyloid peptides in vascular dysfunction and platelet dysregulation in alzheimer's disease. Frontiers in cellular neuroscience. 2015; 9:65.

181. Doré V, Villemagne VL, Bourgeat P, Fripp J, Acosta O, Chetelat G, et al. Cross-sectional and longitudinal analysis of the relationship between a $\beta$  deposition, cortical thickness, and memory in cognitively unimpaired individuals and in alzheimer disease. *JAMA neurology*. 2013; 70(7):903-11.
182. Rowe CC, Bourgeat P, Ellis KA, Brown B, Lim YY, Mulligan R, et al. Predicting alzheimer disease with  $\beta$ -amyloid imaging: Results from the australian imaging, biomarkers, and lifestyle study of ageing. *Annals of neurology*. 2013; 74(6):905-13.
183. Ossenkoppele R, Jansen WJ, Rabinovici GD, Knol DL, van der Flier WM, van Berckel BN, et al. Prevalence of amyloid pet positivity in dementia syndromes: A meta-analysis. *Jama*. 2015; 313(19):1939-50.
184. Lukiw WJ, Li W, Bond T, Zhao Y. Facilitation of gastrointestinal (gi) tract microbiome-derived lipopolysaccharide (lps) entry into human neurons by amyloid beta-42 (a $\beta$ 42) peptide. *Frontiers in Cellular Neuroscience*. 2019; 13.
185. (NIA) NloA [Internet] What happens to the brain in alzheimer's disease? : National Institutes of Health; 2017 [updated May 16, 2017; cited 2020 18/01/2020].
186. Farooq RK, Asghar K, Kanwal S, Zulqernain A. Role of inflammatory cytokines in depression: Focus on interleukin-1 $\beta$ . *Biomedical reports*. 2017; 6(1):15-20.
187. Yue N, Huang H, Zhu X, Han Q, Wang Y, Li B, et al. Activation of p2x7 receptor and nlrp3 inflammasome assembly in hippocampal glial cells mediates chronic stress-induced depressive-like behaviors. *Journal of neuroinflammation*. 2017; 14(1):1-15.
188. Li M, Li C, Yu H, Cai X, Shen X, Sun X, et al. Lentivirus-mediated interleukin-1 $\beta$  (il-1 $\beta$ ) knock-down in the hippocampus alleviates lipopolysaccharide (lps)-induced memory deficits and anxiety-and depression-like behaviors in mice. *Journal of neuroinflammation*. 2017; 14(1):1-12.
189. Bai Z, Stamova B, Xu H, Ander BP, Wang J, Jickling GC, et al. Distinctive rna expression profiles in blood associated with alzheimer's disease after accounting for white matter hyperintensities. *Alzheimer disease and associated disorders*. 2014; 28(3):226.
190. Goshen I, Yirmiya R. Interleukin-1 (il-1): A central regulator of stress responses. *Frontiers in neuroendocrinology*. 2009; 30(1):30-45.
191. Zhao Y, Jaber V, Lukiw WJ. Secretory products of the human gi tract microbiome and their potential impact on alzheimer's disease (ad): Detection of lipopolysaccharide (lps) in ad hippocampus. *Frontiers in cellular and infection microbiology*. 2017; 7:318.
192. Miller CK, Halbing AA, Patisaul HB, Meitzen J. Interactions of the estrous cycle, novelty, and light on female and male rat open field locomotor and anxiety-related behaviors. *Physiology & Behavior*. 2021; 228:113203.
193. Schulz D. Acute food deprivation separates motor-activating from anxiolytic effects of caffeine in a rat open field test model. *Behavioural pharmacology*. 2018; 29(6):543-6.



194. McHail DG, Dumas TC. Hippocampal gamma rhythms during y-maze navigation in the juvenile rat. *Hippocampus*. 2020; 30(5):505-25.
195. Kersten M, Rabbe T, Blome R, Porath K, Sellmann T, Bien CG, et al. Novel object recognition in rats with nmdar dysfunction in ca1 after stereotactic injection of anti-nmdar encephalitis cerebrospinal fluid. *Frontiers in neurology*. 2019; 10:586.
196. Yang L, Zhou R, Tong Y, Chen P, Shen Y, Miao S, et al. Neuroprotection by dihydrotestosterone in lps-induced neuroinflammation. *Neurobiology of disease*. 2020; 140:104814.
197. McKim DB, Weber MD, Niraula A, Sawicki CM, Liu X, Jarrett BL, et al. Microglial recruitment of il-1 $\beta$ -producing monocytes to brain endothelium causes stress-induced anxiety. *Molecular psychiatry*. 2018; 23(6):1421-31.
198. Yu H, Zou Z, Zhang X, Peng W, Chen C, Ye Y, et al. Inhibition of phosphodiesterase 4 by fcpr03 alleviates lipopolysaccharide-induced depressive-like behaviors in mice: Involvement of p38 and jnk signaling pathways. *International journal of molecular sciences*. 2018; 19(2):513.
199. Hara T, Nakamura K, Matsui M, Yamamoto A, Nakahara Y, Suzuki-Migishima R, et al. Suppression of basal autophagy in neural cells causes neurodegenerative disease in mice. *Nature*. 2006; 441(7095):885-9.
200. Umbarawan Y, Syamsunarno MRA, Obinata H, Yamaguchi A, Sunaga H, Matsui H, et al. Robust suppression of cardiac energy catabolism with marked accumulation of energy substrates during lipopolysaccharide-induced cardiac dysfunction in mice. *Metabolism*. 2017; 77:47-57.
201. Qin L, Liu Y, Hong JS, Crews FT. NADPH oxidase and aging drive microglial activation, oxidative stress, and dopaminergic neurodegeneration following systemic lps administration. *Glia*. 2013; 61(6):855-68.
202. Mastinu A, Bonini SA, Rungratanawanich W, Aria F, Marziano M, Maccarinelli G, et al. Gamma-oryzanol prevents lps-induced brain inflammation and cognitive impairment in adult mice. *Nutrients*. 2019; 11(4):728.
203. Hauss-Wegrzyniak B, Vannucchi MG, Wenk GL. Behavioral and ultrastructural changes induced by chronic neuroinflammation in young rats. *Brain research*. 2000; 859(1):157-66.
204. Alvarez-Suarez JM, Gasparrini M, Forbes-Hernández TY, Mazzoni L, Giampieri F. The composition and biological activity of honey: A focus on manuka honey. *Foods*. 2014; 3(3):420-32.
205. Tan Z, Beiser A, Vasan R, Roubenoff R, Dinarello C, Harris T, et al. Inflammatory markers and the risk of alzheimer disease: The framingham study. *Neurology*. 2007; 68(22):1902-8.

206. Iloun P, Abbasnejad Z, Janahmadi M, Ahmadiani A, Ghasemi R. Investigating the role of p38, jnk and erk in lps induced hippocampal insulin resistance and spatial memory impairment: Effects of insulin treatment. *EXCLI journal*. 2018; 17:825.
207. Sriraksa N, Thongrong S. The neuroprotective effect of zingiber cassumunar roxb. Extract on lps-induced neuronal cell loss and astroglial activation within the hippocampus. *BioMed Research International* 2020; 2020:10.
208. Amorim MR, Moreira DA, Santos BM, Ferrari GD, Nogueira JE, de Deus JL, et al. Increased lipopolysaccharide-induced hypothermia in neurogenic hypertension is caused by reduced hypothalamic pge2 production and increased heat loss. *The Journal of Physiology*. 2020; 598(20):4663-80.
209. Shiraki C, Horikawa R, Fujimoto M, Okamoto K, Kurganov E, Miyata S. Role of trpm8 in switching between fever and hypothermia in adult mice during endotoxin-induced inflammation. 2020.
210. Liu E, Lewis K, Al-Saffar H, Krall CM, Singh A, Kulchitsky VA, et al. Naturally occurring hypothermia is more advantageous than fever in severe forms of lipopolysaccharide-and escherichia coli-induced systemic inflammation. *American Journal of Physiology-Regulatory, Integrative and Comparative Physiology*. 2012; 302(12):R1372-R83.
211. Garami A, Steiner AA, Romanovsky AA. Fever and hypothermia in systemic inflammation. *Handbook of clinical neurology*: Elsevier; 2018. p. 565-97.
212. Park KH, Lee KH, Kim H. Effect of hypothermia on coagulatory function and survival in sprague–dawley rats exposed to uncontrolled haemorrhagic shock. *Injury*. 2013; 44(1):91-6.
213. Shohet RV. The cardiovascular system. In: Janson LW, Tischler ME, editors. *The big picture: Medical biochemistry*. New York, NY: McGraw-Hill Education; 2018.
214. Paulsen DF. Chapter 10. Muscle tissue. *Histology & cell biology: Examination & board review, 5e*. New York, NY: The McGraw-Hill Companies; 2010.
215. Barrett KE, Barman SM, Brooks HL, Yuan JXJ. Excitable tissue: Muscle. *Ganong's review of medical physiology, 26e*. New York, NY: McGraw-Hill Education; 2019.
216. Huang S, Xu M, Liu L, Yang J, Wang H, Wan C, et al. Autophagy is involved in the protective effect of p21 on lps-induced cardiac dysfunction. *Cell death & disease*. 2020; 11(7):1-15.
217. Laposata M. Blood vessels. In: Laposata M, editor. *Laposata's laboratory medicine: Diagnosis of disease in the clinical laboratory, 3e*. New York, NY: McGraw-Hill Education; 2019.
218. Mescher AL. The circulatory system. *Junqueira's basic histology text and atlas, 16e*. New York, NY: McGraw Hill; 2021.

219. Ochoa TJ, Contreras CA. *Escherichia coli*. Nelson textbook of pediatrics. 1 ed: Elsevier 2016. p. 1396-400.
220. Xu JC, Lin; Wang, Tingting; Zhang, Peng; Liu, Zhengjun;. Ergosterol attenuates lps-induced myocardial injury by modulating oxidative stress and apoptosis in rats. *Basel*. 2018; 48(2):583-92.
221. Zhou DR, Eid R, Miller KA, Boucher E, Mandato CA, Greenwood MT. Intracellular second messengers mediate stress inducible hormesis and programmed cell death: A review. *Biochimica et Biophysica Acta (BBA)-Molecular Cell Research*. 2019; 1866(5):773-92.
222. Newsholme P, Cruzat VF, Keane KN, Carlessi R, de Bittencourt Jr PIH. Molecular mechanisms of ros production and oxidative stress in diabetes. *Biochemical Journal*. 2016; 473(24):4527-50.
223. Morgan MJ, Liu Z-g. Crosstalk of reactive oxygen species and nf-kb signaling. *Cell research*. 2011; 21(1):103-15.
224. Sun X, Luo S, Jiang C, Tang Y, Cao Z, Jia H, et al. Sodium butyrate reduces bovine mammary epithelial cell inflammatory responses induced by exogenous lipopolysaccharide, by inactivating nf-kb signaling. *Journal of dairy science*. 2020; 103(9):8388-97.
225. Bai Y-Y, Yan D, Zhou H-Y, Li W-X, Lou Y-Y, Zhou X-R, et al. Betulinic acid attenuates lipopolysaccharide-induced vascular hyporeactivity in the rat aorta by modulating nrf2 antioxidative function. *Inflammopharmacology*. 2020; 28(1):165-74.
226. San Chin H, Li MX, Tan IK, Ninnis RL, Reljic B, Scicluna K, et al. Vdac2 enables bax to mediate apoptosis and limit tumor development. *Nature communications*. 2018; 9(1):1-13.
227. Redza-Dutordoir M, Averill-Bates DA. Activation of apoptosis signalling pathways by reactive oxygen species. *Biochimica et Biophysica Acta (BBA)-Molecular Cell Research*. 2016; 1863(12):2977-92.
228. Sharma D, Sharma P, Sharma K, Mathur J, Singh P. Histochemical study of the metabolism and toxicity of mercury. *Current Science*. 1988; 57(9):483-5.
229. Asci H, Ozmen O, Erzurumlu Y, Savas H, Temel EN, Icten P, et al. Ameliorative effects of pregabalin on lps induced endothelial and cardiac toxicity. *Biotechnic & Histochemistry*. 2020:1-12.
230. Sciarretta S, Yee D, Ammann P, Nagarajan N, Volpe M, Frati G, et al. Role of nadph oxidase in the regulation of autophagy in cardiomyocytes. *Clinical Science*. 2015; 128(7):387-403.
231. Avlas O, Bragg A, Fuks A, Nicholson JD, Farkash A, Porat E, et al. Tlr4 expression is associated with left ventricular dysfunction in patients undergoing coronary artery bypass surgery. *PloS one*. 2015; 10(6):e0120175.
232. Bereketeab Haileselassie RM, Amit U. Joshi, Brooke A. Napier, Liliana M. Massis, Nicolai Patrick Ostberg, Bruno B. Queliconi, Denise Monack, Daniel Bernstein and Daria

- Mochly-Rosen. Drp1/fis1 interaction mediates mitochondrial dysfunction in septic cardiomyopathy. *Journal of Molecular and Cellular Cardiology*. 2019; 130:160-9.
233. Bank AJ, Wang H, Holte JE, Mullen K, Shammas R, Kubo SH. Contribution of collagen, elastin, and smooth muscle to in vivo human brachial artery wall stress and elastic modulus. *Circulation*. 1996; 94(12):3263-70.
234. Reesink KD, Spronck B. Constitutive interpretation of arterial stiffness in clinical studies: A methodological review. *American Journal of Physiology-Heart and Circulatory Physiology*. 2019; 316(3):H693-H709.
235. Lacolley P, Regnault V, Segers P, Laurent S. Vascular smooth muscle cells and arterial stiffening: Relevance in development, aging, and disease. *Physiological reviews*. 2017.
236. Laposata M. Blood vessels. In: Laposata M, editor. *Laposatas laboratory medicine: Diagnosis of disease in the clinical laboratory*, 3e. New York, NY: McGraw-Hill Education; 2019.
237. St-Amand R, Sock ÉTN, Quinn S, Lavoie J-M, St-Pierre DH. Two weeks of western diet disrupts liver molecular markers of cholesterol metabolism in rats. *Lipids in Health and Disease*. 2020; 19(1):1-11.
238. Harada K, Kikuchi R, Suzuki S, Tanaka A, Aoki T, Iwakawa N, et al. Impact of high-density lipoprotein 3 cholesterol subfraction on periprocedural myocardial injury in patients who underwent elective percutaneous coronary intervention. *Lipids in health and disease*. 2018; 17(1):21.
239. Varbo A, Nordestgaard BG. Nonfasting triglycerides, low-density lipoprotein cholesterol, and heart failure risk: Two cohort studies of 113 554 individuals. *Arteriosclerosis, thrombosis, and vascular biology*. 2018; 38(2):464-72.
240. Romanelli RJ, Ito MJ, Karalis DG, Huang H-C, Iorga SR, Kam I, et al. Statin prescribing, switching, and low-density lipoprotein cholesterol goal attainment across racial/ethnic groups with atherosclerotic cardiovascular disease. *Circulation*. 2019; 139(Suppl\_1):AP128-AP.
241. Johansen M, De Silva K, Plain K, Begg D, Whittington R, Purdie A. Sheep and cattle exposed to mycobacterium avium subspecies paratuberculosis exhibit altered total serum cholesterol profiles during the early stages of infection. *Veterinary immunology and immunopathology*. 2018; 202:164-71.
242. Nash DT, Fillit H. Cardiovascular disease risk factors and cognitive impairment. *The American journal of cardiology*. 2006; 97(8):1262-5.
243. Jensen HA, Mehta JL. Endothelial cell dysfunction as a novel therapeutic target in atherosclerosis. *Expert review of cardiovascular therapy*. 2016; 14(9):1021-33.

244. Guo L, Ai J, Zheng Z, Howatt DA, Daugherty A, Huang B, et al. High density lipoprotein protects against polymicrobe-induced sepsis in mice. *Journal of Biological chemistry*. 2013; 288(25):17947-53.
245. Wang L, Chen W-Z, Wu M-P. Apolipoprotein ai inhibits chemotaxis, adhesion, activation of thp-1 cells and improves the plasma hdl inflammatory index. *Cytokine*. 2010; 49(2):194-200.
246. Ekstrand M, Gustafsson Trajkovska M, Perman-Sundelin J, Fogelstrand P, Adiels M, Johansson M, et al. Imaging of intracellular and extracellular ros levels in atherosclerotic mouse aortas ex vivo: Effects of lipid lowering by diet or atorvastatin. *PLoS One*. 2015; 10(6):e0130898.
247. Chistiakov DA, Bobryshev YV, Orekhov AN. Macrophage-mediated cholesterol handling in atherosclerosis. *Journal of cellular and molecular medicine*. 2016; 20(1):17-28.
248. Xue F, Nie X, Shi J, Liu Q, Wang Z, Li X, et al. Quercetin inhibits lps-induced inflammation and ox-ldl-induced lipid deposition. *Frontiers in pharmacology*. 2017; 8:40.
249. Bongu A, Chang E, Ramsey-Goldman R. Can morbidity and mortality of sle be improved? *Best practice & research Clinical rheumatology*. 2002; 16(2):313-32.
250. Martins IJ. Bacterial lipopolysaccharides change membrane fluidity with relevance to phospholipid and amyloid beta dynamics in alzheimer's disease. *Journal of Microbial and Biochemical Technology*. 2013; 8(4): 322-4.
251. McMillan KN, Kramer J, Takemoto CM, Ozment CP. Coagulation disorders in congenital heart disease. *Critical heart disease in infants and children: Elsevier* 2019. p. 282-302.
252. Stein ES, Shimon MB, Furman AA, Golderman V, Chapman J, Maggio N. Thrombin inhibition reduces the expression of brain inflammation markers upon systemic lps treatment. *Neural plasticity*. 2018; 2018.
253. Nunes JM, Fillis T, Page MJ, Venter C, Lancry O, Kell DB, et al. Gingipain r1 and lipopolysaccharide from porphyromonas gingivalis have major effects on blood clot morphology and mechanics. *Frontiers in Immunology*. 2020; 11(1551).
254. Zhang G, Han J, Welch EJ, Richard DY, Voyno-Yasenetskaya TA, Malik AB, et al. Lipopolysaccharide stimulates platelet secretion and potentiates platelet aggregation via tlr4/myd88 and the cgmp-dependent protein kinase pathway. *The Journal of Immunology*. 2009; 182(12):7997-8004.
255. Pretorius E, Bester J, Page MJ, Kell DB. The potential of lps-binding protein to reverse amyloid formation in plasma fibrin of individuals with alzheimer-type dementia. *Frontiers in aging neuroscience*. 2018; 10:257.
256. Drabik L, Wołkow P, Undas A. Fibrin clot permeability as a predictor of stroke and bleeding in anticoagulated patients with atrial fibrillation. *Stroke*. 2017; 48(10):2716-22.

257. Undas A. Fibrin clot properties and their modulation in thrombotic disorders. *Thrombosis and haemostasis*. 2014; 112(07):32-42.
258. Levi M, Ten Cate H. Disseminated intravascular coagulation. *New England Journal of Medicine*. 1999; 341(8):586-92.
259. De Waal GM, De Villiers WJ, Forgan T, Roberts T, Pretorius E. Colorectal cancer is associated with increased circulating lipopolysaccharide, inflammation and hypercoagulability. *Scientific Reports*. 2020; 10(1):1-20.
260. Minden-Birkenmaier BA, Meadows MB, Cherukuri K, Smeltzer MP, Smith RA, Radic MZ, et al. Manuka honey modulates the release profile of a dhl-60 neutrophil model under anti-inflammatory stimulation. *Journal of Tissue Viability*. 2020; 29(2):91-9.
261. Ząbczyk M, Majewski J, Lelakowski J. Thromboembolic events are associated with prolonged clot lysis time in patients with permanent atrial fibrillation. *Polskie Archiwum Medycyny Wewnętrznej*. 2011; 121(11).
262. Suzan Hamid WG, Milena Pavlova. Trends in cardiovascular diseases and associated risks in sub-saharan africa: A review of the evidence for ghana, nigeria, south africa, sudan and tanzania. *The Aging male*. 2018:169-76.
263. Kyomuhendo C, Adeola R. Green and grey: Nutritional lifestyle and healthful ageing in rural and urban areas of three sub-saharan african countries. *Business Strategy & Development*. 2021; 4(1):22-33.
264. Fierros-Campuzano J, Ballesteros-Zebadúa P, Manjarrez-Marmolejo J, Aguilera P, Méndez-Díaz M, Prospero-García O, et al. Irreversible hippocampal changes induced by high fructose diet in rats. *Nutritional Neuroscience*. 2020:1-13.
265. Wu J, Dai F, Li C, Zou Y. Gender differences in cardiac hypertrophy. *Journal of cardiovascular translational research*. 2020; 13(1):73-84.
266. Ittner LM, Götz J. Amyloid- $\beta$  and tau—a toxic pas de deux in alzheimer's disease. *Nature Reviews Neuroscience*. 2011; 12(2):67-72.
267. Nortley R, Korte N, Izquierdo P, Hirunpattarasilp C, Mishra A, Jaunmuktane Z, et al. Amyloid  $\beta$  oligomers constrict human capillaries in alzheimer's disease via signaling to pericytes. *Science* 2019; 365(6450).
268. Putakala M, Gujjala S, Nukala S, Bongu SBR, Chintakunta N, Desireddy S. Cardioprotective effect of phyllanthus amarus against high fructose diet induced myocardial and aortic stress in rat model. *Biomedicine & Pharmacotherapy*. 2017; 95:1359-68.